12-1-2011

Assessment of functional characteristics of small GTPases using small molecules

Jacob Agola

Jacob Ongudi Agola

Candidate

Biomedical Sciences

Department

This dissertation is approved, and it is acceptable in quality and form for publication:

Approved by the Dissertation Committee:

Prof. Angela Wandinger-Ness , Chairperson

Prof. Laurie G. Hudson

Prof. Eric R. Prossnitz

Prof. Tione Buranda

Prof. Larry A. Sklar

Assessment of Functional Characteristics of Small GTPases Using Small Molecules

By

Jacob Ongudi Agola

B.S., Chemistry, University of Nairobi, Kenya, 1997

M.S., Chemistry, University of Wyoming, U.S.A, 2006

DISSERTATION

Submitted in Partial Fulfillment of the

Requirements for the Degree of

Doctor of Philosophy

Biomedical Sciences

The University of New Mexico

Albuquerque, New Mexico

December, 2011

DEDICATION

This dissertation is dedicated to the following: My late mother Jane Oyugi Agola (Miyo ber), sisters; Lilian Anyango (Otule), Ruth Apiyo (Nyar gi Obondi) and Caroline Atieno (Ogwela). Further dedication is due to my father Charles Agola Omolo, all my surviving siblings and to every man and woman who has given all to humanity.

ACKNOWLEDGEMENT

This journey has been long and would not have come this far without the support of many. I wish to extend my sincere thanks to Prof. Angela Wandinger-Ness, my advisor and dissertation chair, for her assistance and patience through the years I had the privilege of working under her supervision. Her guidance and mentorship come with a motherly touch and will remain with me as I continue my career. I would also like to thank my dissertation committee members; Prof. Laurie G. Hudson, Prof. Eric R. Prossnitz, Prof. Tione Buranda and Prof. Larry A. Sklar for their valuable advice and recommendations pertaining to this study.

Message of thanks also goes to colleagues in the Wandinger-Ness research group. It was a cherished moment to work with each and every member of the group. I also extend special thanks to the UNM Center for Molecular Discovery (UNMCMD) and UNM Microscopy teams, Kansas University Chemistry Center and the entire UNM fraternity. Their collective assistance is highly acknowledged. Dr. Zurab Surviladze formerly of UNMCMD, is also specially acknowledged for carrying out the initial small molecule screening which paved the way for further work. At a family level, I am indebted to my late mother, Jane Oyugi Agola who even though never went beyond grade school, **would**

always stress the importance of education. My father Charles Agola and all my siblings deserve equal praise. UNM, National Science Foundation (NSF), National Institute of Health (NIH) also receive my special thanks for both direct and indirect funding which supported this work. Finally, all glory to God of Abraham, Isaac and Jacob.

Assessment of Functional Characteristics of Small GTPases Using Small Molecules

By

Jacob Ongudi Agola

ABSTRACT OF DISSERTATION

Submitted in Partial Fulfillment of the

Requirements for the Degree of

Doctor of Philosophy

Biomedical Sciences

The University of New Mexico

Albuquerque, New Mexico

December, 2011

Assessment of Functional Characteristics of Small GTPases Using Small Molecules

By

Jacob Ongudi Agola

B.S., Chemistry, University of Nairobi, 1997

M.S., Chemistry, University of Wyoming, 2006

Ph.D., Biomedical Sciences, University of New Mexico, 2011

ABSTRACT

Rab and Rho subfamilies of GTPases are functionally linked to intracellular trafficking and organization of the cytoskeleton respectively. Despite their roles, use of small molecule inhibitors or activators to map the functionality of these GTPases remains largely underexplored due to lack of suitable compounds. In this dissertation, we report on the functional characterization of Rab7 and Rac1 GTPases using small molecules. 2-(benzoylcarbamothioylamino)-5,5-dimethyl-4,7- dihydrothieno[2,3-c]pyran-3-carboxylic acid (PubChem #: CID1067700) has been used to characterize Rab7. Using bead based flow cytometry, CID1067700 was found to have significant inhibitory potency on Rab7 nucleotide binding with a respective inhibitory efficacy of 80% for BODIPY-GTP and

60% for BODIPY-GDP binding. Rac1 has been functionally characterized by non-steroidal anti-inflammatory drug (NSAID), R-Naproxen in the context of ovarian cancer. R-Naproxen isoform functionally inhibited Rac1 in the cell lines assayed relative to S-Naproxen and structurally similar 6-methoxy-2-naphthylacetic Acid (6-MNA). Inhibition is based on interference with membrane distribution of Rac1 rather than overall protein levels. Taken together, this study has identified the first competitive GTPase inhibitor (CID1067700) and also demonstrated the potential utility of the compound for dissecting GTPase enzymology. The study has also shown that R-Naproxen blocks activation of Rac1 small GTPase in ovarian cancer cells with implications for the inhibition of ovarian cancer cell proliferation, migration, and invasion.

Key Words: Rab, Rho, Rac, Cdc42 and Ras GTPases; drug discovery; fluorescent GTP and GDP; enzyme kinetics; GEF; flow cytometry, ovarian cancer, competitive and allosteric inhibitors.

TABLE OF CONTENTS

LIST OF FIGURES

LIST OF TABLES

LIST OF KEY ABBREVIATIONS

6-MNA: 6-Methoxy-2-Napthalene Acetic acid

BSA: Bovine Serum Albumin

BODIPY-GTP: BODIPY FL GTP 2'-(or 3')-O-[N-(2-aminoethyl)urethane

BODIPY-GTP: BODIPY FL GDP 2'-(or-3')-O-[N-(2-aminoethyl)urethane

DMSO: Dimethyl sulfoxide

EDTA: Ethylenediaminetetraacetic acid

GTP: Guanosine Triphosphate

GDP: Guanosine Diphosphate

GST: Glutathione-S-Transferase

GEF: Guanine Nucleotide Exchange Factor

GAP: GTPase Activating Protein

GDI:GDP dissociation Inhibitor

LCMS: Liquid Chromatography Mass Spectrometry

NMR: Nuclear Magnetic Resonance

NSAID: Non-Steroidal Anti-Inflammatory Drug

PAK1: p21-Activated Kinase

PIP2: Phosphatidylinositol 4,5-bisphosphate

CHAPTER ONE

INTRODUCTION

Overall introduction: Ras superfamily of GTPases

Small GTPases (Ras superfamily) are intracellular, molecular switches that activate downstream signaling molecules in response to extracellular and intracellular cues. There are five families: Ras, Rho, Arf/Sar1, Rab, and Ran. Biochemical studies have revealed many commonalities between small GTPases with respect to synthesis, post-translational modification, activation, inactivation, and transmission of signals to downstream effector molecules. Characteristically, small GTPases switch between inactive [guanosine diphosphate (GDP) bound] and active [guanosine triphosphate (GTP) bound] conformational states (Fig. 1) (1-4). The conformational switch involves specific regulatory proteins. While guanine nucleotide exchange factors (GEFs) catalyze release of bound GDP to allow for GTP binding by small GTPases (5), GTPase activating proteins (GAPs) on the other hand, facilitate hydrolysis of GTP on the membrane bound small GTPase proteins.

Conversion between GTP- and GDP-bound states is also associated with transitions between membrane and cytosolic compartments, respectively (Fig. 1). Translocation of

the small GTPase to the cytosolic compartment is facilitated by guanine dissociation inhibitors (GDI-1 or GDI-2), while membrane association is facilitated by Rab escort protein (REP) immediately after synthesis and prenylation or by GDI during membrane recycling (Fig. 1) (6). Upon activation, the GTP-bound, membrane associated small GTPases bind to and transmit signals to multiple effector molecules. Besides regulating vital cellular processes such as cell signaling, members of Ras superfamily of GTPases via interdigitated functions of Ras, Rho, Arf/Sar1, Rab, and Ran individual subfamily members, regulate intracellular trafficking, nuclear translocation and cytoskeletal rearrangements that occur in response to extracellular signals and cellular needs. Together the GTPase regulated cascades enable metabolic homeostasis, cell migration, cell growth and division, cell differentiation and polarization.

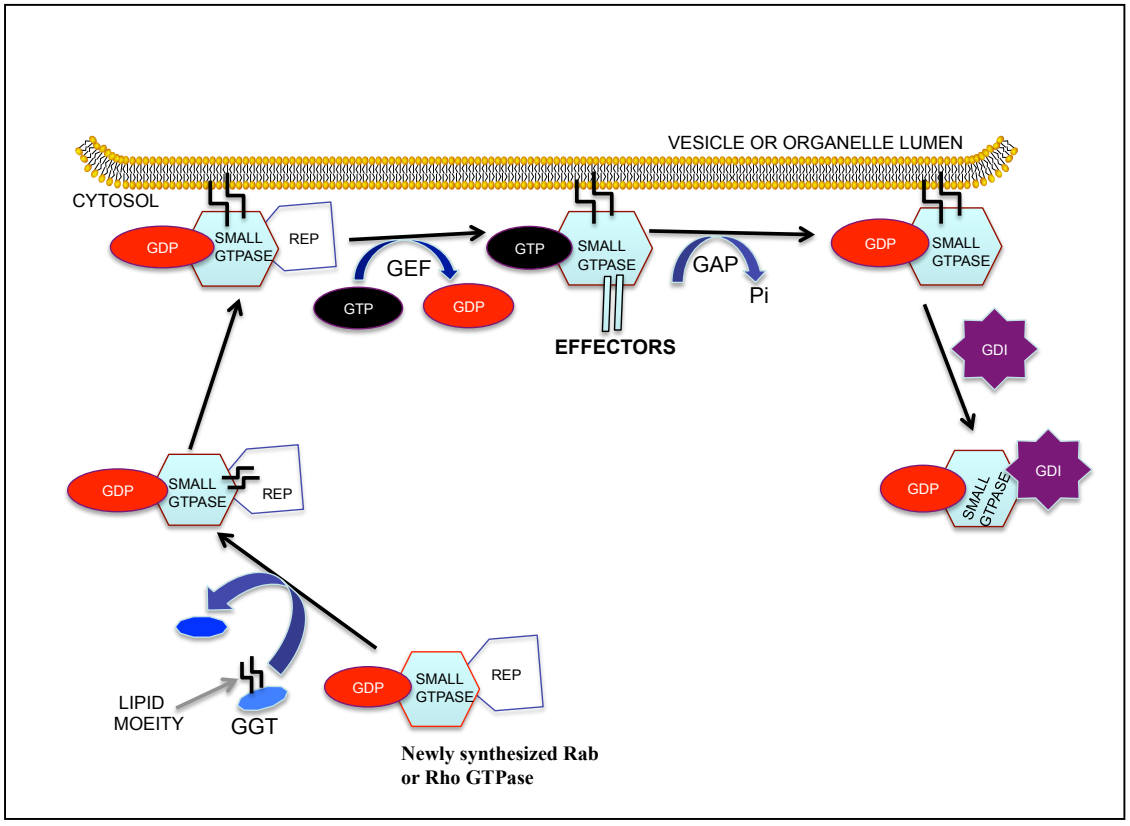

Figure 1. Principal processes governing the regulation of small GTPases. Newly synthesized small GTPases are modified on C-terminal cysteine residues by lipid moieties (prenyl or farnesyl chains) to ensure membrane recruitment via REP. GEFs and GAPs act as small GTPase signal activators and attenuators, respectively. GDI serves to regulate membrane-cytosol cycling.

The involvement of small GTPases in diverse human diseases presents the small GTPases as novel targets for therapeutic intervention hitherto not extensively explored. Diverse points of small molecule modulation of small GTPase function are possible ranging from prenylation inhibition to protein-protein interaction regulation (Fig. 1). A precedent already exists with respect to the use of small molecule inhibitors to prevent small GTPase membrane recruitment, through inhibition of protein prenylation or inhibition of regulatory protein interactions (7, 8). Because of the broad cellular importance of lipid modifications for protein function, the former approach has not however yielded the selectivity necessary for many applications, though the identification of more specific prenylation inhibitors remains under active investigation (9-12).

The inhibition of regulatory protein interactions on the other hand holds promise for being more specific, with the best-characterized example provided by brefeldin A mediated inhibition of Arf GEF activity (13). Within the Rho-family GEFs, a few successful attempts have been made to identify inhibitors through screening and rationale drug design (13-16). It is important to point out that these successes have not been replicated in any of the members of the Rab family of GTPases whether in terms of nucleotide binding inhibitors or modulators of protein-protein interactions, in spite of their cellular importance in cancer and genetic diseases (17, 18).

Different strategies can be applied to realize the therapeutic potential of small GTPases. One strategy is to target the central regulatory properties of small GTPases based on the switch between GDP and GTP bound states, by finding a small molecule that can modulate nucleotide binding by the small GTPase. A second strategy is to identify small molecules that inhibit protein-protein interactions required for GTPase function. The use of a small molecules is also important to characterize protein function and has advantages to traditional approaches that rely on dominant negative mutants. These include, but are not limited to; fast and often-reversible inhibition of protein function, informative dose–response data, providing room for studying protein of interest in a multimeric complex without the latter falling apart and availability of small molecule compounds. All these advantages collectively can lead to a novel endpoint and that is, providing new insights into mechanistic details of GTPase functions in cellular processes. In this study, we have sought to assay how small GTPases can be functionally modulated by small molecules in vitro as well as in a cellular context.

Hypothesis of the dissertation study

Small GTPases are functional targets of small molecules that act as competitive or allosteric inhibitors.

Aims of the study

The central goal of the study was to identify and characterize small molecule inhibitors of Ras-related GTPases. The stated hypothesis is addressed through two specific aims. Aim 1 utilizes an in vitro, flow cytometry based assay to distinguish the mechanism of small molecule action on the Rab7 GTPase. Aim 2 utilizes in vitro and cell based assays to characterize functional inhibition of the Rac1 GTPase.

Aim1: Mechanism of small molecule Rab7 GTPase inhibition.

The first aim of the study was designed to characterize the mechanism of inhibition of Rab7 by a sulphur based small molecule; 2-(benzoylcarbamothioylamino)-5,5-dimethyl-4,7- dihydrothieno[2,3-c]pyran-3-carboxylic acid (CID 1067700; PubChem CID1067700). CID1067700 was identified at the University of New Mexico Center for Molecular Discovery (UNMCMD) by screening the NIH Roadmap library of over 300,000 compounds (Pubchem AID 1333, 1334, 1340). To address the first aim, a bead based flow cytometry approach was used (Fig. 2), where gluthione-S-transferase (GST) tagged Rab7 was mobilized on a glutathione bead and then the effect of CID1067700 assayed in terms of loss of BODIPY-GTP or -GDP binding by Rab7. The approach enables distinction of allosteric or competitive inhibition of nucleotide binding (Fig. 2).

Using the bead based approach; the effect of CID1067700 on Rab7 was assayed in dose dependent binding assays and kinetic measurements of nucleotide binding and dissociation. Structure activity relationships of several chemical analogs of CID1067700 were also tested to establish essential features for small molecule inhibition.

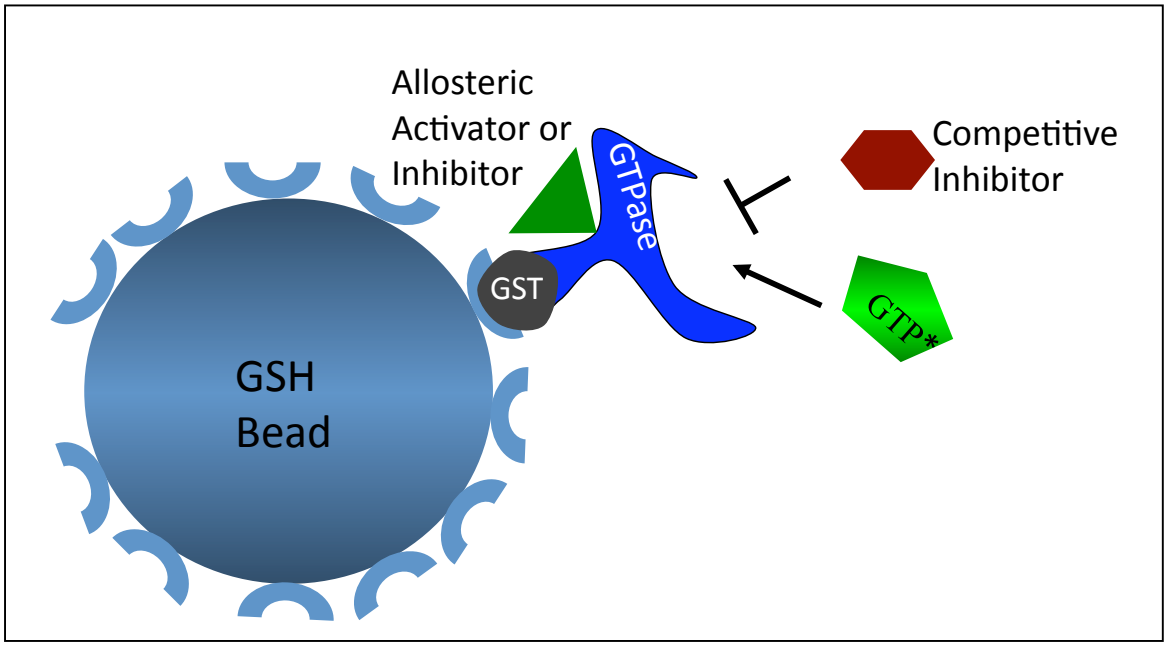

Figure 2: Design of glutathione bead based high throughput screening (HTS) to identify small GTPase activators and inhibitors. GST-tagged small GTPase is immobilized on a gluthathione bead of definite mean diameter (13 μm). The effect of the small molecule on the fluorescent nucleotide binding by the GTPase is then assayed using flow cytometry. Competitive inhibitor binds the same site as the nucleotide while allosteric modulator (activator or inhibitor) binds the indicated site (typically GTPase switch region) outside the nucleotide binding pocket. The read out of the assay is mean channel fluorescence.

Aim 2: In vitro and cell based assays to study functional inhibition of Rac1 GTPase

The second aim was centered on the small molecule inhibition of the Rac1 GTPase. Functional modulation of Rac1 small GTPase by the non-steroidal anti-inflammatory drug (NSAID), R-Naproxen was assessed in the context of ovarian cancer cells. R-Naproxen was identified the University of New Mexico Center for Molecular Discovery (UNMCMD) by screening a Prestwick chemical library of off-patent molecules. The effects of R-Naproxen on Rac1 activation status, Tiam1 GEF interaction, membrane distribution and overall Rac1 protein levels were measured.

Biological and chemical connection between Rab7 and Rac1

In terms of function, the Rab5, Rab7 and Rac1 GTPases are intimately linked to enable coordination between molecular trafficking and actin cytoskeletal remodeling, respectively (Fig. 3). It has been shown that Rac1 interaction with endosomes is dependent on Rab5 GTPase and that the Rab5-Rac1 circuitry is significant in the role of Rac1 in modulating cell motility (19, 20). This is supported by evidence showing that, ectopic expression of Rab5 in HeLa cells increases early endosomal accumulation of active Rac1 and Tiam1 GEF as well as induction both lamellipodia and circular dorsal ruffles (19). Since Rab5-Rab7 conversion is an important regulatory process in cargo

trafficking as will be explained later, one can speculate that it may also be involved in Rab5 mediated Rac1 trafficking. Also, Armus which is a Rac1 effector (21, 22), is reported to inactivate Rab7 by facilitating nucleotide hydrolysis again suggesting a cross talk between Rab7 and Rac1 in trafficking and regulation of actin assembly. The composite data emphasize that the cellular role of Rac1 cannot be divorced from the endocytic trafficking pathway. We can also emphasize a common denominator with respect to chemical connection between Rab7 and Rac1. The current study is about CID1067700 and R-Naproxen small molecules capable of functionally impacting Rab7 and Rac1 respectively. CID1067700 which competitively inhibits nucleotide binding by Rab7, may also inhibit Rac1 by binding the nucleotide binding site since among the Ras family of GTPases, the principal amino acid residues of the nucleotide binding site are evolutionarily conserved. The potency of inhibition may however vary due to differences in the orientation of the nucleotide pocket between the two GTPases. R-Naproxen in this study displays characteristics typical of allosteric inhibitor. Thus, its ability to inhibit Rac1 may not be replicated in Rab7 due to differences in amino acid residues on its binding site between the two GTPases and also the ensuing potential differences in the protein conformation which may be caused by its binding. Thus, within the broader context of biological and chemical connection, both Rab7 and Rac1 are functionally

interdependent and may be modulated in a similar way by a small molecule that displays competitive characteristics.

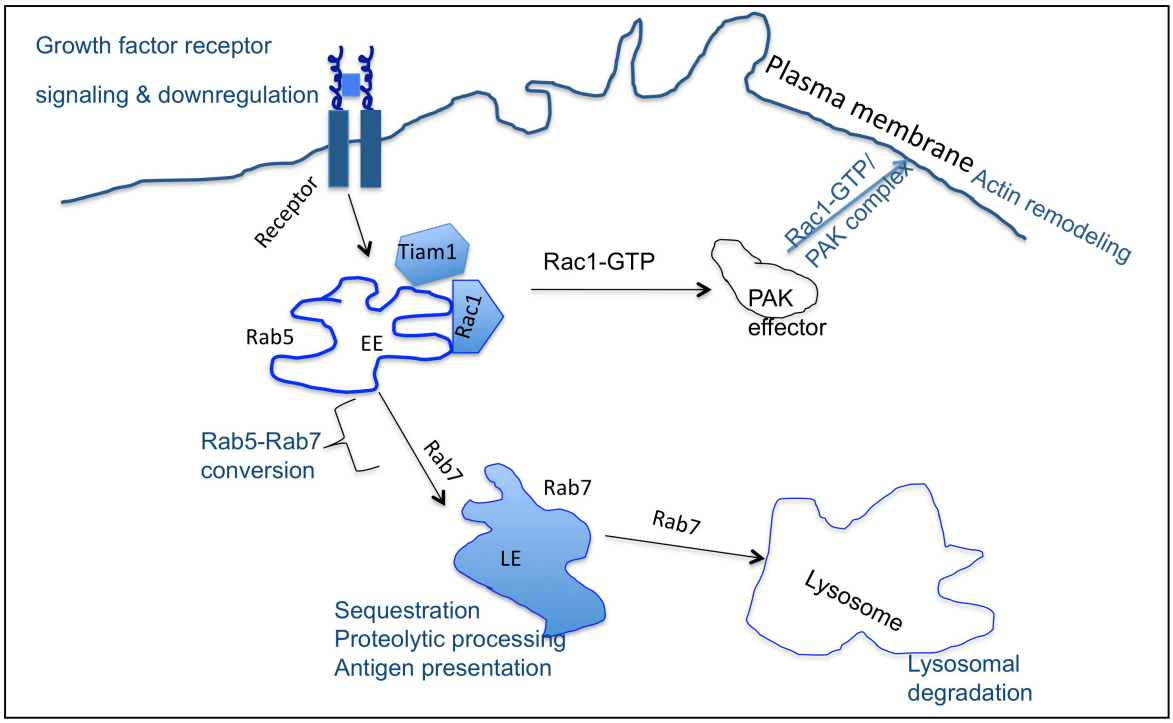

Figure 3: Roles of Rab7 and Rac1 small GTPases in molecular trafficking and actin remodeling. GDP bound Rac1 is localized at early endosomal membranes where it interacts with Tiam1 GEF, converting the protein to the active GTP bound state. Active Rac1 interacts with PAK1 effector at the plasma membrane and induces actin remodeling. Rab7 is transiently localized to early endosomes where it facilitates Rab5-Rab7 conversion and transport of cargo to late endosomes. Rab7 is important in the regulation of antigen processing, growth factor sequestration and lysosomal degradation, among other functions.

CHAPTER TWO

CHARACTERIZATION OF RAB7 SMALL GTPASE WITH CID1067700

Abstract

Rab7 plays a significant role in late endocytic events of mammalian cells that serve to regulate growth factor downregulation, pathogen degradation, autophagy, among other events central to normal cell physiology. Here we report on the small chemical molecule 2-(benzoylcarbamothioylamino)-5,5-dimethyl-4,7- dihydrothieno[2,3-c]pyran-3-carboxylic acid (CID 1067700; PubChem CID1067700) as an inhibitor of nucleotide binding by Rab7 and possibly other Ras-related GTPases. The mechanism of action of this pan-GTPase inhibitor has been characterized in the context of the Rab7 GTPase as there are no known inhibitors of Rab GTPases. Bead-based flow cytometry was used to establish that CID1067700 had significant inhibitory potency on Rab7 nucleotide binding with a respective inhibitory efficacy of 80% for BODIPY-GTP and 60% for BODIPY-GDP binding. The compound behaves like a competitive inhibitor of Rab7 nucleotide binding based on both equilibrium binding and kinetic assays. Molecular docking analyses are compatible with CID1067700 fitting into the nucleotide binding pocket of the GTP-conformer of Rab7. Structural features pertinent to CID1067700 inhibitory activity have been identified through an initial structure activity analyses. These studies

identified a molecular scaffold that may serve in the generation of more selective probes for Rab7 and other GTPases. Using effector protein interaction, we have also shown that when CID1067700 is bound to the nucleotide binding site, Rab7 does not adapt conformational state analogous to GTP bound (active) state. Taken together, this study has identified the first competitive GTPase inhibitor and demonstrated the potential utility of the compound for dissecting the enzymology of the Rab7 GTPase as well as serving as a model for other small molecular weight GTPase inhibitors.

Introduction

The founding Rab GTPase family members were identified in secretion deficient yeast mutants and in mammalian brain, thereby revealing their essential roles in the regulation of membrane trafficking (23-25). The human genome encodes more than 70 Rab GTPases and Rab-like proteins (26-28). Still only a fraction of these Rab GTPases have been studied in significant detail. Currently there are ~25 Rab GTPases with characterized functions in endoctyosis and related processes (**Appendix A**) and (29). Rab7 is one of the most studied endocytic Rab GTPases due to its pivotal roles in shunting molecules for recycling through the Golgi, back to the plasma membrane or to degradation (Fig. 4).

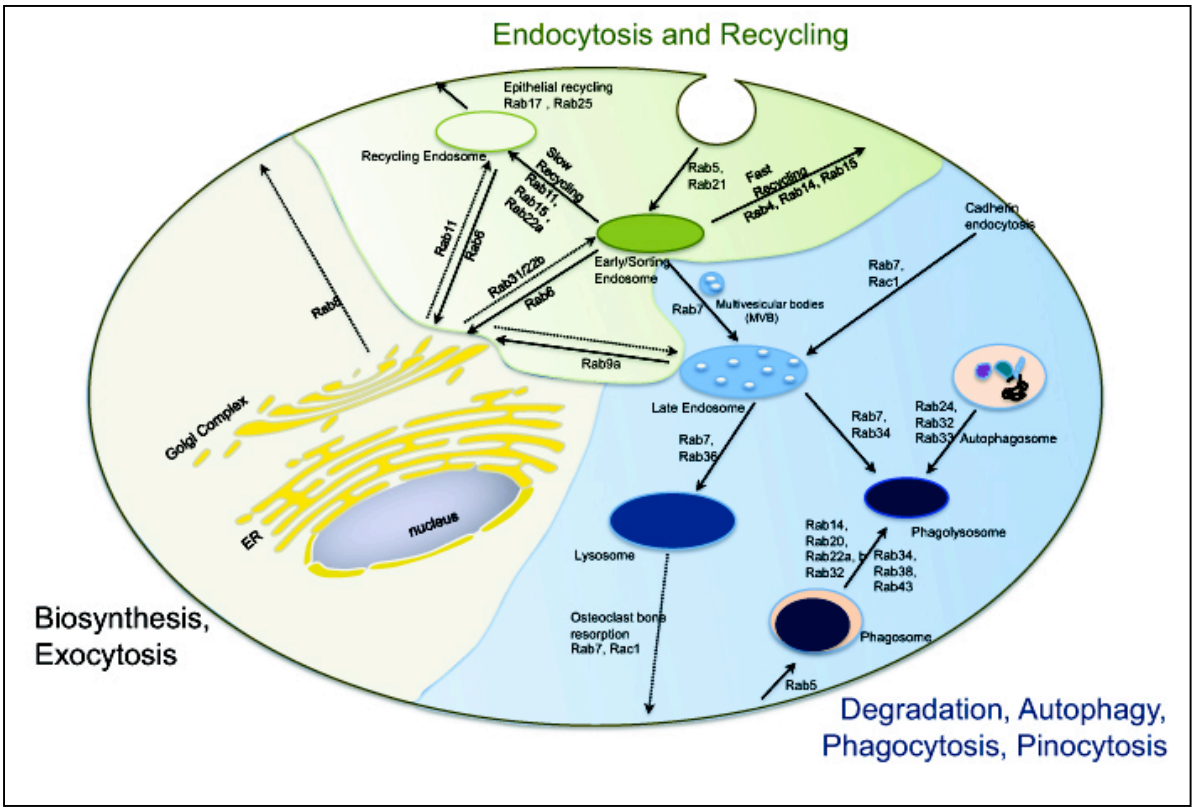

Figure 4: **Intracellular trafficking pathways associated with Rab7.** Rab7 regulates cargo trafficking to the lysosomes for degradation via late endosomes, cargo recycling through the Golgi back to the plasma membrane, autophagy, phagolysosome fusion and osteoclast-mediated bone resorption.

Functional role of Rab7

Rab7 plays a significant role in endocytic trafficking and other degradative pathways such as autophagy and phagocytosis (27, 29, 30). Rab7 regulated pathways are important for normal cell physiology as illustrated by the following examples. Firstly, Rab7 and its effectors are central to the regulation of growth factor signaling and receptor down regulation through lysosomal degradation (31-33). Increased receptor downregulation may be pertinent to reducing hyperactive signaling in cancers where expression of epidermal growth factor receptor is elevated and/or constitutively active, where Rab7 is also overexpressed (34, 35). Upregulation of active Rab7 may lead to modest increases in growth factor receptor degradation.

Secondly, Rab7 participates in phagocytic and autophagic processes. Rab7 facilitates the fusion of autophagosomes with lysosomes that is important in nutrient regulation, clearance of cytoplasmic protein aggregates and degradation of organelles (36-42). Imbalances in autophagy are associated with immune dysregulation, cancer, and neurodegeneration (43, 44). Extracellular pathogens and dead cells engulfed into phagosomes are known to be cleared through a maturation phase requiring phagosome fusion with endosomes (45, 46). The maturation process is characterized by formation of

a late phagosome and a subsequent phagolysosome, thus degradation of pathogens and cellular debris are dependent on Rab7 (47, 48).

Thirdly, Rab7 is important for the biogenesis of secretory lysosomes such as melanosomes and lytic granules secreted by immune cells that are important in normal pigmentation and immune cell function. Rab7 has been shown to associate with early and intermediate stage melanosomes during melanosomal transport (49-51). This was further illustrated in human amelanotic melanoma cells (SK-mel-24) where expression of dominant negative Rab7 impaired vesicular transport of tyrosinase and TRP-1 proteins from the trans-Golgi network to maturing melanosomes (52), and also in MMAc melanoma cells, where the GTP-bound (active) form of Rab7 promoted melanogenesis by regulating gp100 maturation (51). Secretory lysosome exocytosis also accompanies bone remodeling events during which formation of a ruffled border facilitated by Rac1 is accompanied by transport and fusion of acidic intracellular vesicles with the plasma membrane in a Rab7 regulated process (53-55). Improper transport of melanosomal and lytic substances can potentially be cytotoxic to cells coupled with defects in pigmentation, poor immune system regulation and bone defects. This therefore emphasizes the important role Rab7 is playing in secretory lysosome biogenesis and function.

Fourthly, Rab7 is important for the regulation of lipid homeostasis and lipid signaling in the control of vesicle trafficking. Proper sphingolipid (SLs) transport and metabolism is important for membrane structure, cell signaling, regulation of cell growth and the cell cycle and when aberrant leads to sphingolipid storage disorders that cause mental retardation and premature death (56-58). Nieman-Pick type C (NPC) disease is characterized the accumulation of sphingolipids in late endosomes and lysosomes in tissues such as liver, spleen and brain (59, 60). The defects in cholesterol and sphingolipid storage are dramatically improved by the overexpression of Rab7, which enhances intracellular trafficking of cholesterol and sphingolipids (61). Rab7 together with the lipid kinase hVps34/hVps15 (62) and the myotubularin lipid phosphatases (MTM1 and MTMR2) serves as a molecular switch controlling the sequential synthesis and degradation of endosomal PI(3)P important for the spatial and temporal regulation of vesicle budding and fusion (63, 64). Lipid homeostasis also involves the function of ORP1L which is a Rab7 effector. In Mel JuSo cells cells, ORPIL was shown to act as a sensor of cholesterol accumulation in late endosomes in addition to transmitting information to the Rab7–RILP–p150 glued complex through the formation of endoplasmic reticulum– late endosome membrane contact sites (65). Normal cellular lipid levels dictate processes ranging from vesicular trafficking, signaling to receptor

degradation among others, defects in which may result in human disease. These confirm the importance of Rab7 in lipid synthesis and trafficking.

Fifthly, Rab7 is important in regulating cell-cell adhesion. Cell differentiation is characterized by epithelial cells undergoing epithelial–mesenchymal transition (66). This change is marked by down-regulation and intracellular sequestration of E-cadherin and other cell-cell junction proteins that are later trafficked via the endocytic pathway to the lysosomes (66). Enhanced transport of ubiquitinated E-cadherin to the lysosomes occurs through hepatocyte growth factor-regulated tyrosine kinase substrate (Hrs) and v-Src-induced activation of Rab7 mediated transport, thereby contributing to the regulation of cell-cell adhesion (67).

The enumerated Rab7 functions in endocytic membrane transport occur in different cellular contexts yet overall serve to regulate key cellular functions that dictate cell viability and differentiation. All Rab7 functions depend on coordinated spatial and temporal interactions between Rab7 and other regulatory partner molecules as discussed further in the following section.

Rab7 and its accessory effector molecules

Membrane trafficking requires a series of discrete temporally and spatially regulated steps that include: 1) cargo selection and clustering, 2) vesicle coat protein recruitment, vesicle budding through the action of membrane curvature inducing proteins, 3) cytoskeleton mediated translocation, and 4) docking and fusion with the target membrane. Rab GTPases are known to function in all aspects of transport through the sequential interaction with different effectors. Rab7 interacts with multiple effector molecules to regulate endocytic transport, including proteins regulating phosphoinositide signaling, motor proteins controlling bidirectional cytoskeletal transport, proteasome subunits controlling degradation, among others (62, 63, 68-71) (**Appendix B**).

One of the best characterized Rab7 effector proteins is the Rab7 interacting lysosomal protein (RILP) which is important for cargo sorting and retrograde cytoskeletal translocation. Upon RILP recruitment to late endosomes and lysosomes binds and prolongs the Rab7 activation (GTP bound state) (68, 72-76). A complex of Rab7 and RILP induces recruitment of dynein-dynactin motor complexes to Rab7-containing late endosomes and lysosomes (69, 77, 78). RILP in turn mediates the membrane recruitment of VPS22 and VPS36 of the ESCRT-II machinery, which is responsible for

multivesicular body formation through intraluminal vesicle invagination and important in exosome formation and growth factor receptor sorting (31, 79). Depletion of RILP leads to elevated levels of four late endosomal molecules (lysobisphosphatidic acid, Lamp1, CD63 and cation-independent mannose-6-phosphate receptors) besides inhibiting ligand-mediated degradation of epidermal growth factor receptors [EGFRs] (31). Thus, Rab7 together with RILP controls late endosomal sorting of lipids and proteins associated with cargo delivery. RILP has been shown to function in concert with ORP1L effector whereby, a complex involving RILP, Rab7, p150Glued and ORP1L activates microtubule (dynein) motors and initiates translocation of late endosomes on microtubules (80) to facilitate vesicular transport to lysosomes.

The ubiquitin–proteasome pathway is a well-known mechanism for the targeted degradation of cytosolic proteins (81, 82). The proteasome mediated by the α-subunit XAPC7 (also known as PSMA7, RC6-1, and HSPC) has been shown to interact specifically with Rab7 that aids in its recruitment to the membranes of multivesicular late endosomes (71, 82). The XAPC7 interaction facilitates the connection between cargo sorting and degradative events.

Rabring7 (Rab7-interacting ring finger protein) originally isolated using a CytoTrap system (83), is also a downstream effector protein of Rab7 involved in EGFR trafficking for lysosomal degradation through its E3 ligase activity. Overexpression of Rabring7 was shown to alter EGFR degradation besides inducing perinuclear aggregation of lysosomes (84, 85). High cellular levels of Rabring7 are also marked by enhanced accumulation of the acidotropic probe LysoTracker (83), a phenomenon which implicates Rabring7 protein in lysosome biogenesis and receptor degradation. Internalization of polyubiquitylated TrkA involves its interaction with Unc51.1 and p62, the atypical protein kinase C interacting protein and this degradative process is also thought to involve the Rabring7 effector.

Rab7 interacts with hVps34 kinase, its adaptor protein p150 and phosphatidylinositol 3-kinase (18, 27, 63). The complex ensures regulated phosphatidylinositol 3-phosphate synthesis on early and late endosomes (62). Phosphatidylinositol 3-phosphate enriched membrane domains facilitate membrane fusion through the recruitment of FYVE domain containing proteins, and intraluminal vesicle sequestration of growth factors (86). Myotubularin phosphatase mediated degradation of phosphatidylinositol 3-phosphate terminates the signal and is accompanied by a requisite dissociation of the Rab7/Vps34 complex (64).

As illustrated by the given examples, coordinate interactions between Rab7 and multiple effector proteins cut across key processes that are crucial to cell function. Misregulation leads to various disease states such as cancer, neurodegenerative disease and cell infection by pathogens. Collectively, the data implicate Rab7 as an important small molecule target.

Regulation of Rab7

The principal processes pertinent to regulation of Rab7 include prenylation and membrane insertion, nucleotide binding and hydrolysis, and effector protein interaction (Fig. 1) (28, 87). The function of Rab GTPases are primarily dictated by both proper membrane association and a nucleotide exchange mechanism that turns the protein on through GTP binding and off through GTP hydrolysis based on nucleotide dependent conformational changes. In mammalian cells, Rab7 can localize to late endosomes, lysosomes, cytosol, phagosomes, melanosomes and exosomes (27, 30, 37, 39, 52, 88, 89). Location of Rab7 at these sites depends on whether the GTPase is in the 'active' or 'inactive' state. After translation, cytosolic GDP bound Rab7 undergoes post-translational geranylgeranylation which enables it to associate reversibly with intracellular membranes and thus is critical to its biological function (90-97).

The process of Rab7 geranylgeranylation proceeds in a sequential manner. Newly synthesized Rab7 protein first associates with Rab escort protein (REP-1) via its alpha-subunit (98). Rab7 then interacts with the Rab binding platform of REP-1 via an extended interface involving the Switch 1 and 2 regions of Rab7 with the C terminus of the REP-1 molecule functioning as a mobile lid covering a conserved hydrophobic patch of REP-1 (99). The integrity of this interaction is significant since mutations in the REP-1 gene in humans have been associated with X-chromosome-linked defect, choroideremia, a progressive disease that inevitably culminates in complete blindness (99-102).

Once bound to Rab7, REP-1 presents the GTPase to the Rab geranylgeranyl transferase (RabGGTase) enzyme loaded with the isoprenoid donor geranylgeranyl pyrophosphate, GGpp (103). The enzyme then catalyzes covalent modification of the Rab protein at the C-terminal cysteine motifs with two geranylgeranyl (GG) moieties (98, 104). The highly variable C-terminal domain of Rab7 contains two cysteine residues that are subject to prenylation (97, 105). The addition of lipid moieties on Rab7 is similar for all Rab proteins and is crucial for membrane recruitment (90-94).

Rab7 delivery to the target membrane involves release of GDI. This is accomplished by a membrane associated protein factor called GDI-displacement factor (GDF) (106).

GDFs are present either in the early secretory pathway or within the endocytic pathway (94). The current model has it that once delivered to the membrane and GDI extracted by GDF, Rab7 diffuses within the plane of the membrane and is then stabilized by relevant effector binding (107). This model still needs to be refined since there are studies suggesting that the necessity of GDF to extract GDI may not be thermodynamically tenable (96). Delivered GDP bound Rab7 can then undergo nucleotide exchange by losing its GDP for GTP in order to perform downstream functions. Following GEF catalyzed activation, Rab7 GTPase interacts in a temporally and spatially regulated manner with specific effector molecules (**Appendix B**). These include sorting adaptors, tethering factors, kinases, phosphatases and motor proteins that ensure cargo sorting, vesicle transport and fusion (2). Unlike Rab5 with a known GEF as Rabex5, the Rab7 GEF is still under investigation. Ccz1-Mon1 acts as the yeast Ypt7 GEF(108), an orthologue of mammalian Rab7. Termination of Rab7 GTPase activation is achieved by intrinsic GTPase hydrolysis and GAP stimulated catalysis (109). Currently, some TBC domain containing proteins such as TBC1D5 and TBC1D15 have been identified as Rab7 GAP (21, 109, 110).

Another regulatory mechanism with significant control on Rab7 activity is Rab5-Rab7 conversion (Fig. 3). Conversion is thought to confer directionality to the membrane

trafficking events leading to membrane maturation (111-116). It involves HOPS complex mediated recruitment of Rab7 into Rab5 positive organelles (112, 113). There are suggestions that hVps39 may also be involved in this process as part of the complex (108, 114, 115).

Association of the Rab7 GTPase with human disease

Rab7 has been associated with different types of diseases ranging from those due to mutations in the Rab7 encoding gene to others that may result from manipulation of the transport role of Rab7 by pathogens **(117)**. Diseases associated with Rab7 arising from genetic mutations tend to be primarily peripheral neuropathies. The latter can be caused by mutations in multiple genes required for axon viability or Schwann cell dependent myelination (118, 119). Charcot-Marie-Tooth type 2B (CMT2B) disease (also known as hereditary sensory neuropathy 1C) causes axonal degeneration and has been linked to four missense mutations in Rab7 gene (29, 33, 120-122). The mutations target highly conserved residues that reside on the surface of Rab7 and affect nucleotide exchange (33, 123-125). In neuronal N2A and PC12 cell lines, expression of the mutant proteins inhibits neurite outgrowth (126). Such changes in neuronal differentiation are likely due to prolonged phosphorylation of the TrkA receptor and altered Erk nuclear signaling

caused by the expression of the mutant Rab7 proteins (33). Patients with CMT2B disease usually manifest severe sensory loss, distal muscle weakness and a high frequency of foot ulcers and infections with frequent digit amputations (127, 128). Because CMT2B is an autosomal dominant disease, it is predictable that selective inhibition of the mutant protein or enhancement of wild-type Rab7 activity might be beneficial therapeutic interventions.

With respect to the usual Rab7 role, CMT2B mutant proteins may potentially alter Rab5-Rab7 conversion, Rab7-effector protein interactions and therefore impact Rab7-regulated trafficking to and from the cell body that are required for maintenance of axon viability and normal impulse transmission. For example the CORVET and HOPS protein complexes identified in yeast and conserved in mammalian systems are thought to enable transition of cargo from early to late endosomes and lysosomes (129). GTP-bound Rab7 recruits the dynein/dynactin motor complex through the Rab interacting lysosomal protein (RILP) and in conjunction with Rabring7 promotes growth factor degradation (68, 83, 85).

Taken together, the enumerated roles of Rab7 in addition to its regulation and effector protein interactions coupled with its overexpression in cancer and mutant Rab7 associated with peripheral neuropathies, make Rab7 an important candidate for small molecule modulation. Such molecules could have utility both for dissecting the mechanistic details of processes governed by Rab7, as well as for the future development of targeted therapies (18, 130). This by extension may provide a platform for small molecule modulation of other members of the Rab family, a growing number of which are implicated in diseases ranging from pigmentation and bleeding disorders to bone diseases and thereby address questions that remain regarding ubiquitous and cell type specific functions of Rab GTPases and how these may contribute to disease pathogenesis. More so, this approach may provide detailed understanding of how Rab GTPases coordinate with regulatory proteins, downstream effector proteins and other GTPases to effect cargo selection, vesicle formation, translocation through cytoskeletal networks, and targeted vesicle fusion (131, 132). Thus, we sought to investigate how Rab7 function may be modulated by a small molecule both in the context of understanding normal Rab7 function as well as in terms of characterizing Rab7 as a potential therapeutic target. This is a new area that has not been investigated despite the important cellular functions and disease pathologies associated with Rab7. For this purpose, I used a sulfur based small

chemical molecule herein called; 2-(benzoylcarbamothioylamino)-5,5-dimethyl-4,7-dihydrothieno[2,3-c]pyran-3-carboxylic acid (Pubchem #: CID1067700).

Materials and Methods

Reagents

Reagents used in this study were obtained from Sigma unless otherwise indicated. Sephadex G-25, glutathione (GSH) Sepharose 4B, and Superdex peptide beads (13 μm with an exclusion limit of 7 kDa) were from Amersham Biosciences. BODIPY (4,4-difluoro-4-bora-3a,4a-diaza-s-indacene or dipyrromethene boron difluoride) nucleotide analogues (BODIPY FL GTP 2'-(or 3')-O-[N-(2-aminoethyl)urethane] G-35778 and BODIPY FL GDP 2'-(or-3')-O-[N-(2-aminoethyl)urethane], G-22360) were from Invitrogen Molecular Probes (Carlsbad, CA, USA). Concentrations of BODIPY nucleotides were based on absorbance measurements and an extinction coefficient value of 80,000 M^{-1} cm^{-1}. 2-(benzoylcarbamothioylamino)-5,5-dimethyl-4,7-dihydrothieno[2,3-c]pyran-3-carboxylic acid with compound identification number (CID1067700) was from ChemDiv.

Expression and purification of GST-Rab7

GST–Rab7 protein was expressed in E. coli BL21 (DE3). Cultures were grown at 37°C to a bacterial density of 0.5-0.7 absorbance units at 595 nm and protein induced by transfer to room temperature and addition of 0.2 mM isopropyl-beta-D-1-thiogalactopyranoside (IPTG) for 16-18 h to maximize yield of properly folded active fusion protein. Purification of GST-Rab7 was performed according to standard procedures and as previously described (133).

Synthesis of glutathione beads for flow cytometry assay

High GSH density beads used for flow cytometry were synthesized by loading Superdex peptide beads with GSH as previously reported (133, 134).

Immobilization of Rab7 on GSH beads for flow cytometry

All nucleotide binding to Rab7 and measurements were performed in the HPS buffer (30 mM Hepes, pH 7.5, 20 mM NaCl and 100 mM KCl) containing 1 mM EDTA. A BectonDickinson FACScan flow cytometer with a 488-nm excitation laser and standard detection optics was used for all assays (133). Pure GST-Rab7 protein was incubated in 96-well plates at 4°C overnight with 10^5 GSH beads in a total volume of 100 μl of HPS

buffer containing 1 mM EDTA and 1 mM dithiothreitol (DTT) added fresh. Unbound protein was removed by centrifugation washes by spinning GST-Rab7 bound to GSH beads twice at 800 g followed by resuspension of washed protein in fresh HPS buffer containing 1 mM EDTA and 1 mM dithiothreitol (DTT).

Dose response or competition binding assays

Dose response assays were conducted in two different modes. In the first case, $5x10^3$ GSH beads loaded with GST-Rab7 were incubated with a fixed concentration of nucleotide (GDP or GTP) for 1 h in the presence of 1% DMSO (final) or increasing concentrations of CID1067700 (10^{-3} – 100 μM) in 1% DMSO and a total volume of 20 μl on a 96-well plate. A stock solution of CID1067700 (10 mM) was prepared in 100% DMSO and stored in single use aliquots at -80°C. In the second mode, $5x10^3$ GSH beads loaded with GST-Rab7 protein were incubated for 2 h 15 min at 4 °C with varying concentrations of fluorescent guanine nucleotide (0–2 μM) in a total volume of 20 μl on a 96-well plate in the presence of either 1 % DMSO or a fixed CID1067700 concentration (0.1 – 1μM). For measurements on the flow cytometer, samples were transferred to a falcon tube (BD Bioscience) for flow cytometry and were diluted at least 10-fold in HPS buffer. This dilution step was necessary to ensure discrimination of bead-associated

fluorescence and background fluorescence of soluble proteins and also ensured sufficient sample volume for the measurement.

Nucleotide dissociation assays in the presence of CID1067700

Nucleotide dissociation under equilibrium conditions was accomplished by first incubating $1.5x10^5$ GSH bead bound GST-Rab7 with fixed BODIPY-GTP (100 nM) or BODIPY-GDP (40 nM) for 2hr 15 min at 4 ^oC followed by initiating release of bound nucleotide with either unlabeled GDP (10 μM) or CID1067700 (10 μM). As a negative control, GST-Rab7 was preloaded with unlabelled GDP (1 mM) for 2hr 15 min at 4^oC prior to adding BODIPY-GTP or BODIPY–GDP at the above concentrations for a further 2hr 15 min and then similarly initiating release of bound BODIPY-linked nucleotide with unlabeled GDP (10 μM) to obtain fluorescence for non-specific binding under equilibrium binding conditions. This low level bead associated fluorescence was subtracted from specific binding to obtain accurate measurement of the off rates.

Molecular docking of CID1067700 on Rab7

Docking calculations were performed using OpenEye Fred (Fred, version 2.2.5, OpenEye Scientific Software, Inc., Santa Fe, NM, USA, www.eyesopen.com, 2010) docking software. Rab7 crystal structures (PDB code: 1T91 GDP-conformer, 1VG8 GNP-conformer) were used to dock CID1067700 on Rab7 for the wild type. Chemgauss3

scoring function was used to evaluate ligand binging potential. Docking simulations provide only a qualitative assessment of binding probability of our ligand to Rab7 and should be examined with care, however the results indicate that CID1067700 can potentially bind to Rab7 nucleotide binding site and no steric constrains were observed

Data analyses

All data processing and analyses employed GraphPad Prism software (GraphPad Software, San Diego). For kinetic experiments, raw data acquired were first processed using IDLE query software (obtained from University of New Mexico Center for Molecular Discovery, UNM CMD) before further analysis using GraphPad Prism. All experiments are representative of at least three independent trials.

Synthesis of CID1067700 derivatives for structure activity analyses

Structure activity relationship (SAR) was performed to understand the relationship between the chemical structure of CID1067700 and its activity. A lot of times, the activity of a small molecule can be a pharmacological response, binding, toxicity or any other quantifiable event. In our context, the activity of interest was pharmacological response marked by modulation of nucleotide binding by Rab7 by CID1067700. Derivatives of CID1067700 were synthesized and analyzed for purity by collaborating laboratory at University of Kansas. The steps involved were carried out using standard

chemical synthesis protocol. Below is a sequential summary of the methods employed.

Chemistry and analytical details

^{1}H and ^{13}C NMR spectra were recorded on a Bruker AM 400 spectrometer (operating at 400 and 101 MHz respectively) in $CDCl_3$ with 0.03% TMS as an internal standard or DMSO-d_6. The chemical shifts (d) reported are given in parts per million (ppm) and the coupling constants (*J*) are in Hertz (Hz). The spin multiplicities are reported as s = singlet, br. s = broad singlet, d = doublet, t = triplet, q = quartet, dd = doublet of doublet and multiplet. The LCMS analysis was performed on an Agilent 1200 RRL chromatograph with photodiode array UV detection and an Agilent 6224 TOF mass spectrometer. The chromatographic method utilized the following parameters: a Waters Acquity BEH C-18 2.1 x 50 mm, 1.7 um column; UV detection wavelength = 214 nm; flow rate = 0.4 ml/min; gradient = 5 - 100% acetonitrile over 3 minutes with a hold of 0.8 minutes at 100% acetonitrile; the aqueous mobile phase contained 0.15% ammonium hydroxide (v/v). The mass spectrometer utilized the following parameters: an Agilent multimode source which simultaneously acquires ESI+/APCI+; a reference mass solution consisting of purine and hexakis (1H, 1H, 3H-tetrafluoropropoxy) phosphazine; and a make-up solvent of 90:10:0.1 MeOH:Water:Formic Acid which was introduced to the LC flow prior to the source to assist ionization. Melting points were determined on a

Stanford Research Systems OptiMelt apparatus. Synthesized analogs were prepared by the general route depicted in Fig. 5. Stepwise procedures for all synthesized analogs and intermediates are described. Analytical characterization is provided for all tested commercial and synthetic compounds itemized in this section.

Figure 5. General scheme used for synthetic analogs

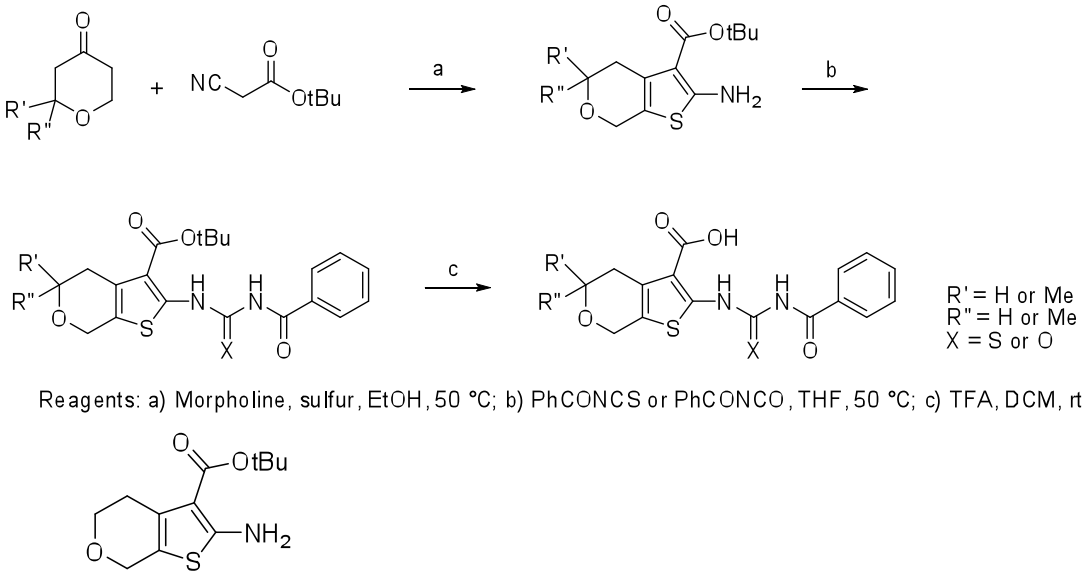

Reagents: a) Morpholine, sulfur, EtOH, 50 °C; b) PhCONCS or PhCONCO, THF, 50 °C; c) TFA, DCM, rt.

***tert*-Butyl 2-amino-5,7-dihydro-4H-thieno[2,3-c]pyran-3-carboxylate.** Following a previously reported procedure. Tetrahydro-4*H*-pyran-4-one (0.28 mL, 3.0 mmol, 1 equiv.), *tert*-butyl cyanoacetate (0.47 mL, 3.3 mmol, 1.1 equiv.), sulfur (0.106 g, 3.30 mmol, 1.1 equiv.), and morpholine (0.39 mL, 4.5 mmol, 1.5 equiv.) were dissolved in EtOH (9 mL) and stirred at 50 ^{o}C1 for 16 h. The solvent was removed and water (7 mL) was added. The product was extracted with EtOAc (2 × 7 mL) and purified by

preparatory HPLC (0-20% EtOAC:hexanes). The product was isolated as a clear, pale yellow oil (0.77 g, quantitative yield). ^{1}H NMR (400 MHz, $CDCl_3$) δ 5.98 (s, 2H), 4.55 (t, J = 2.0 Hz, 2H), 3.90 (t, J = 5.6 Hz, 2H), 2.79 (ddd, J = 7.6, 3.8, 2.0 Hz, 2H), 1.54 (s, 9H). ^{13}C NMR (101 MHz, $CDCl_3$) δ 165.38, 161.65, 130.33, 114.60, 106.76, 80.37, 65.20, 64.66, 28.57, 27.94.

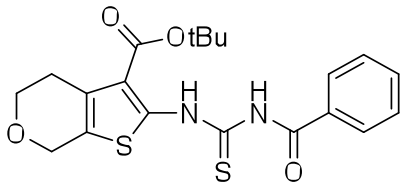

***tert*-Butyl 2-(3-benzoylthioureido)-5,7-dihydro-4H-thieno[2,3-c]pyran-3-carboxylate.** *tert*-Butyl 2-amino-5,7-dihydro-4H-thieno[2,3-c]pyran-3-carboxylate (0.099 g, 0.39 mmol, 1 equiv.) and PhCONCS (0.06 mL, 0.4 mmol, 1 equiv.) were dissolved in THF (2 mL) and stirred at 50 ^{o}C for 16 h. The solvent was removed and the product was purified by preparatory HPLC (0-30% EtOAC:hexanes). The product was isolated as a white solid (0.131 g, 80% yield). ^{1}H NMR (400 MHz, $CDCl_3$) δ 14.75 (s, 1H), 9.21 (s, 1H), 7.92 (dd, J = 5.2, 3.3 Hz, 2H), 7.64 – 7.57 (m, 1H), 7.54 – 7.46 (m, 2H), 4.71 (s, 2H), 3.94 (t, J = 5.6 Hz, 2H), 2.90 (t, J = 5.6 Hz, 2H), 1.63 (s, 9H). ^{13}C

NMR (101 MHz, $CDCl_3$) δ 173.72, 165.23, 164.54, 147.15, 133.48, 131.81, 129.36, 129.04, 127.77, 125.77, 117.76, 82.36, 65.20, 64.71, 28.51, 27.38.

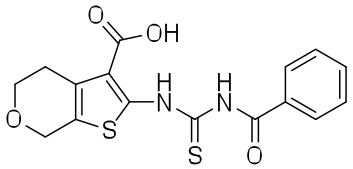

SID 99381129
CID 46916266

2-(3-benzoylthioureido)-5,7-dihydro-4H-thieno[2,3-c]pyran-3-carboxylic acid (SID 99381129, CID 46916266). To a solution of *tert*-Butyl 2-(3-benzoylthioureido)-5,7-dihydro-4H-thieno[2,3-c]pyran-3-carboxylate (0.104 g, 0.25 mmol, 1 equiv.) in DCM (10 mL) was added TFA (2 mL, 26 mmol, 100 equiv.), and the reaction was stirred at rt for 16 h. The solvent was removed and the product was triturated with 1:1 Et_2O/hexanes (25 mL) and filtered. The product was purified by mass-directed reverse-phase chromatography and isolated as a white solid (3 mg, 3% yield). ^{1}H NMR (400 MHz, $CDCl_3$) δ 14.92 (br s, 1H), 9.02-9.09 (m, 1H), 7.83-7.91 (m, 1H), 7.55-7.66 (m, 2H), 7.41-7.50 (m, 2H), 7.19-7.23 (m, 1H), 4.69-4.76 (m, 2H), 3.92-3.98 (m, 2H), 2.88-3.03 (m, 2H). LCMS retention time: 2.955 min; LCMS purity at 215 nm = 100%. HRMS *m/z* calculated for $C_{16}H_{15}N_2O_4S_2$ [M^++1]: 363.0468, found 363.0464.

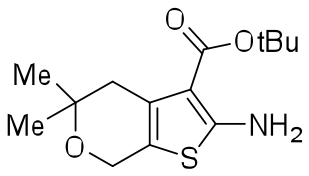

***tert*-Butyl 2-amino-5,5-dimethyl-5,7-dihydro-*4H*-thieno[2,3-c]pyran-3-carboxylate**.

A mixture of 2,2-dimethyldihydro-2H-pyran-4(*3H*)-one (0.300 g, 2.34 mmol, 1 eq), *tert*-butyl cyanoacetate (0.37 mL, 2.57 mmol, 1.1 eq), sulfur (0.083 g, 2.57 mmol, 1.1 eq), morpholine (0.30 mL, 3.51 mmol, 1.5 eq), and ethanol (7 mL) was heated at 50 °C for 16 h. The reaction mixture was then filtered, and the filter cake washed with ethyl acetate (20 mL). Purification by silica gel chromatography (0-20% EtOAc:Hex ramp over 20 min) afforded the desired product *tert*-butyl 2-amino-5,5-dimethyl-5,7-dihydro-*4H*-thieno[2,3-c]pyran-3-carboxylate as a yellow solid (0.631 g, 2.23 mmol, 95 % yield). ^{1}H NMR (400 MHz, CDCl3) δ 5.88 (s, 2H), 4.52 (t, *J* = 1.9, 2H), 2.64 (t, *J* = 1.9, 2H), 1.53 (s, 9H), 1.26 (s, 6H).

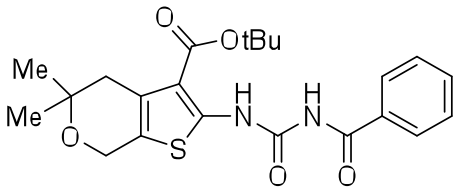

***tert*-Butyl 2-(3-benzoylureido)-5,5-dimethyl-5,7-dihydro-4H-thieno[2,3-c]pyran-3-carboxylate.** *tert*-Butyl 2-amino-5,5-dimethyl-5,7-dihydro-4H-thieno[2,3-c]pyran-3-carboxylate (0.116 g, 0.41 mmol, 1 equiv.) and PhCONCO (0.06 mL, 0.5 mmol, 1.2 equiv.) were dissolved in THF (2 mL) and stirred at 50 ^{o}C for 16 h. The solvent was removed and the product was purified by preparatory HPLC (0-40% EtOAC:hexanes). The product was isolated as a white solid (0.105 g, 59% yield). ^{1}H NMR (400 MHz, $CDCl_3$) δ 13.26 (s, 1H), 9.81 (s, 1H), 8.13 (d, *J* = 7.0 Hz, 2H), 7.65 (d, *J* = 6.7 Hz, 3H), 4.72 (s, 2H), 2.75 (s, 2H), 1.64 (s, 9H), 1.32 (s, 6H).

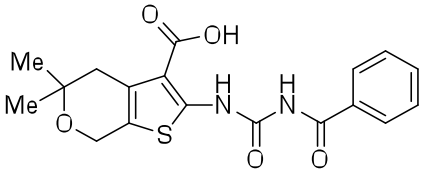

SID 99381130
CID 46916265

2-(3-Benzoylureido)-5,5-dimethyl-5,7-dihydro-4H-thieno[2,3-c]pyran-3-carboxylic acid (SID 99381130, CID 46916265). To a solution of *tert*-butyl 2-(3-benzoylureido)-5,5-dimethyl-5,7-dihydro-4H-thieno[2,3-c]pyran-3-carboxylate (0.105 g, 0.24 mmol, 1 equiv.) in DCM (10 mL) was added TFA (0.5 mL, 6.5 mmol, 27 equiv.), and the reaction was stirred at rt for 5 days. The solvent was removed under reduced pressure and the product was purified by preparatory HPLC (0-5% MeOH/DCM), followed by mass-

directed reverse-phase chromatography and isolated as a white solid (6 mg, 7% yield). ^{1}H NMR (400 MHz, DMSO) δ 13.11 (s, 1H), 11.39 (s, 1H), 8.05 – 7.99 (m, 2H), 7.69 – 7.63 (m, 1H), 7.55 (t, *J* = 7.7 Hz, 2H), 4.62 (s, 2H), 2.71 (s, 2H), 1.22 (s, 6H). LCMS retention time: 2.872 min; LCMS purity at 215 nm = 100%. HRMS *m/z* calculated for $C_{18}H_{19}N_2O_5S$ [M^++1]: 375.1009, found 375.1013.

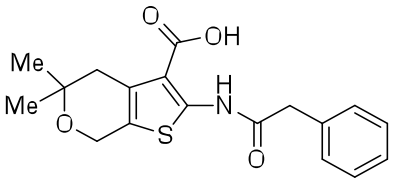

SID 99381117
CID 740871

5,5-dimethyl-2-(2-phenylacetamido)-5,7-dihydro-4H-thieno[2,3-c]pyran-3-carboxylic acid (SID 99381117, CID 740871). 5,5-Dimethyl-2-(2-phenylacetamido)-5,7-dihydro-4H-thieno[2,3-c]pyran-3-carboxylic acid was purchased from ChemBridge (CAS 303966-15-6) and purified by mass-directed reverse-phase chromatography and isolated as a white solid (3 mg, 100% purity). ^{1}H NMR (400 MHz, $CDCl_3$) δ 10.88 (s, 1H), 7.43 – 7.37 (m, 2H), 7.33 (dd, *J* = 6.7, 4.3 Hz, 3H), 4.72 (s, 2H), 3.85 (s, 2H), 2.85 (s, 2H), 1.35 (s, 6H). LCMS retention time: 3.045 min; LCMS purity at 215 nm = 100%. HRMS *m/z* calculated for $C_{18}H_{20}NO_4S$ [M^++1]: 346.1108, found 346.1110.

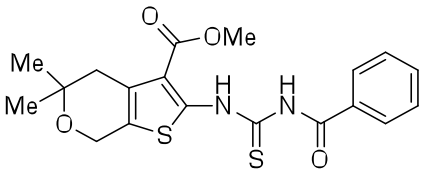

SID 99381118
CID 1251121

Methyl 2-(3-benzoylthioureido)-5,5-dimethyl-5,7-dihydro-4H-thieno[2,3-c]pyran-3-carboxylate (SID 99381118, CID 1251121). To a combined mixture of methyl 2-amino-5,5-dimethyl-5,7-dihydro-4H-thieno[2,3-c]pyran-3-carboxylate (ChemBridge, CAS 713111-73-0, 31 mg, 0.13 mmol, 1 equiv.) and PhCONCS (0.02 mL, 0.15 mmol, 1.2 equiv.) was added THF (0.7 mL). The resulting solution was stirred at 50 ^{o}C for 3 days. The solvent was then removed under reduced pressure and the crude product was triturated with hexanes, filtered, and rinsed with hexanes (4 × 5 mL). The product was further purified by preparatory HPLC (0-50% EtOAC:hexanes) and isolated as a white solid (38 mg, 72% yield). ^{1}H NMR (400 MHz, $CDCl_3$) δ 14.83 (s, 1H), 9.14 (s, 1H), 7.98 (dd, J = 8.4, 1.2 Hz, 2H), 7.72 – 7.63 (m, 1H), 7.56 (dd, J = 10.5, 4.8 Hz, 2H), 4.77 (t, J = 1.5 Hz, 2H), 4.04 (s, 3H), 2.85 (s, 2H), 1.35 (s, 6H). LCMS retention time: 3.508 min; LCMS purity at 215 nm = 96%. HRMS *m/z* calculated for $C_{19}H_{21}N_2O_4S_2$ [M^++1]: 405.0937, found 405.0942.

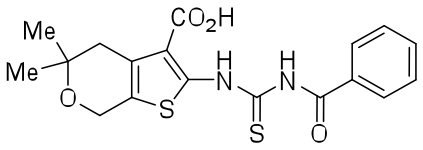

SID 85747738
CID 1067700

2-(3-benzoylthioureido)-5,5-dimethyl-5,7-dihydro-4H-thieno[2,3-c]pyran-3-carboxylic acid (SID 85747738/ CID 1067700). 2-(3-benzoylthioureido)-5,5-dimethyl-5,7-dihydro-4H-thieno[2,3-c]pyran-3-carboxylic acid was purchased from Chemdiv Inc. (CAS 314042-01-8) and purified by mass-directed reverse-phase chromatography to yield a white solid (6 mg). ^{1}H NMR (400 MHz, DMSO) δ 14.84 (s, 1H), 13.39 (s, 1H), 11.81 (s, 1H), 7.98 (dd, *J* = 1.2, 8.4, 2H), 7.74 – 7.62 (m, 1H), 7.55 (t, *J* = 7.7, 2H), 4.67 (s, 2H), 2.75 (s, 2H), 1.24 (s, 6H). ^{13}C NMR (101 MHz, DMSO) δ 174.43, 166.86, 165.35, 146.72, 133.08, 132.06, 129.10, 128.75, 128.41, 124.09, 116.50, 70.14, 58.82, 37.27, 26.19. LCMS retention time: 1.871 min; LCMS purity at 214 nm = 92.8%. HRMS *m/z* calculated for $C_{18}H_{19}N_2O_4S_2$ [M^++1]: 391.0781, found 391.0777.

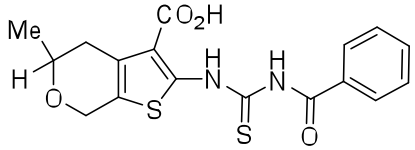

SID 9931128
CID 46916263

2-(3-benzoylthioureido)-5-methyl-5,7-dihydro-*4H*-thieno[2,3-c]pyran-3-carboxylic acid (SID 9931128/ CID 46916263). To tert-butyl 2-(3-benzoylthioureido)-5-methyl-5,7-

dihydro-4H-thieno[2,3-c]pyran-3-carboxylate (0.028 g, 0.065 mmol, 1 eq.) was added a 40% v/v solution of trifluoroacetic acid in dichloromethane (2.5 mL). After stirring the solution for 4 hours at rt, the solvent was evaporated in vacuo, and the residue purified by reverse-phase chromatography to yield the product as a white semi-solid (0.011 g, 0.029 mmol, 46% yield). ^{1}H NMR (400 MHz, Acetone) δ 8.07 (d, J = 7.4, 2H), 7.68 (t, *J* = 7.0, 1H), 7.56 (t, *J* = 7.5, 2H), 4.76 (q, *J* = 14.7, 2H), 3.82 – 3.68 (m, 1H), 3.05 (d, 1H), 1.47 (d, *J* = 6.5, 1H), 1.32 (d, *J* = 6.1, 3H). ^{13}C NMR (126 MHz, Acetone) δ 175.37, 166.92, 165.37, 161.89, 148.65, 134.12, 133.28, 131.39, 129.62, 129.28, 126.49, 71.61, 65.11, 35.05, 21.82. LCMS retention time: 3.095 min; Purity at 214 nm = 93.3%. HRMS *m/z* calculated for $C_{17}H_{17}N_2O_4S_2$ [M^+ + 1] 377.0624, found 377.0622.

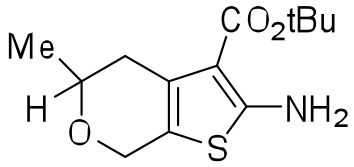

***tert*-butyl 2-amino-5-methyl-5,7-dihydro-*4H*-thieno[2,3-c]pyran-3-carboxylate.** A mixture of 2-methyldihydro-*2H*-pyran-4(*3H*)-one (0.320 g, 2.80 mmol, 1 eq), *tert*-butyl cyanoacetate (0.44 mL, 3.08 mmol, 1.1 eq), sulfur (0.099 g, 3.08 mmol, 1.1 eq), morpholine (0.36 mL, 4.21 mmol, 1.5 eq), and ethanol (7 mL) was heated at 50 °C for 16

hours. The reaction mixture was then filtered, and the filter cake washed with ethyl acetate (20 mL). Purification by silica gel chromatography (0-30% EtOAc:Hex ramp over 20 min) afforded the desired product *tert*-butyl 2-amino-5-methyl-5,7-dihydro-4H-thieno[2,3-c]pyran-3-carboxylate as a pale yellow solid (0.745 g, 2.77 mmol, 99 % yield). ^{1}H NMR (400 MHz, CDCl3) δ 5.90 (s, 2H), 4.71 – 4.49 (m, 2H), 3.82 – 3.65 (m, 1H), 2.86 – 2.73 (m, 1H), 2.52 – 2.37 (m, 1H), 1.52 (d, *J* = 1.4, 9H), 1.31 (dd, *J* = 2.1, 6.2, 3H).

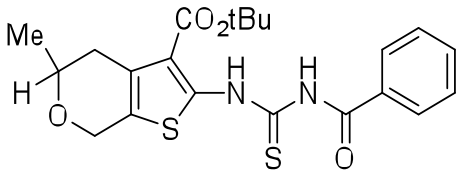

***tert*-butyl 2-(3-benzoylthioureido)-5-methyl-5,7-dihydro-*4H*-thieno[2,3-c]pyran-3-carboxylate**. To a solution of *tert*-butyl 2-amino-5-methyl-5,7-dihydro-4H-thieno[2,3-c]pyran-3-carboxylate (0.104 g, 0.386 mmol, 1 eq) in dry ethanol (1 mL)under argon was added benzoyl isothiocyanate (0.15 mL, 1.08 mmol, 2.8 eq). The mixture was heated at reflux for 16 hours. The solvent was evaporated in vacuo. Purification by reverse-phase chromatography (10-100% CH_3CN: Water ramp over 20 min) afforded the desired product *tert*-butyl 2-(3-benzoylthioureido)-5-methyl-5,7-dihydro-*4H*-thieno[2,3-c]pyran-3-carboxylate as a pale yellow oil (0.057 g, 0.132 mmol, 34 % yield). ^{1}H NMR (400

MHz, DMSO) δ 14.72 (s, 1H), 11.89 (s, 1H), 8.06 – 7.95 (m, 2H), 7.69 (t, *J* = 7.4, 1H), 7.57 (t, *J* = 7.7, 2H), 4.78 (d, *J* = 14.8, 1H), 4.66 (d, *J* = 15.0, 1H), 3.80 – 3.63 (m, 1H), 2.93 (d, *J* = 16.7, 1H), 2.50 – 2.44 (m, 1H), 1.59 (s, 9H), 1.30 (d, *J* = 6.1, 3H).

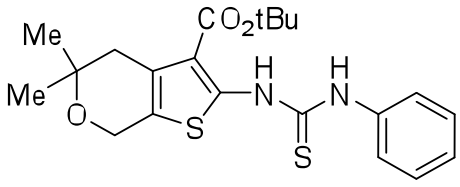

***tert*-butyl 5,5-dimethyl-2-(3-phenylthioureido)-5,7-dihydro-*4H*-thieno[2,3-c]pyran-3-carboxylate**. . To a solution of *tert*-butyl 2-amino-5,5-dimethyl-5,7-dihydro-*4H*-thieno[2,3-c]pyran-3-carboxylate (0.100 g, 0.353 mmol, 1 eq) in dry tetrahyrofuran (5 mL) under argon was added phenyl isothiocyanate (0.05 mL, 0.388 mmol, 1.1 eq). The mixture was heated at reflux for 16 hours. The solvent was evaporated in vacuo. Purification by reverse-phase chromatography (0-100% CH_3CN: Water ramp over 20 min) afforded the desired product *tert*-butyl 5,5-dimethyl-2-(3-phenylthioureido)-5,7-dihydro-*4H*-thieno[2,3-c]pyran-3-carboxylate as a yellow solid (0.045 g, 0.108 mmol, 30 % yield). ^{1}H NMR (400 MHz, DMSO) δ 11.92 (s, 1H), 11.05 (s, 1H), 7.50 (d, *J* = 7.6, 2H), 7.42 (t, *J* = 7.9, 2H), 7.26 (t, *J* = 7.3, 1H), 4.61 (s, 2H), 2.65 (s, 2H), 1.53 (s, 9H), 1.23 (s, 6H).

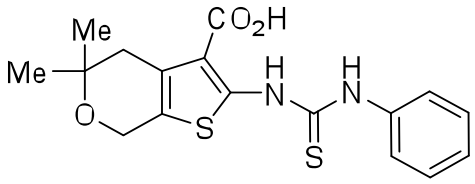

5,5-dimethyl-2-(3-phenylthioureido)-5,7-dihydro-*4H*-thieno[2,3-c]pyran-3-carboxylic acid (SID 99381127/ CID 1280844). To 5,5-dimethyl-2-(3-phenylthioureido)-5,7-dihydro-4H-thieno[2,3-c]pyran-3-carboxylic acid (0.037 g, 0.088 mmol, 1 eq.) was added a 40% v/v solution of trifluoroacetic acid in dichloromethane (2.5 mL). After stirring the solution for 4 hours at rt, the solvent was evaporated in vacuo and the residue purified by reverse-phase LCMS to yield the product as a white solid (0.020 g, 0.065 mmol, 63% yield). ^{1}H NMR (400 MHz, Acetone) δ 7.97 (d, J = 7.7, 2H), 7.88 (t, J = 7.7, 2H), 7.73 (t, J = 6.9, 1H), 4.32 (s, 2H), 3.11 (s, 2H), 1.73 (s, 6H). LCMS retention time: 3.113 min; Purity at 214 nm = 100%. HRMS *m/z* calculated for $C_{17}H_{19}N_2O_3S_2$ [M^+ + 1] 363.0832, found 363.0829.

Results

Identification of CID1067700 as an inhibitor of nucleotide binding by Rab7

CID1067700 was identified as an inhibitor of GTP-binding using a high throughput screen that was described previously in the context of an allosteric Rho GTPase inhibitor (135). Briefly, six sets of beads (each with a unique red fluorescence intensity) were individually coated with six representative GST-tagged Ras-related GTPases (Cdc42 wt, Rac1wt, Rac1Q61L, Rab2 wt, Rab7wt, and H-Ras wt) (Fig. 6a). The individually conjugated beads were then assayed in the presence of individual compounds in the Molecular Libraries Small Molecule Repository using HyperCyt flow cytometry to identify molecules that altered the binding of fluorescent nucleotide to Ras-family GTPases (136). CID1067700 **(**Fig. 6b), was identified as a hit that decreased fluorescent nucleotide (GTP) binding in the primary screen and was confirmed in secondary, multiplex dose response assays to have an EC_{50} of 20-500 nM and at least 40% inhibition against all tested GTPases **(**Fig. 6c). CID1067700 was the only compound identified in the screen to have significant inhibitory activity against the Rab GTPases (Rab2 and Rab7). Because of its pronounced inhibitory effect (>80%) on Rab7 and the absence of any known chemical inhibitors for Rab-family GTPases, I further characterized the mechanism of CID1067700 inhibition using Rab7 as a model protein.

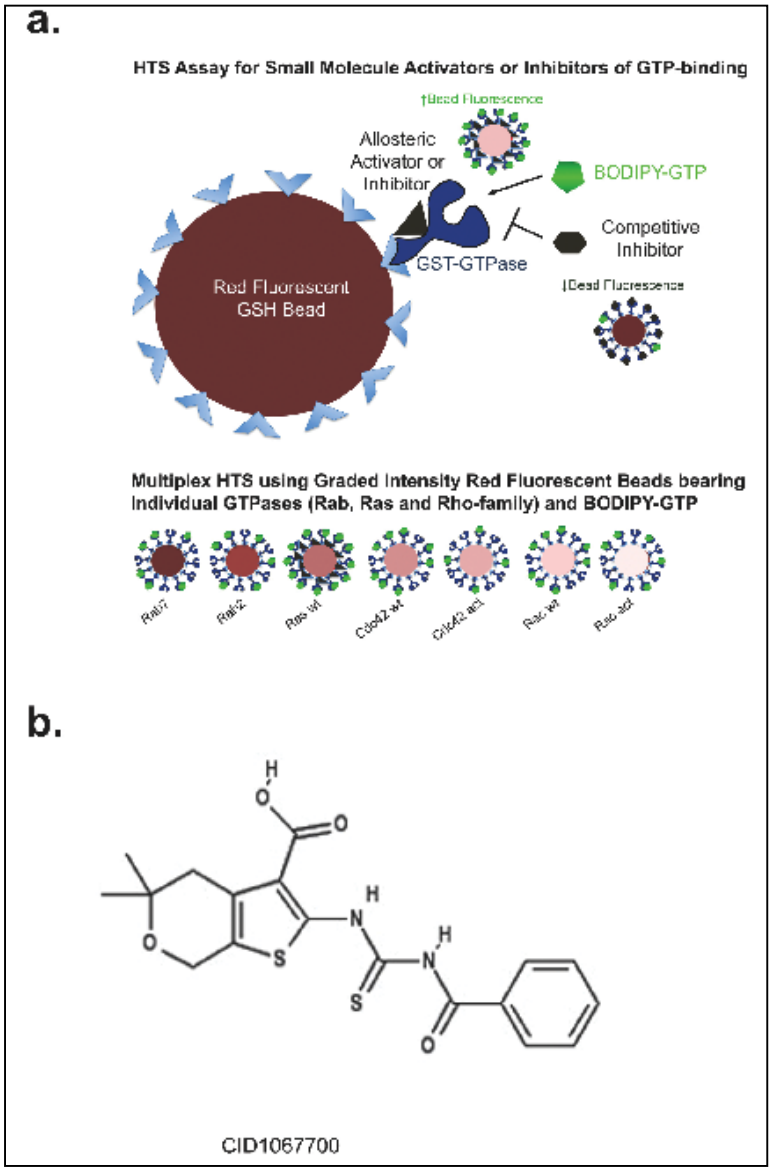

Figure 6. Identification of CID1067700 as a pan GTPase inhibitor using high-throughput screening on small GTPases. (**a**) Schematic diagram of the bead based assay used to measure fluorescent guanosine triphosphate (GTP) binding by flow cytometry to glutathione-S-transferase (GST)–GTPase chimeras immobilized on GSH-beads. For HTS beads of varying red fluorescence intensities were used as identifiers for individual protein-conjugated bead sets. (**b**) Chemical structure of CID1067700 an inhibitor of nucleotide binding.

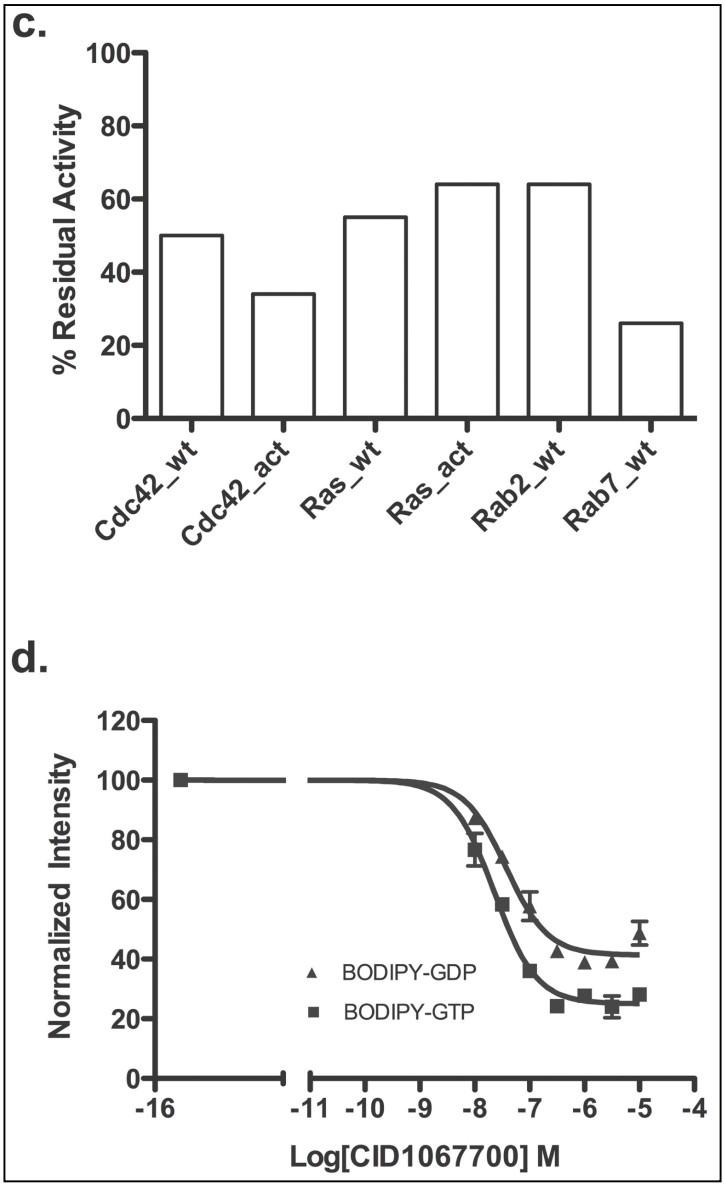

Figure 6. (c) Activity of CID1067700 against multiple GTPases measured as residual nucleotide binding activity (BODIPY-GTP, 100 nM) in the presence of increasing concentrations of compound. (**d**) Nanomolar concentrations of CID1067700 inhibit Rab7wt protein nucleotide binding; BODIPY-GTP (100 nM, filled squares) and BODIPY-GDP (40 nM, filled triangles).

Dose dependent inhibition of Rab7 nucleotide binding by CID1067700

Single-plex dose response measurements were used to determine the effect of CID1067700 on nucleotide binding by Rab7 small GTPase. To achieve this, the BODIPY-GDP and BODIPY-GTP concentrations in the assay were fixed to the previously determined equilibrium dissociation constants (K_d=100 nM BODIPY-GTP; K_d=40 nM BODIPY-GDP) for the wild-type (wt) Rab7 protein (133). Increasing CID1067700 concentrations resulted in strong inhibition of both BODIPY-GDP and BODIPY-GTP binding by Rab7wt with EC_{50} values of 25 nM for BODIPY-GTP and 40 nM for BODIPY-GDP **(**Fig. 6d**).** The deduced efficacy of inhibition was 80% for BODIPY-GTP and 60% for BODIPY-GDP. These results demonstrate high efficacy and potency of the CID1067700 molecule with respect to inhibition of Rab7 nucleotide binding. Maximum inhibition by CID1067700 occurred at 1-10 μM CID1067700 concentration range. Lower inhibitory efficacy against BODIPY-GDP binding may either represent a preference for one nucleotide conformer over another by Rab7 or the established higher affinity of Rab7 for GDP than for GTP (133, 137).

Inhibition of Rab7wt nucleotide binding by CID1067700 could be effected through allosteric or competitive binding. To distinguish between the two scenarios, we tested the inhibition of Rab7wt by CID1067700 under conditions where CID1067700 concentration

was held at a fixed concentration (100-200 nM) while increasing the concentration of the fluorescent nucleotide competitor (Fig. 7a-h). These values were equivalent to approximately 5 times the observed EC_{50} for CID1067700 using each of the two nucleotides. The inhibitory effect of CID1067700 was most pronounced at lower nucleotide concentrations, resulting in an overall rightward shift of the dose response curves (Fig. 7b, d). Significantly, both control (DMSO only) and inhibitor (CID1067700 treated) curves had statistically similar B_{max} values that correspond to the number of binding sites on Rab7 (Fig. 7a, c). Thus, at high concentrations, the nucleotide out competes the CID1067700 compound for the binding pocket, accounting for the B_{max} values that are not statistically different. In contrast, there was ≤3-fold increase in the observed EC_{50} for both nucleotides in the presence of CID1067700 indicating competition of nucleotides by the inhibitor. Calculated inhibitor constants (K_i) for both nucleotides (Table 1) show a 2-fold increase between inhibition of BODIPY-GTP and BODIPY-GDP confirming that CID1067700 is better at inhibiting BODIPY-GTP binding than BODIPY-GDP binding. Analysis of the constitutively active Rab7Q67L and dominant negative Rab7T22N mutants, that mimic the GTP-bound and GDP-bound conformers respectively showed that both were similarly inhibited by CID1067700 (Fig.

7e-h). The composite data suggest that the CID1067700 compound and the nucleotide most likely compete for the nucleotide binding pocket of Rab7.

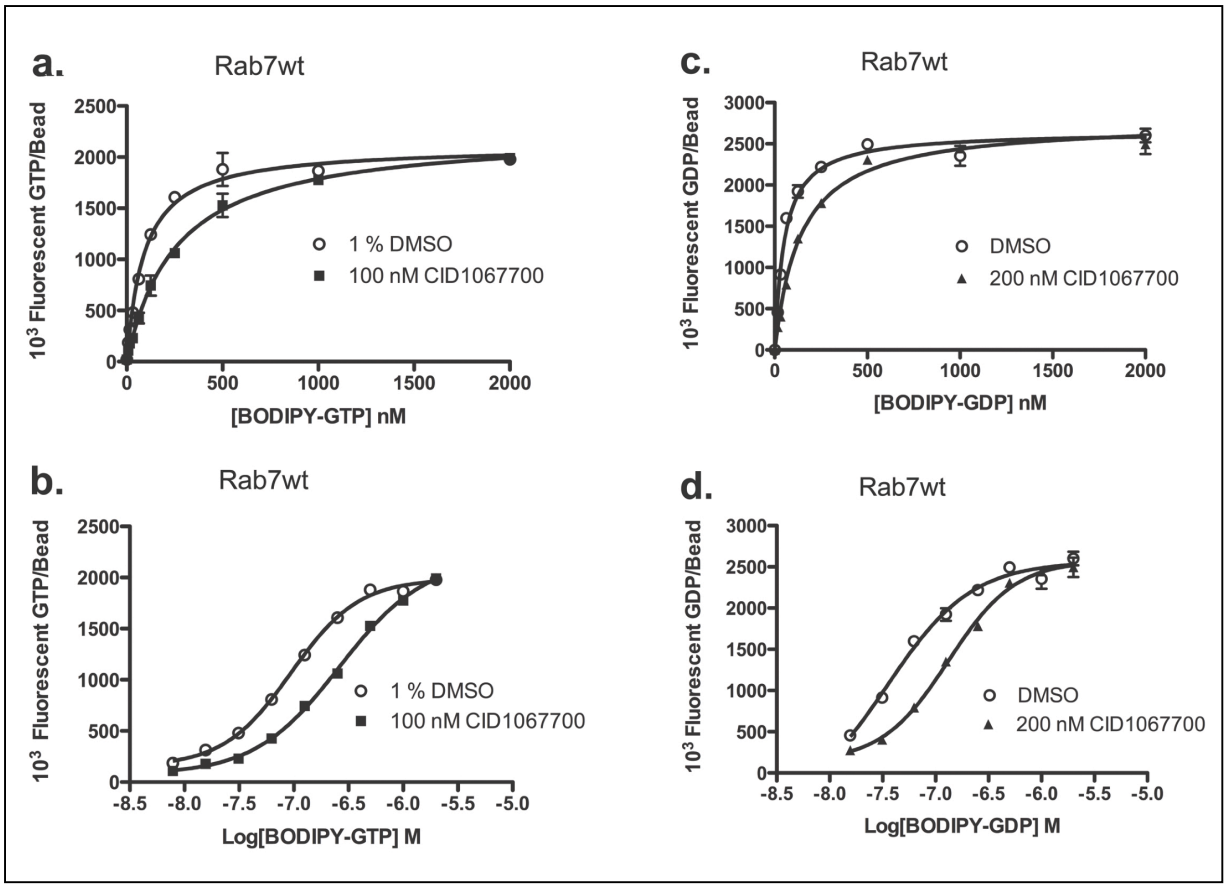

Figure 7. CID1067700 competitively inhibits BODIPY-linked nucleotide binding by wild type and mutant forms of Rab7. (**a-b**) CID1067700 (100 nM) does not alter Rab7wt B_{max} for BODIPY-GTP, but does alter apparent EC_{50} for GTP (filled squares); observed as a rightward shift of log plot of BODIPY-GTP binding by Rab7wt. (**c-d**) CID1067700 (200 nM) does not alter Rab7wt B_{max} for BODIPY-GDP; but does alter apparent EC_{50} for GDP (filled triangles); observed as rightward shift of log plot of BODIPY-GDP binding by Rab7wt.

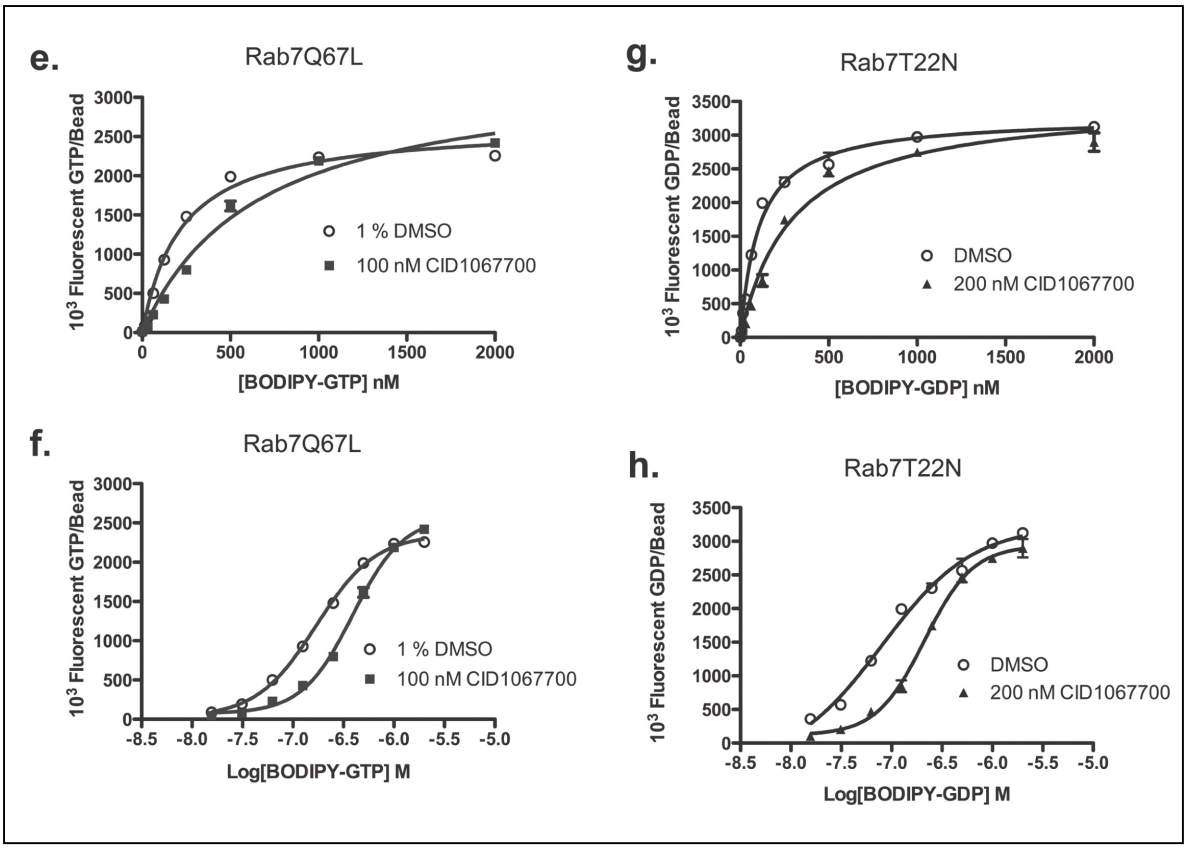

Figure 7. (**e-f).** CID1067700 (100 nM) does not alter constitutively active Rab7Q67L mutant B_{max} for BODIPY-GTP, but does alter apparent EC_{50} for GTP (filled squares); observed as a rightward shift of log plot of BODIPY-GTP binding by Rab7Q67L. (**g-h**) CID1067700 (200 nM) does not alter Rab7T22N B_{max} for BODIPY-GDP; but does alter apparent EC_{50} for GDP (filled triangles); observed as rightward shift of log plot of BODIPY-GDP binding by Rab7T22N. In all experiments, equilibrium binding reactions performed in 1% DMSO served as the controls (open circles).

Table 1. Equilibrium binding parameters deduced from Figure 7.

	Rab7wt		Rab7Q67L	Rab7T22N
Nucleotide:	GTP*	GDP*	GTP*	GDP*
[a]B_{max} (BODIPY/bead): Control	2110.00 ± 42.88	2651.00 ± 57.56	2660.00 ± 83.51	3275.00 ± 76.61
B_{max} (BODIPY/bead): Treated	2250.00 ± 55.75	2779.00 ± 57.58	3372.00 ± 187.40	3515.00 ± 148.30
[b]EC_{50} (nM): Control	90.89 ± 7.19	51.57 ± 4.97	220.50 ± 22.30	106.70 ± 9.42
EC_{50} (nM): Treated	258.4 ± 19.79	140.4 ± 10.42	654.40 ± 86.32	294.50 ± 37.15
[c]K_i (nM)	54.39	116.11	51.04	113.83

Equilibrium binding off rates

[d]BODIPY-GTP:

CID1067700 competitor (K_{-1} sec^{-1}): 0.02617 ± 0.00261

Unlabeled GDP competitor (K_{-1} sec^{-1}): 0.02659 ± 0.00119

[e]BODIPY-GDP:

CID1067700 competitor (K_{-1} sec^{-1}): 0.00110 ± 5.33760e-005

Unlabeled GDP competitor (K_{-1} sec^{-1}): 0.00137 ± 4.46200e-005

[a]Maximal number of bound BODIPY-nucleotide molecules per bead (Bmax) and [b]EC_{50} values were calculated simultaneously using the GraphPad Prism software to fit dose dependence to equation; where B represents the number of Rab7. $$B = B_{\max}\frac{[Nucleotide]}{EC_{50}+[Nucleotide]}$$

Cytometry detector output was converted to BODIPY-Nucleotide/bead using standard fluorescein beads from Invitrogen after correcting for the non-specific binding

[c]Inhibitor constant (K_i) was calculated using Cheng Prusoff equation; $$K_i = \frac{[Inhibitor]}{\frac{EC_{50\,Inhibitor}}{EC_{50,Control}} - 1.0}$$ where EC_{50} is obtained from equilibrium nucleotide binding experiments

[d]Off rates were calculated using two phase exponential to fit BODIPY-GTP kinetic data obtained under equilibrium conditions.

[e]Off rates were calculated using equation; $$B = Plateau\left(e^{-k_{off}(t-t_0)}\right)$$ to fit BODIPY-GDP kinetic data obtained under equilibrium conditions.

**The samples labeled control were treated with 1 % DMSO final while those labeled treated were subjected to CID1067700 treatment.

CID1067700 does not affect nucleotide release by Rab7

To further confirm the mode of Rab7 nucleotide inhibition by CID1067700, we analyzed the fluorescent nucleotide dissociations rates from Rab7 in the presence of CID1067700. The experiment was carried out by pre-binding BODIPY-GTP or –GDP to GST-tagged Rab7 protein up to equilibrium nucleotide exchange point and then assaying for the loss of fluorescence over time occasioned by the release of bound nucleotide (Fig. 8a-d). As a competitor, we used CID1067700 (10 μM) or unlabeled GDP (10 μM). Dissociation rate constants were calculated from data fit to exponential functions using Prism software. K_{off} values of Rab7wt obtained at room temperature were statistically similar between unlabeled GDP and CID1067700 competitor for both BODIPY-GTP or –GDP (Table 1). Together the data confirm that the CID1067700 compound has no effect on the rate of release of bound fluorescent GTP or GDP by Rab7, ruling out allosteric binding of the CID1067700 inhibitor in preference to competitive binding to the nucleotide pocket.

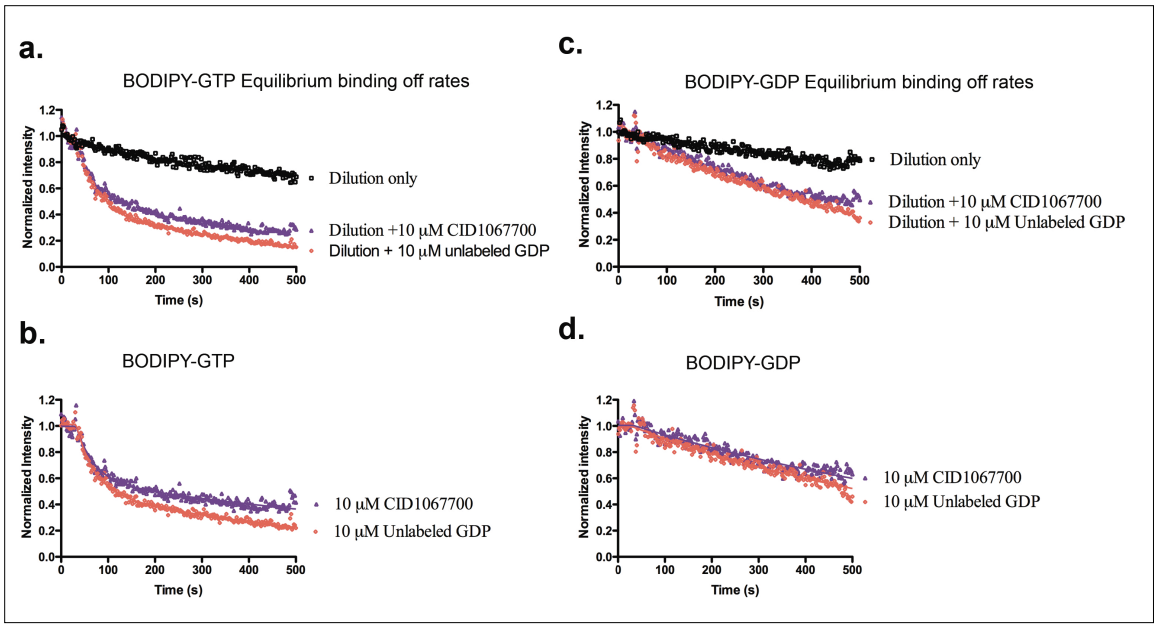

Figure 8: CID1067700 has no effect on the rate of release of bound BODIPY-linked nucleotide by wild type Rab7 under equilibrium binding conditions. (**a)** Rab7 was pre-incubated with BODIPY-GTP (100 nM) for 2 h 15 min at 4°C, conditions that allow nucleotide binding to equilibrium. Dissociation assays were initiated by dilution +/- the addition of either CID1067700 (10 µM) or unlabeled GDP (10 µM) and decrease in fluorescence due to nucleotide dissociation was measured in real time. (**b**) Two-phase exponential analysis of **a,** normalized by subtraction of dilution only values. (**c**). Rab7 was preincubated with BODIPY-GDP (40 nM) for 2 h 15 min at 4°C as for (a). Dissociation assays were initiated by dilution +/- CID1067700 (10 µM) or unlabeled GDP (10 µM) and decrease in fluorescence due to nucleotide dissociation was measured in real time. (**d**) Single phase exponential analysis of **c,** normalized by subtraction of dilution only values.

In another approach, in the absence of excess unlabeled GTP, CID1067700 and BODIPY-nucleotide competitively substitute for each other at the binding site when direct ligand competition was assayed. BODIPY-GTP or GDP (25-200 nM) was allowed to bind Rab7wt protein for 100 s in the absence of DMSO or CID1067700. At the indicated times, either 1% DMSO or 10 μM CID1067700 (final) was added as fluorescent nucleotide loading was allowed to continue in real time (Arrows, Fig. 9a-b, 9d-e). Relative to DMSO, addition of CID1067700 resulted in an immediate reduction in further nucleotide binding/loading. Statistical normalization of the fluorescence in the CID1067700 treated samples, revealed maximal competition between BODIPY-GTP and CID1067700 when the inhibitor was in 50-fold excess over the nucleotide (200 nm BODIPY-GTP vs. 10 μM) (Fig. 9c). Thus, binding of CID1067700 behaves as the rate limiting step in this circumstance. In contrast, BODIPY-GDP outcompetes CID1067700 with nearly complete efficacy (Fig. 9f).

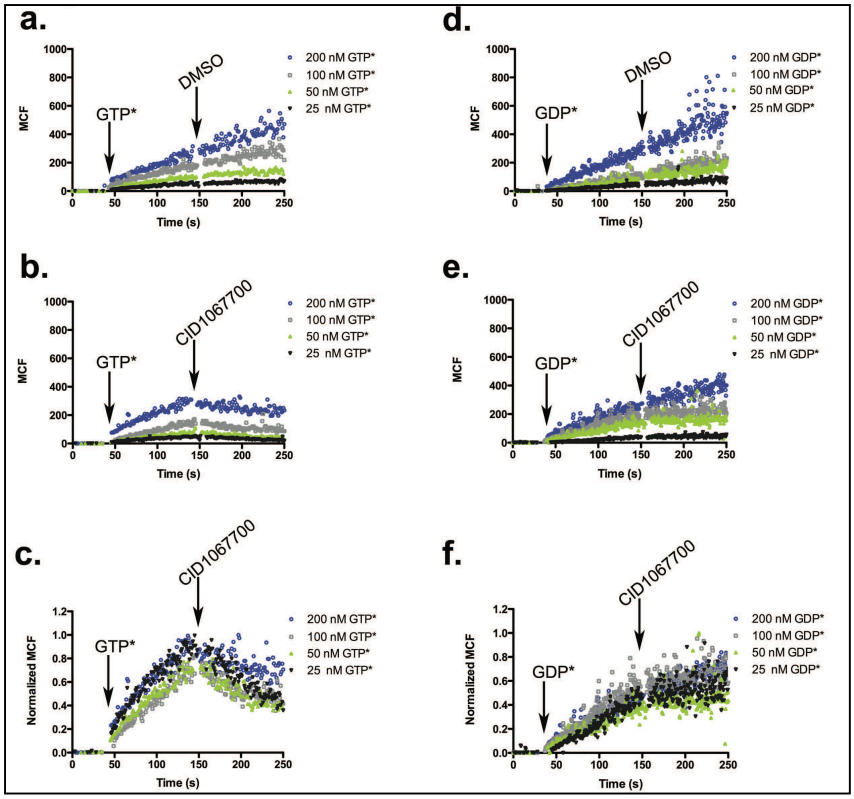

Figure 9: CID1067700 precludes nucleotide loading through direct displacement of fluorescent nucleotide. (**a-c**) Rab7 first incubated with BODIPY-GTP and then 1% DMSO final added at the point indicated by an arrow or (**b)** Rab7 first bound with BODIPY-GTP and then 10 μM of CID1067700 final added at the point indicated by an arrow and (**c**). Normalization of (**b**) reveals competition between BODIPY-GTP and CID1067700 at 200 nM concentration of the BODIPY-GTP and that binding of CID1067700 is the rate limiting step. (**d-f**) Rab7 first bound with BODIPY-GDP and then 1% DMSO final added at the point indicated by an arrow or (**e).** Rab7 first bound with BODIPY-GDP and then 10 μM CID1067700 final added at the point indicated by an arrow and (**f**). Normalization of (**e**) reveals that BODIPY-GDP outcompetes CID1067700 better than BODIPY-GTP. Comparison made with (**c**).

Nucleotide binding kinetics in the presence of CID1067700 indicates competitive mechanism

To obtain an alternative confirmation of the mechanism of CID1067700 inhibition and therefore binding kinetic parameters, real time on rate kinetic measurements were made using bead-based flow cytometry, as previously described (133). Varying the concentration of CID1067700 over a 10-fold range revealed that the compound saturates binding sites on Rab7 at 1 μM concentration (Fig. 10a and Fig. 10d). On-rate kinetic measurements of BODIPY-GTP and BODIPY-GDP binding in the presence of a fixed concentration of CID1067700 (1 μM for maximum inhibition) or DMSO control (2 min pre-incubation) revealed CID1067700 decreased Rab7 BODIPY-nucleotide (GTP and GDP) binding over a 4-fold nucleotide concentration range (Fig. 10b-c, e-f). Statistically, there was no effect on the observed association rate constant (k_{ob}), a parameter that may reflect the affinity of nucleotide for Rab7. Kinetic analyses corroborated the equilibrium binding data and supported a competitive inhibition of Rab7 nucleotide binding by CID1067700.

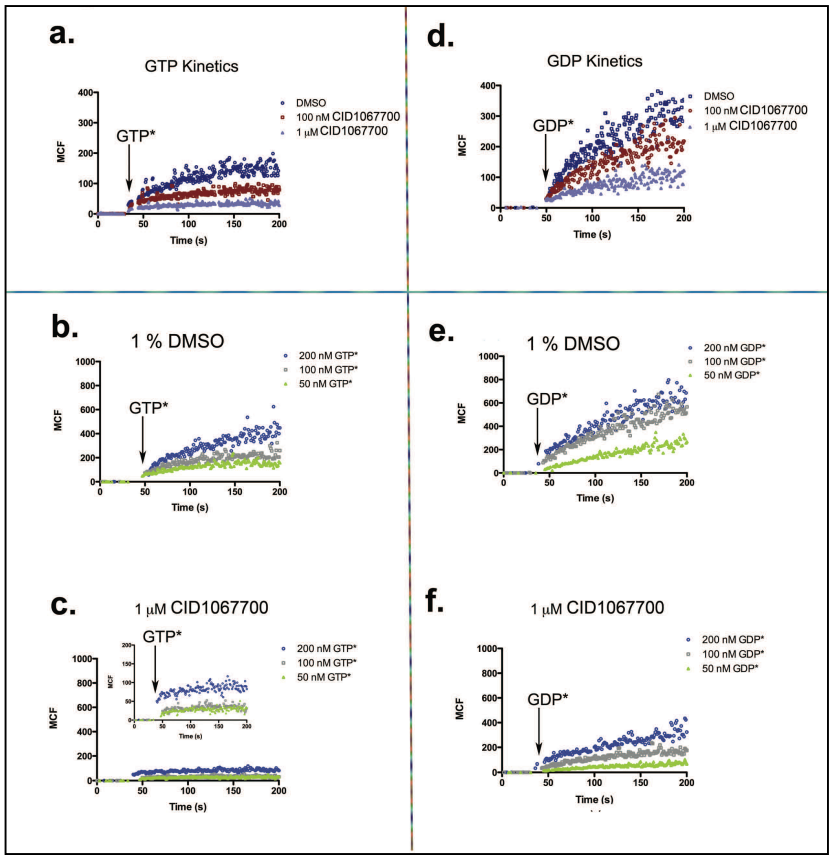

Figure 10: CID1067700 has a fast binding equilibrium and reduces the apparent number of binding sites for fluorescent nucleotide on wild type Rab7. (**a**) Rab7wt was preincubated with either 1% DMSO (blue) or CID1067700 (0.1 or 1μM) for 2 min at 4°C before addition of 100 nM BODIPY-GTP or (**b-c)** Rab7wt pre-incubated with either 1% DMSO or CID1067700 (1 μM) for 2 min at 4°C before addition of (50-200 nM) BODIPY-GTP. (**d**). Rab7wt was preincubated with either 1% DMSO (blue) or CID1067700 (0.1 or 1μM) for 2 min at 4°C before addition of 40 nM BODIPY-GDP. (**e-f**) Rab7wt pre-incubated with either 1% DMSO or CID1067700 (1 μM) for 2 min at 4°C before addition of (50-200 nM) BODIPY-GDP. Baseline fluorescence reading shown for first 50s after which kinetics of BODIPY-nucleotide binding was measured for 200s. Added nucleotide concentration ranged from 50-200 nM are color coded.

Molecular docking of CID1067700 on Rab7wt GDP and GTP bound crystal structures predicts optimal binding to the nucleotide binding pocket of the GTP-conformer

The molecular docking of CID1067700 in the nucleotide binding site of Rab7 as predicted by the experimental data was examined using molecular docking OpenEye Fred docking software (Fig. 11a-h). Docking of CID1067700 on the GDP- and GTP-conformers of Rab7 revealed that the molecule fills the nucleotide binding pocket of both conformers in a manner that mimics the nucleotides (Fig. 11a-d). However, the interaction map revealed that the compound had fewer potential interactions with GDP-conformer where the binding pocket is more exposed to solvent, which may also explain why BODIPY-GDP outcompetes CID1067700 better than the BODIPY-GTP (Fig. 11e-f**)**. Comparatively, the good alignment between CID1067700 and GNP where 5,7-dihydro-4H-thieno[2,3-c]pyran ring system has the same orientation as guanine ring system may suggest the binding mode of the small molecule in nucleotide binding pocket. However, a crystal structure determination study involving both CID1067700 and Rab7 will be required to confirm the most likely binding mode.

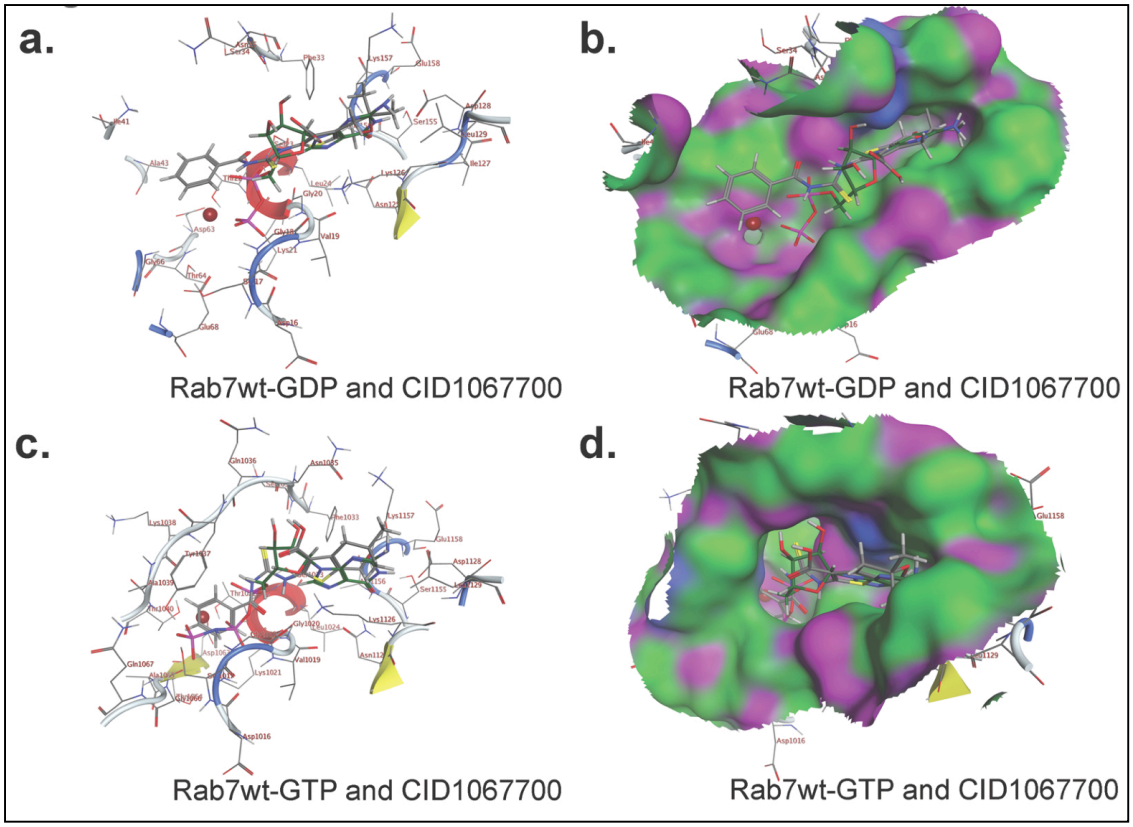

Figure 11: CID1067700 docks optimally in the nucleotide binding pocket of Rab7 in the GTP-bound conformation. (**a-d**) CID1067700 docked in the nucleotide binding site of Rab7 in the (GNP)- bound (PDB 1VG8) and GDP-bound (PDB 1VG9) conformations. Molecular docking carried out using Fred docking software. Both GTP or GDP and CID1067700 are shown simultaneously docked in the pocket for purposes of comparing their orientations in the pocket.

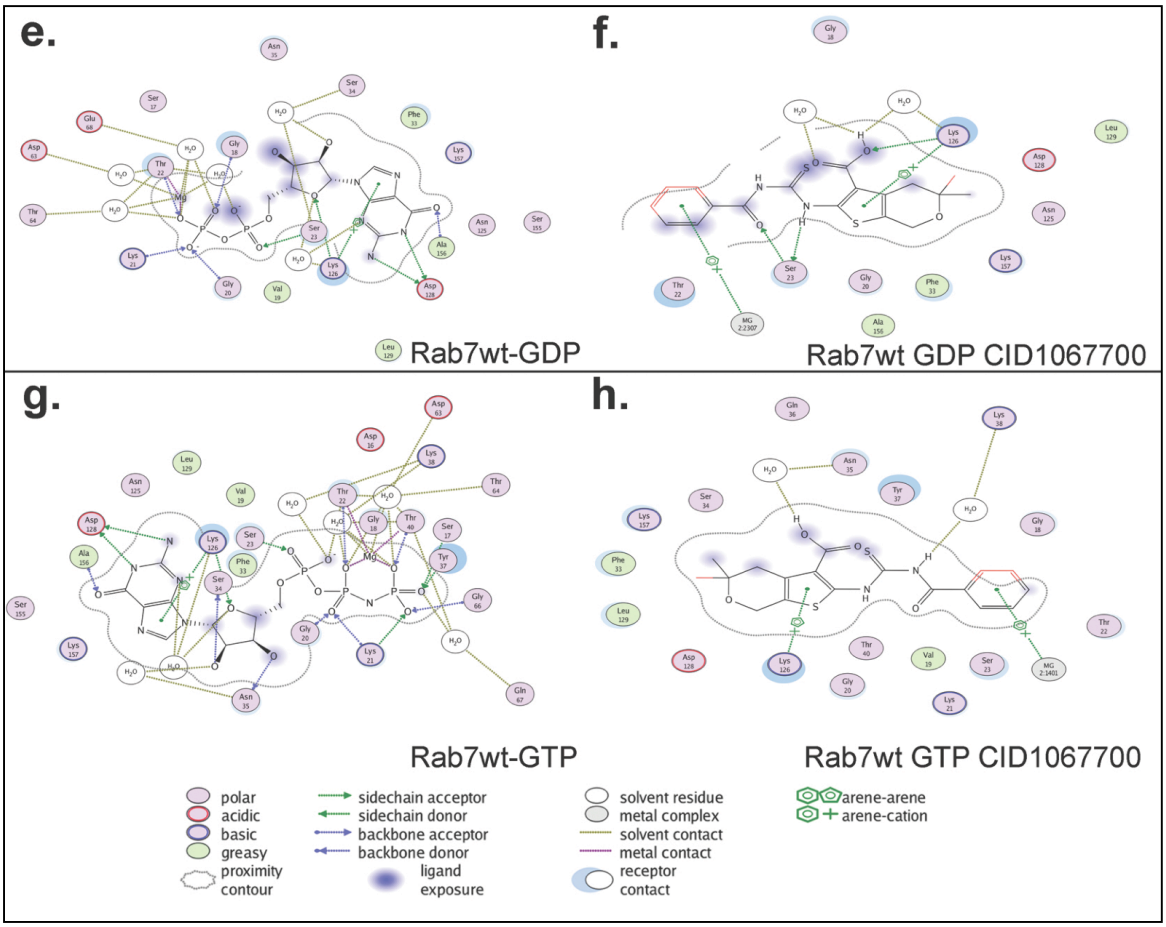

Figure 11. (**e-h)** Interaction maps for Rab7-GNP vs. CID1067700 and Rab7-GDP vs. CID1067700 illustrate differences in number and sites of interaction.

Structure activity analyses identify critical determinants for competitive inhibition

To determine structure activity relationships (SAR), eighteen variants of the parent compound were evaluated. This preliminary SAR set was obtained through synthetic effort (11 compounds) or commercial acquisition (7 compounds). The parent scaffold, represented by CID1067700, was modified in any of three major regions to afford the initial analog collection. The structural alterations focused on esterification of the carboxylic acid (R_1), geminal substitution changes on the fused pyran ring (R_2, R_3), mutation of the ring-fused pyran to an *N*-methylated ring-fused piperidine, or revision of the N-acyl thiourea linker (L). Only three of the compounds retained activity in a multiplex GTPase screen with all other derivatives being inactive (Table 2). The parent and the three active derivatives were assayed in single-plex dose response assays and EC_{50} determined against Rab7 (Fig. 12a-e and Table 5). Esterification of the carboxylic acid moiety resulted in loss of inhibition, a finding that supports the suggested participation of this group in hydrogen bonding (Fig. 11). Removal of one or both of the gem-dimethyl groups from the parental thiophenylpyran structure (R_2-R_3) resulted in a 10- or 20-fold loss in potency, respectively. The effect on potency observed with the gem dimethyl substitution suggested an advantageous lipophilic ligand-binding site interaction that is lost upon substituent removal. Alteration of the *N*-acyl thiourea linker

further attenuated potency, as demonstrated by the 35-fold loss in potency observed with *N*-acyl urea CID46916265, and the complete loss of activity for thiourea CID1280844 and amide CID740871. While further SAR work is required to attribute specific linker functionality with preferred binding interactions, these preliminary results indicate that the orientation of tethered groups, and the length and hydrogen-bonding character of the linker region are critical to maintaining a beneficial activity profile.

Table 2: Molecular scaffolds responsible for CID1067700 inhibitory activity

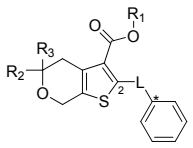

Entry	Pubchem SID	Pubchem CID	R_1	R_2	R_3	L	EC_{50} (μM)
1	57578339	1067700	H	Me	Me	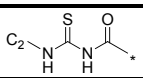	0.024
2	99381128	46916263	H	Me	H	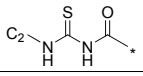	0.27
3	99381129	46916266	H	H	H	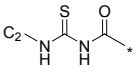	0.50
4	99361118	1251121	Me	Me	Me	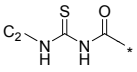	> X (limits of assay)
5	99381130	46916265	H	Me	Me	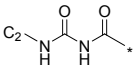	0.83
6	99381127	1280844	H	Me	Me	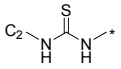	> X (limits of assay)
7	99381117	740871	H	Me	Me	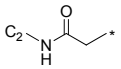	> X (limits of assay)

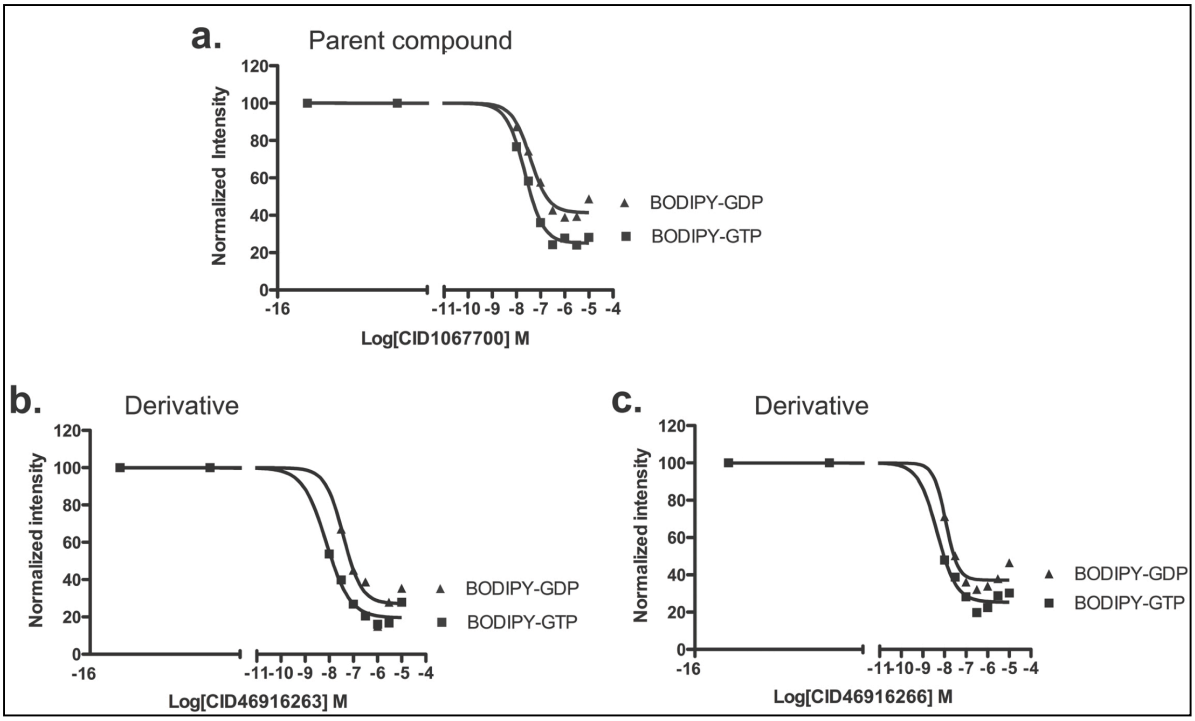

Figure 12: Structure activity relationships identify importance of linker and R-groups in inhibitory activity of CID1067700. (**a**). Fig. 1 (**d**) included for comparison with derivatives of CID1067700. (**b**) Nanomolar concentrations of CID46916263 derivative with only single methyl replacement on the pyran group and intact carbamothioylamino linker inhibit Rab7wt protein nucleotide binding; BODIPY-GTP (100 nM, filled squares) and BODIPY-GDP (40 nM, filled triangles). (**c**) Nanomolar concentrations of CID46916266 derivative with only two methyl replacement on the pyran group and intact carbamothioylamino linker inhibit Rab7wt protein nucleotide binding; BODIPY-GTP (100 nM, filled squares) and BODIPY-GDP (40 nM, filled triangles).

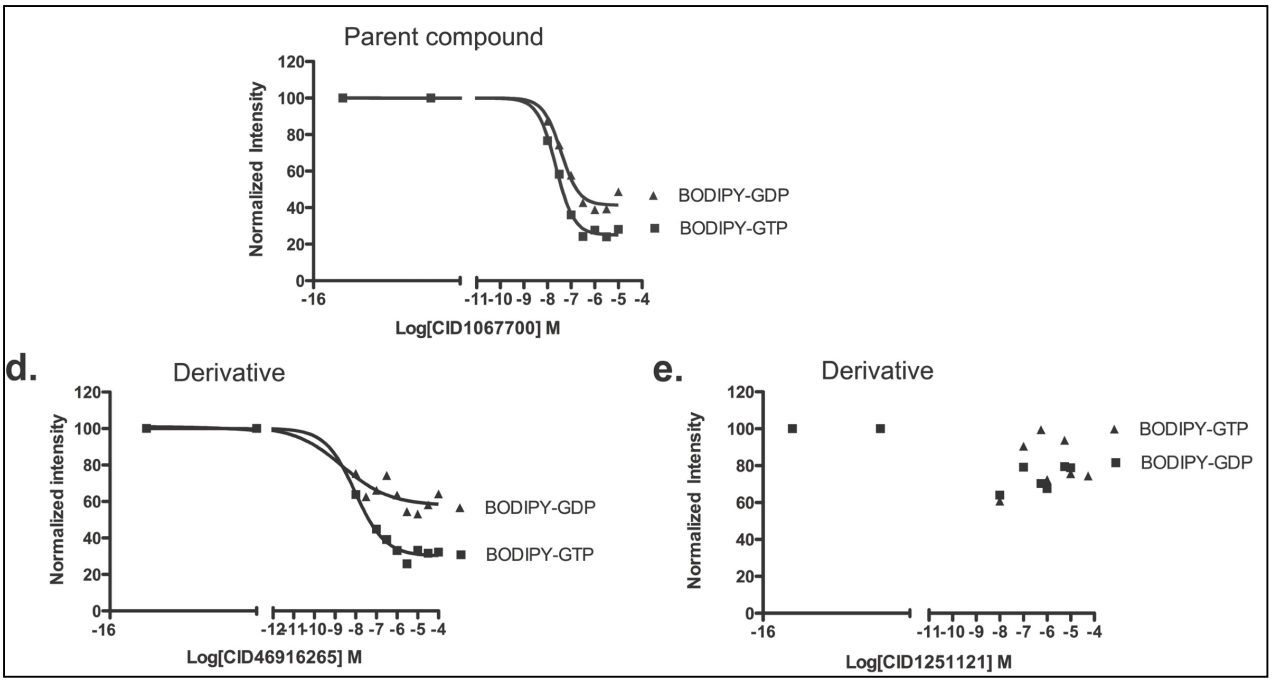

Figure 12. (**d**) Nanomolar concentrations of CID46916265 derivative with only alteration of the thiourea moiety of the carbamothioylamino linker inhibit Rab7wt protein nucleotide binding; BODIPY-GTP (100 nM, filled squares) and BODIPY-GDP (40 nM, filled triangles). (**e**) Nanomolar concentrations of CID1251121 derivative with alteration of the carboxylic acid group only do not show any activity towards inhibition of nucleotide binding by Rab7wt protein.

Discussion and conclusion

In this chapter, a small molecule (CID1067700) identified from high throughput screening has been shown to inhibit nucleotide binding by Rab7 in the nanomolar range with EC_{50} values of 25 nM for BODIPY-GTP and 40 nM for BODIPY-GDP plus calculated efficacy of nucleotide binding inhibition of 60% for BODIPY-GDP and 80% for BODIPY-GTP. Kinetic and equilibrium binding studies demonstrate that the compound acts as a competitive inhibitor and exhibits a good fit to the nucleotide binding pockets of both the GTP- and GDP-bound conformations of Rab7. By assaying rate kinetics of Rab7 nucleotide binding in the presence of CID1067700, we noted a decrease in the number of BODIPY-GTP and BODIPY-GDP binding sites on Rab7 across the entire nucleotide concentration range considered. Based on equilibrium dissociation measurements, we also showed that CID1067700 does not affect how fast or slow Rab7 releases bound nucleotide suggesting that CID1067700 inhibits Rab7 nucleotide binding through a competitive mechanism.

Initial structure activity relationships demonstrate a dependence on the lipophilic interactions with the substituted ring-fused pyran, the hydrogen bonding capability of the carboxylic acid, and the integrity of an extended *N*-acyl thiourea linker to properly extend

and orient the tethered aryl functionality. Although our assays have focused on characterizing the small molecule on Rab7, CID1067700 also exhibits inhibitory activity on other small GTPases (Fig. 6c). To the best of our knowledge CID1067700 is the first example of a competitive inhibitor for small GTPases. CID1067700 was found to also inhibit nucleotide binding by both the Rab7Q67L and Rab7T22N mutants that are known to be constitutively in the GTP and GDP bound states, respectively (30). Although the Q67L mutation lies in the nucleotide binding pocket of Rab7, the actual location of the Gln67 residue in the pocket is remote from all predicted contacts with CID1067700. From analysis of the crystal structure Thr22 residue is involved in forming interactions with Mg^{+2} cofactor which is required for GTP/GDP binding, and although CID1067700 small molecule inhibitor has a similar binding mode to nucleotides, molecular docking studies suggest that magnesium cofactor may not be essential for its binding. Another important question that the current findings raise is about the conformational state Rab7 may adopt once bound to CID1067700. This question is significance because Rab7 downstream function in cells is entirely dependent on its active (GTP-bound) state. To address this question, an in vitro effector protein binding assay was carried out and demonstrated that when Rab7 is bound to CID1067700, Rab7 is not able to bind its Rab interacting lysosomal protein (RILP) effector (**Appendix C**). This suggests that when

CID1067700 binds Rab7 the complex mimics the inactive GDP conformational state. This finding is in agreement with data that in cells incubated CID106770 epidermal growth factor receptor downregulation is impaired, consistent with inhibition of Rab7 function (Hong, Basuray, Sklar and Wandinger-Ness, unpublished observation).

Implications and significance of CID1067700 functional inhibition of Rab7

The identification of CID1067700 as a competitive inhibitor of Rab7 nucleotide binding presents an exciting and novel route to characterize Rab family proteins. Most small molecules reported to be active against low molecular GTPases are allosteric inhibitors and have activities that are restricted to the Rho-family GTPases based on their mechanism of action of blocking GEF interactions with Cdc42, Rac1 and RhoA (138). Thus, the identification of CID1067700 together with analyses of structure activity relationships suggest that it may be possible with further development to prepare more specific analogs with unique advantages when compared to traditional approaches of studying cell physiology such as conditional knock out or RNA interference as a means to perturb Rab GTPase functionality. Small molecules also can be applied to cells to rapidly and often reversibly inhibit targets. This is exemplified by Brefeldin A, an allosteric inhibitor of Arf GTPases (13) and inhibitors of phosphoinositide 3-kinases that

have been shown to inhibit specific kinase isoforms (139, 140). Moreover, Rab7 function depends on numerous protein-protein interaction partners including hVps39 (141), TBC1D15 (109, 142), RILP (36, 129, 143), ORPIL (65, 78), Rabring7 (83, 84) and the alpha proteasome subunit XAPC7 (71, 82) whose interaction with Rab7 may be potential candidates for small molecule modulation. A small molecule might also be useful for dissecting the order of protein binding to a multimeric complex and/or the importance of nucleotide for stability of the protein complex involving Rab7. Taken together, our findings present CID1067700 as a novel competitive inhibitor of small GTPase nucleotide binding that has potential for dissecting protein function in vitro. It may serve as a springboard for further development of families of compounds selective for individual GTPases like members of the Rho family of GTPases.

CHAPTER THREE

FUNCTIONAL CHARACTERIZATION OF RAC1 USING R-NAPROXEN ISOFORM

Abstract

Abnormal function of Rho family GTPases has been associated with human tumors of the colon, breast, lung, head and neck. Because of their roles in cell adhesion and migration, Rho family GTPases have been suggested as potential therapeutic targets in human cancers. In collaborative studies, Rac1 is identified as over expressed in human ovarian cancer and thus a novel target. Inhibition of Rac1 GTPase function by the R-Naproxen isoform is demonstrated, and shown to be distinct from the commercially marketed S-Naproxen. R-Naproxen was initially identified by flow cytometry based high throughput screening of the Prestwick compound library as a select non-steroidal anti-inflammatory drug (NSAID) that targets Rac1. R-Naproxen inhibits EGF-stimulated Rac1 activation as well as altering sub-cellular localization of Rac1 and its guanine nucleotide exchange factor (GEF), Tiam1 at physiologically relevant doses. In vitro assays show that R-Naproxen does not inhibit Rac1 interaction with its Tiam1 guanine exchange factor (GEF). Molecular docking predicts that R-Naproxen can favorably bind the nucleotide pocket of the GDP-bound Rac1, but not the GTP-bound Rac1, suggesting

potential inhibition through stabilization of the inactive protein. Taken together, the findings present R-Naproxen as a potential therapeutic molecule for further consideration in metastatic ovarian cancer research.

Introduction

Like the Rab family, Rho GTPases play important and diverse roles that ensure normal cellular physiology. Ten different mammalian Rho GTPases, some with multiple isoforms; Rho (A, B, C isoforms), Rac (1, 2, 3 isoforms), Cdc42 (Cdc42Hs, G25K isoforms), Rnd1\Rho6, Rnd2\Rho7, Rnd3\ RhoE, RhoD, RhoG, TC10 and TTF have been identified to date (144). Rho, Rac and Cdc42 GTPases are the most characterized members though more research continues to accumulate in this area. Currently, about 22 genes encoding different members of the Rho family have been identified in the human genome (145).

Functional role of Rac1

The primary role of Rho GTPases is centered on the assembly and organization of the actin cytoskeleton. In response to extracellular cues, activation of Rho, Rac, or Cdc42 small GTPase leads to the assembly of contractile actin:myosin filaments, protrusive actin-rich lamellipodia, and protrusive actin-rich filopodia, respectively (146-150). The

effects on the actin cytoskeleton suggest well coordinated signal transduction pathways controlled by each GTPase leading to both the formation (actin polymerization) and the organization (filament bundling) of actin filaments. The integrity of the cytoskeletal network influences processes such as cytokinesis(151-153), phagocytosis (154, 155), pinocytosis (148), cell migration (156, 157), morphogenesis (158) and axon guidance (159). These processes are highly impacted in various disease conditions like cancer. A member of the Rho family of GTPases particularly associated with coordination of cell proliferation, adhesion, and migration/invasion is Rac1. Among the Rac isoforms, Rac1 is ubiquitously expressed, Rac2 is a hematopoietic lineage-specific GTPase regulating superoxide generation via the NADPH oxidase in phagocytes, and Rac3 is expressed primarily in the brain (160-163).

The role of Rac1 in cell proliferation has been demonstrated through several findings. In cholangiocarcinomas cells, it was shown that blocking Rac1 using siRNA significantly suppressed cell proliferation and induced apoptosis (164). In another study, knock down of Rac1 using siRNA was found to impair proliferation of bovine aortic endothelial cells (165). In MDA-MB-231 cells, blocking of Rac1 using NSC23766, a small molecule which inhibits Rac1 interaction with its Tiam1 GEF, was reported to induce G1 cell cycle arrest and prevent cell proliferation (138). Rac1 activation is also associated with

cadherin-mediated cell-cell adhesion (166). This was demonstrated in normal human keratinocytes where expression of dominant negative N17Rac1 was found to inhibit E-Cadherin mediated cell-cell adhesion (167).

Cell migration plays a central role in processes such as embryonic development, wound repair, inflammatory response and tumor metastasis. The migrating cell requires actin-dependent protrusions at the front and contractile actin:myosin filaments at the rear besides stabilization of microtubules originating from the centrosome in the direction of migration (168-170). These actin based structures are to enhance targeted vesicle trafficking from the Golgi apparatus to the leading edge. Rac1 functioning in concert with WAVE and Arp2/3 promotes cell migration at the leading edge where it induces the formation of actin-rich lamellipodia protrusions, serving as the major driving force of cell motility (156, 171-174). In chemotaxing neutrophils, accumulation of Rac1 at the leading edge is aided by PI(3)-kinase and its product, phosphatidylinositol 3-phosphate (PI3P) (175). In neutrophil models, it has been shown that the polarized accumulation of PIP3 is aided by localization of the lipid phosphatase PTEN to the sides and rear of the migrating cell (176, 177). In addition to WAVE and Arp2/3 proteins in cell migration, the functional role of Rac1 in cell migration is also dependent on other interacting effector proteins. For example; DOCK180 which despite lacking requisite DbI homology-

pleckstrin homology (DH-PH) tandem domain, regulates GDP-GTP exchange of Rac and facilitates its cell migration role (178, 179).

In disease conditions such as cancer, processes of cell proliferation, adhesion, and migration are key determinants of disease severity. More often the lethality of cancer is heavily influenced by how far the tumor cell has spread from the point of origin. This situation thus makes therapeutic targeting of Rac1 as well as Rac1 driven migratory processes a tractable strategy. As alluded to above, whether under physiologically normal conditions or in disease states, all Rac1 associated functions do not occur in isolation but rather depend on their interaction with regulatory effector molecules.

Regulation of Rac1

Like the Rabs, Rho GTPases also undergo prenylation prior to membrane recruitment (146). They equally cycle between an active GTP-bound state and an inactive GDP-bound state (Fig. 1). This transition is similarly controlled by (a) Rho guanine nucleotide exchange factors (GEFs) (180); (b) Rho GTPase- activating proteins (GAPs) (181); and (c) Rho guanine nucleotide dissociation inhibitors (GDIs), that block spontaneous activation (182). Many Rho GEFs were originally identified as oncogenes after transfection of immortalized fibroblast cell lines with cDNA expression libraries (183).

Characteristically, nearly all Rho GEFs share DH (Dbl homology) domain adjacent to a PH (pleckstrin homology) domain features. Notable among the Rho GEFs is the T-cell invasion and metastasis 1 (Tiam1) protein. Tiam1 was originally identified in a retroviral insertional mutagenesis screen of murine T-lymphoma cells (184). Tiam1 possesses the characteristic Dbl homology (DH)–pleckstrin homology (PH) domain combination and is widely expressed (185). The Tiam1 protein consists of two N-terminal PEST domains, an N-terminal PH domain (PHn), a coiled-coil region with adjacent sequence (named CC-ex) (186, 187), a Ras-binding domain (RBD) (188), a PSD-95/DlgA/ZO-1 domain and the characteristic catalytic DH–PH (named PHc) combination.

In the cell, Tiam1 is primarily localized on the membranes, an environment found to be crucial to its induction of Rac-mediated membrane ruffles and activation of c-Jun N-terminal kinase (187). While the presence of a lipid domain is key to Tiam1 GEF activity, phosphorylation is another event that may directly trigger its membrane translocation and/or GEF activity. Tiam1 is reported to be phosphorylated on threonine residues by Ca^{2+}/calmodulin kinase II (CaMK-II) and protein kinase C (PKC) in vitro and upon treatment of Swiss 3T3 fibroblasts with lysophosphatidic acid (LPA) and PDGF in vivo (189-191). Thanks to virtual screening and rationale design, the small molecule

NSC23766 was identified and confirmed as an inhibitor of Rac1 interaction with Tiam1 (138).

Like the GEFs, a large number of Rho GTPase family GAPs have been identified to date (181). For the case of Rac1, β2-chimaerin, ArhGAP1, and YopE have been identified to possess GAP activity (192-194). As opposed to YopE, which possesses GAP activity towards Rac1, Rho and Cdc42 (193), β2-chimaerin GAP activity was shown to be phospholipid dependent and more specific towards Rac1 than Rho and Cdc42 (194). In both Rab7 and Rac1 GTPases, the regulatory process involving GEFs, GAPs and effector molecules is conceptually analogous to an electronic circuit system in which GEFs act as electronic signal amplifiers, while GAPs that inactivate the GTPase present as signal attenuators. Effector molecules that couple GTP bound (active) GTPase proteins with downstream signaling events are analogous to electronic signal integrators. Granted the dependence of Rab or Rho GTPase function on partner molecules, careful elucidation of both regulatory factors and effectors is crucial for effective implementation of therapeutic strategies taking into consideration the need to avoid pathways with functional redundancies.

Association of Rac1 GTPase with human disease: Rac1 and cancer

Mounting evidence has linked Rho GTPases with cancer development (**Appendix D**) (195-198). Abnormal function of Rho GTPases has been associated with human tumors of the colon, breast, lung, head and neck, and ovary (199-203). A member of the Rho GTPases widely expressed in several human cancers is Rac GTPase (204-206). Its role in cell migration is a key determinant of tumor cell metastasis (Fig. 13).

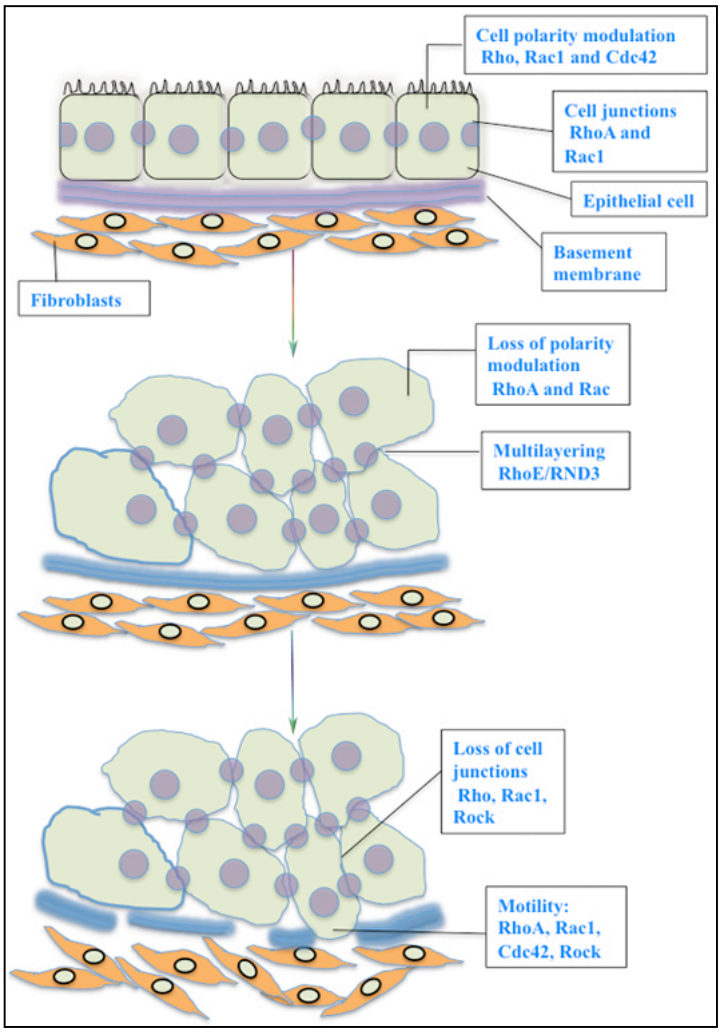

Figure 13: Rho family of GTPases in tumor metastasis. Rac1 is involved in processes leading to loss of cell polarity, loss of cell-cell junctions and cell motility. Rho like Rac1, regulates processes that coordinate loss of cell polarity and multilayering, loss of cell-cell junctions and cell motility. These are characterized by formation of stress fibers and focal adhesion that in turn ensure both amoeboid and mesenchymal migration. Cdc42 is associated with processes that establish normal cell polarity as well as migratory polarity with the latter marked by protrusive actin-rich filopodia at the leading edge of the cell.

The role played by Rac1 GTPase in cancer pathogenesis has been well documented. In proliferating epithelial breast cells and breast cancer, Rac1 protein was found to be highly expressed and to be linked to metastasis of these cells (207). In the same vein, in a breast cancer cell line, inhibition of Rac1 using Rac inhibitor EHT1864 down-regulated ERα expression and breast cancer cell proliferation (208). ERα plays a critical role in the pathogenesis of the breast cancer disease (209-211). Another group showed that Rac1 is critically involved in non-small cell lung adenocarcinoma (NSCLA) cell migration, invasion and lung metastasis of SP cells (212) which echoed previous research linking tumorigenesis in LSL-K-rasG12D mouse model of lung adenocarcinoma with the expression levels of Rac1 (213).

In many colorectal cancers, Rac1 or the Rac1 specific GEF (Tiam1) is over expressed (214-216). Tiam1 in colorectal cancers is a transcriptional regulator of the canonical Wnt signalling pathway (215, 217). The synergy of Rac1 and Tiam1 expression levels in colorectal cancers correlate with the findings that showed that an interplay of Rac1 and Tiam1 modulates Wnt target gene transcription by associating with the β-catenin/TCF transcription factor complex at Wnt-responsive promoters (218). Dysregulation in Wnt signaling is associated with the development of many cancers including colorectal cancer (219). The role of Rac1in some cancers sometimes may depend on a more complicated

pathway. For example, in SKOV3 ovarian cancer cell line, the Rac1 role in cancer development was found to be dependent on the Crk/Dock180/Rac1 pathway (220) and important in ovarian cancer cell proliferation, motility and invasion (220).

Ovarian cancer occurs with high prevalence, killing about 20,000 women annually (221, 222). Most cases of ovarian cancer are diagnosed when the cancer has already spread, leading to 5-year survival rate of less than 40 % (222). The main reasons behind this poor prognosis are: (i) lack of understanding of the molecular underpinnings of the disease and (ii) predominant localization of ovarian cancer cells within the peritoneal region which complicates early diagnosis (222). At the molecular level, one strategy for addressing the ovarian cancer problem is through targeting a protein that is directly associated with cancer cell metastasis such as Rac1 GTPase. This strategy is not only vital in the context of having a grasp of the ovarian cancer disease etiology but also may present Rac1 as a potential therapeutic target in ovarian cancer disease.

For many years, dominant negative mutants of Rac have been the preferred choice in studying Rac function in cells. However, given the difficulty of introducing high concentrations of the Rac mutants into primary cells coupled with non-specific effects of the mutants on effector molecules such as Rho guanine nucleotide exchange factor (GEF)

activities, it has become desirable to explore the use of small molecules to target Rac activities. Different strategies have been applied for this purpose. In one approach small molecules to modulate Rac1 nucleotide binding and therefore interfere with downstream events linked to Rac1 activation have been developed. One such inhibitor is EHT1864 (223). Functionally, EHT1864 inhibits Rac family GTPases by placing Rac1 in an inert and inactive state (guanine nucleotide displacement mechanism) and thus impairing Rac1-mediated functions in vivo (223). The second approach involves small molecule interference of Rac1 protein-protein interactions with the best characterized one being NSC23766 specific inhibition of Rac1-Tiam1 interaction (14, 14, 138, 224-226).

A strategy for targeting Rac1 protein function through non-steroidal anti-inflammatory drugs (NSAIDs) has established by the Wandinger-Ness lab in collaboration with Hudson, Sklar and colleagues. NSAIDs are commonly used for pain management and best known for their inhibitory activity on cyclooxygenase enzymes. Preliminary data accumulated from high throughput screening (HTS) performed by the UNM Center for Molecular Discovery suggested that Rac1 may be functionally regulated by NSAIDs (unpublished). The limited, documented studies on the use of NSAIDs to manage human cancer have tended to be mainly epidemiological with little thrust on the molecular basis of the disease (227-229), which may provide beneficial effects in terms of cancer stage

and age of onset. It was therefore the aim of the dissertation work to elucidate how the NSAID drug, Naproxen, may regulate Rac1 protein function in an ovarian cancer cell line.

Naproxen comes in two isomeric forms, R-isomer and S-isomer (Fig. 14). Both have the same chemical formula but different conformations in space at the chiral center (230). The two different conformations can induce different chemical behaviors between the two isomeric forms that will be shown in the results section. This is in line with the increasing experimental evidence showing that chiral NSAIDs inhibit both COX-2 and COX-1 isoenzymes with comparable stereoselectivity (231, 232). For instance, in an in vitro system of guinea pig whole blood, lipopolysaccharide (LPS)-stimulated human monocytes, and purified preparations of COX-2 from sheep placenta, S-enantiomers of ketoprofen, flurbiprofen, and ketorolac were found to display exclusive inhibitory effect on COX-2 enzyme as opposed to COX-1 (232). In cancer studies as well, R-etodolac was shown to be better at inducing apoptosis of prostate cancer cells than the S-etodolac (233). In this study, we provide evidence that the R-enantiomer of Naproxen as opposed to the S-enantiomer functionally inhibited Rac1 and its associated downstream cellular processes in ovarian cancer cell lines. A related NSAID, 6-methoxy-2-napthalene acetic

acid (6-MNA) compound (Fig. 14**)** which is structurally very similar to Naproxen but lacks chiral center was used as a negative control.

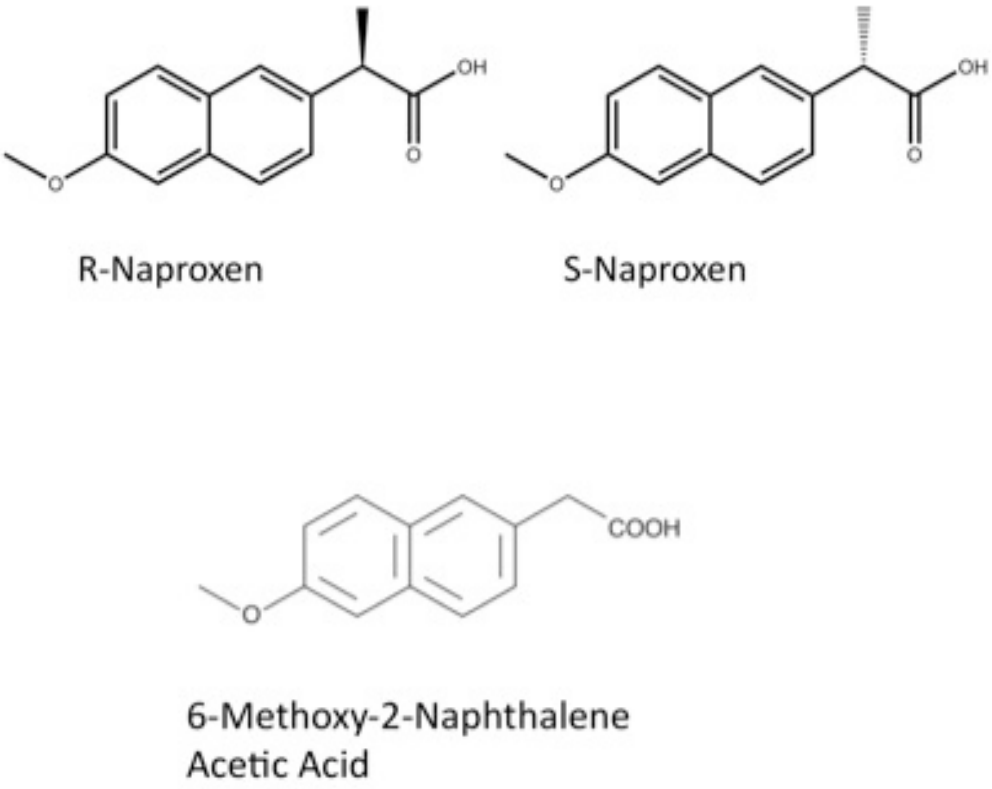

Figure 14: Molecular structures of the NSAID compounds used in the study

Materials and Methods

Reagents

Reagents used in this part of the study were obtained from different sources as indicated. G-LISA™ Rac Activation Assay kit (Cytoskeleton, Denver, CO, USA), RhoGEF exchange assay kit (Cytoskeleton, Denver, CO, USA), DMEM and MEM media (Invitrogen, Carlsbad, CA, USA) and c-Myc Tag IP/Co-IP Kit (Thermo Fisher Scientific, Rockford, IL, USA). R-Naproxen, S-Naproxen and 6-methoxy-2-napthalene acetic acid (6-MNA) were obtained from the chemical library of off patent drugs (Prestwick, Washington DC, USA), Sigma-Aldrich (St. Louis, MO, USA) and Cayman Chemical (Ann Arbor, MI, USA), respectively.

Rac1 activation assay in the presence of Naproxen

The Rac1 activation assay was carried out using G-LISA™ Rac Activation Assay kit procedures (Cytoskeleton, Denver, CO, USA). The principle of the assay is based on the interaction of active Rac (Rac-GTP) with its p21-kinase (PAK1) effector. The bound active Rac is detected with a Rac specific antibody. The extent of Rac activation is based on the absorbance readings (read at 490 nm) between the activated cell lysates versus non-activated cell lysates. The assay was carried out in Swiss 3T3 fibroblast and

OVCA433 cell lines. Swiss 3T3 cells are known to a show robust Rac1 activation upon EGF stimulation and were therefore used for baseline kinetic measurements. The Swiss 3T3 cells were cultured in DMEM media (DMEM, L-glutamine, Penicillin/Streptomycin antibiotic and fetal calf serum) and then subjected to a two-step starvation by sequentially scaling down the concentration of fetal calf serum (FCS). The OVCA433 cells were first cultured in MEM media (MEM, L-glutamine, Penicillin/Streptomycin

antibiotic and 10% fetal calf serum) for 24 h and then starved for 24 h in the culture media containing 0.1 % bovine serum albumin (BSA). A time course of EGF-dependent Rac1 activation was first carried out in both cell lines without any small molecule. This established 2 min of EGF stimulation for maximal Rac1 activation.

In the presence of small molecule, the starved OVCA433 cells were appropriately treated for 1 hour with R-Naproxen (300 μM final), S-Naproxen (300 μM final), and 6-MNA (300 μM final) dissolved in aqueous buffer system. To enhance the dissolution of R-Naproxen and 6-MNA in aqueous buffers, the pH of the solution had to be adjusted to at least 8.0 using 40 mM Tris-Base while S-Naproxen was dissolved in double distilled water. One set of treated cells was then stimulated with EGF (10 ng/ml final) for 2 minutes before harvesting and storing the cell lysate as per prescriptions of the G-LISA™

Rac Activation Assay kit. The starved Swiss 3T3 cells were subjected to a time dependent treatment with R-Naproxen and 6-MNA before stimulation with EGF (10 ng/ml) for 2 minutes. Harvesting and storage followed the same procedure as for the OVCA433 cells.

Rac1 guanine exchange factor (GEF) assay in the presence of Naproxen

The Rac1 GEF assay was carried out according to the protocol outlined in the RhoGEF exchange assay kit, BK100 (Cytoskeleton, Denver, CO, USA). Immunoprecipitated myc-tagged Tiam1 was used in the assay for GEF activity. HeLa cells were cultured for transfection using standard cell culture procedures. At 80% confluency, the cells were transfected with myc-Tiam1 plasmid using Lipofectamine^{TM} 2000. The cell lysate was harvested according to procedures stipulated in the c-myc tag IP/co-IP kit (Thermo Scientific, Pierce Biotechnology, Rockford USA) and then stored at -80^{o}C. To carry out the Rac1 GEF assay in the presence of small molecule, the following procedure was adopted. Phosphatidylinositol 4,5-bisphosphate (PIP2) lipid in $CHCl_3$: MeOH:H_2O mixture was dried under vacuum and then redispersed in immunoprecipitation elution buffer (50 μl) using intermittent bath sonication and vortexing. The equivalent of 10 μM of PIP2 lipid (final) was incubated with 1 μM Myc-Tiam1 (full length) solution for 5

minutes at room temperature as reported earlier (234) and then put on ice. His-Rac1 (45 μM final) constituted in sterile water was mixed with nucleotide exchange buffer (20 mM Tris-HCl pH = 7.5, 50 mM NaCl, 10 mM $MgCl_2$, 5 % BSA and 0.75 μM Mant-GTP) in a 100 μl volume (final) in a light sensitive 96 well plate. 1 % DMSO (final), 100 μM R-Naproxen in 1 % DMSO (final) and 100 μM 6-MNA in 1 % DMSO (final) were then added accordingly. The mixture was briefly shaken on a bench top shaker for 30 sec before further incubation for 5 minutes at room temperature. Initial fluorescence measurements were obtained for 5 minutes on the fluorimeter plate reader (1420 Multichannel counter, PerkinElmer) by exciting mant-GTP at 360 nm and recording emitted fluorescence at 440 nm. PIP2 lipid bound Myc-Tiam1 (10 μM final) was then added to appropriate wells and fluorescence changes monitored. Control wells in the assay consisted of Rac1 treated with H_2O only and 1% DMSO. PIP2 served as a Tiam1 GEF activator in the assay by binding lipid homology domains of Tiam1 (234).

Molecular docking of R-Naproxen on Rac1

Docking calculations were performed using OpenEye Fred (Fred, version 2.2.5, OpenEye Scientific Software, Inc., Santa Fe, NM, USA, www.eyesopen.com, 2010) docking software. Rac1 crystal structure (PDB code: 1I4D) was used to dock R-Naproxen on Rac1 wild type crystal structure. Chemgauss3 scoring function was used to

evaluate ligand binding potential. Docking simulations provide only a qualitative assessment of binding probability of R-Naproxen ligand to Rac1 and should be examined with care.

R-Naproxen inhibition of COX enzymes relative to S-Naproxen

The R-Naproxen inhibitory effect on COX enzymes relative to S-Naproxen was assayed by a contracted commercial company (CEREP, Seattle, USA). The following procedures obtained from CEREP were used. For COX-1, the test compound, reference compound or water (control) were first pre-incubated for 20 min at 22°C with the enzyme (≈ 5 μg) in a buffer containing 90 mM Tris-HCl (pH 8.0), 2 mM phenol and 1 μM hematine. Thereafter, the reaction was initiated by adding 4 μM arachidonic acid and the mixture incubated for 5 min at 22°C. Following incubation, the reaction was stopped by the addition of 1 M HCl then 1 M Tris/HCl (pH 8.0) followed by cooling to 4°C. For basal control measurements, arachidonic acid was omitted from the reaction mixture.

The fluorescence acceptor (D2-labeled PGE2) and the fluorescence donor (anti-PGE2 antibody labeled with europium cryptate) were then added. After 120 min, the fluorescence transfer was measured at λex=337 nm, λem=620 and λem=665 nm using a microplate reader (EnVision, Perkin Elmer). The enzyme activity was determined by dividing the signal measured at 665 nm by that measured at 620 nm (ratio). The results

were finally expressed as a percent inhibition of the control enzyme activity. The standard inhibitory reference compound was diclofenac, which was tested in each experiment at several concentrations to obtain an inhibition curve from which its IC_{50} value was calculated.

On the other hand, the approach followed to assay inhibition of COX-2 enzyme was slightly different from that used for COX-1. The test compound, reference compound or water (control) were pre-incubated for 20 min at 22°C with the enzyme (≈ 0.2 µg) in a buffer containing 90 mM Tris-HCl (pH 8.0), 2 mM phenol and 1 µM hematine. Thereafter, the reaction was initiated by addition of 2 µM arachidonic acid and the mixture was incubated for 5 min at 22°C. For basal control measurements, arachidonic acid was also omitted from the medium. Following incubation, the reaction was similarly stopped by the addition of 1 M HCl then 1 M Tris/HCl (pH 8.0) followed by cooling to 4°C. Fluorescence acquisition and calculation of percent inhibition were then carried out in the same way as in the COX-1 assay. Unlike in the case of COX-1, they used NS398 as the standard inhibitory reference compound.

Results

R-Naproxen inhibits Rac1 GTPase in ovarian (OVCA433) and Swiss 3T3 cell lines

As discussed previously, Rac1 plays a critical role in several aspects of tumorigenesis, cancer progression, invasion, and metastasis. Rac proteins are overactive or over-expressed but not mutated in most invasive human cancers. In this study, isomeric R-Naproxen was used to characterize Rac1 function in ovarian cancer (OVCA433) and Swiss 3T3 fibroblast cell lines with and without EGF stimulation. This quantitative assay takes advantage of the interaction between activated Rac1 (Rac1-GTP) and GST tagged p21-activated kinase (PAK1) effector mobilized on a well. PAK1 is one of the six members of the family of serine/threonine protein kinases functioning as an effector of Rho GTPases (235). PAK1 controls the dynamics of cell motility by linking a variety of extracellular signals to changes in actin cytoskeleton organization, cell shape, and adhesion dynamics besides modulating cell division, apoptosis, and gene transcription processes (236). PAK1 pull down depends on Rac1 being in the GTP-bound state.

To obtain the optimum time point where maximum Rac1 activation occurs, the two cell lines used in the study were first subjected to time dependent EGF stimulation. The premise is that prior to EGF stimulation, serum starvation of the cells keeps Rac1 GTPase

predominantly in the GDP state (in the cytosol) such that EGF stimulation triggers a cascade of events that activate Rac1 and convert it to the GTP-bound state. As shown in Fig. 15a-b, both OVCA433 and Swiss 3T3 fibroblast cell lines showed maximum EGF dependent Rac stimulation after 2 min of treatment. Swiss 3T3 cells were included in the study not only to elucidate R-Naproxen effect on Rac1 in a non-cancerous cell line but also due to its robust response to EGF stimulation. Pretreatment of Swiss 3T3 cells with R-Naproxen yielded a time dependent inhibition of EGF-dependent Rac1 activation, with maximal inhibition after 1 h of drug pretreatment (Fig. 15c). While the 1 hr R-Naproxen treatment of Swiss 3T3 cells reduced EGF stimulated Rac1 activation to a level comparable to the serum starved basal level of Rac-GTP, treatment with 6-MNA followed by EGF stimulation showed modest and statistically insignificant inhibition of Rac1 activation. Time dependent inhibition of Rac1 by R-Naproxen suggests that Rac1 may be a direct target of R-Naproxen in Swiss 3T3 cells. OVCA433 cells were treated with a fixed therapeutically relevant concentration of R-Naproxen, S-Naproxen and 6-MNA (300 μM) for 1 hour before stimulating cells with EGF for 2 min. R-Naproxen blocked EGF-mediated activation of Rac1 relative to S-Naproxen and 6-MNA treated sets (Fig. 15d). Given that the assay measures levels of Rac1-GTP, the results obtained

show that R-Naproxen, but less so S-Naproxen, acts as an inhibitor of Rac1 activation in cell based assays.

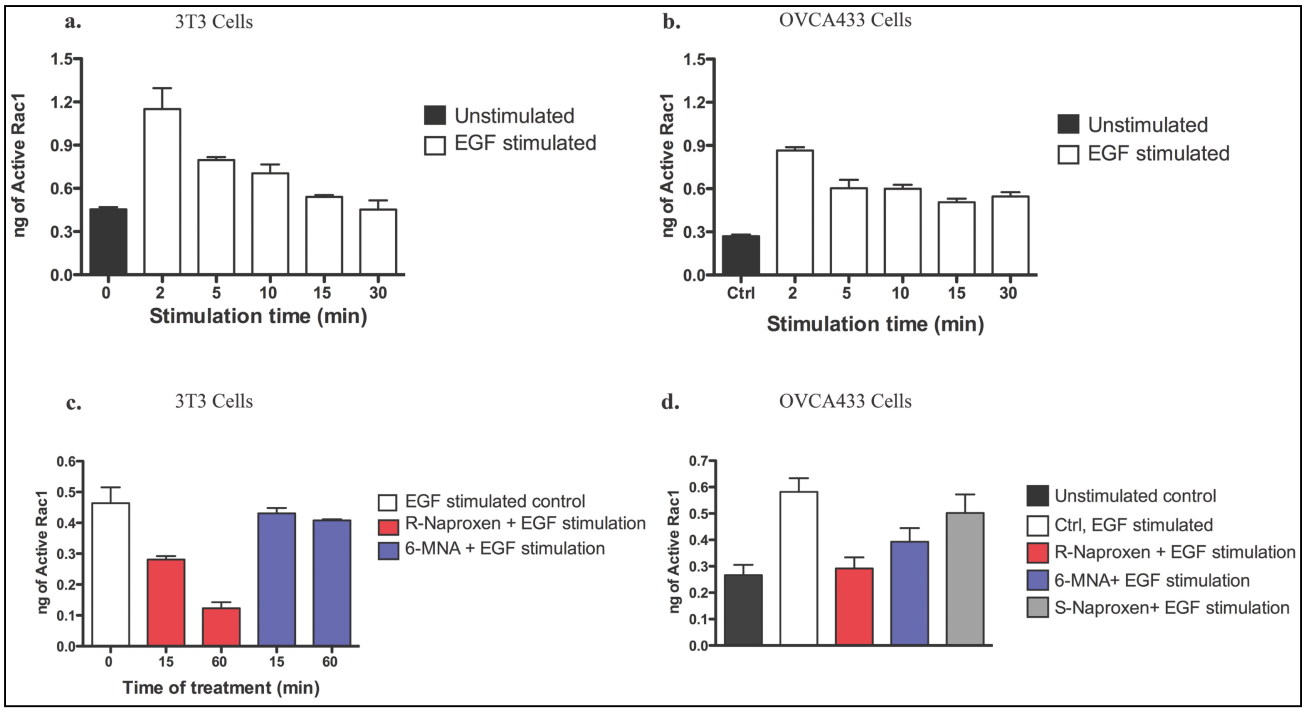

Figure 15: R-Naproxen blocks epidermal growth factor mediated Rac1 activation in OVCA433 and Swiss 3T3 cells. (**a**) Time course of epidermal growth factor mediated Rac1 activation in Swiss 3T3 cells. (**b**). Time course of epidermal growth factor mediated Rac1 activation in OVCA433 cells. (**c**). 300 μM R-Naproxen pretreatment blocks epidermal growth factor mediated Rac1 activation in Swiss 3T3 cells in a time dependent way. (d). 300 μM R-Naproxen blocks epidermal growth factor mediated Rac1 activation in OVCA433 cells after 1 h treatment. Both OVCA433 and Swiss 3T3 cells stimulated with EGF for 2 min during drug treatment.

As an independent measure of Rac1 activation status in the presence of R-Naproxen treatment, the active Rac1 membrane bound pool and the overall protein levels of Rac1 were measured by a combination of immunofluorescence and Western blot analyses. Findings are shown in Fig. 16a-c. R-Naproxen reduced the membrane bound pools of Rac1 (Fig. 16a**)** and its Tiam1 GEF (Fig. 16b**)** without affecting overall protein levels of Rac1 (Fig. 16c**)**, in agreement with the Rac1 GLISA data. Compared to R-Naproxen, treatment of OVCA433 cells with the NSAIDs of Aspirin, Ibuprofen, Fenoprofen and Ketoprofen did not cause appreciable/significant redistribution of Rac1 from the plasma membrane to the cytosol (**Appendix E**). In a wider context, inhibition of Rac1 is predicted to impair actin based processes of cell proliferation, adhesion and migration. Dr. Laurie Hudson (collaborator in the project) and colleagues measured the effects of R-Naproxen on ovarian cancer cell proliferation, adhesion and migration and determined that, R-Naproxen inhibited all the three actin based processes, a finding which correlated with inhibition of Rac1 GTPase activation. Studies conducted on OVCA429 cells by an undergraduate student in the laboratory, Anna Vestling, also showed that R-Naproxen but not 6-MNA, inhibited formation of protrusive actin-rich lamellipodia, and protrusive actin-rich filopodia (unpublished), which correlated with inhibition of Rac1 and Cdc42 GTPases respectively.

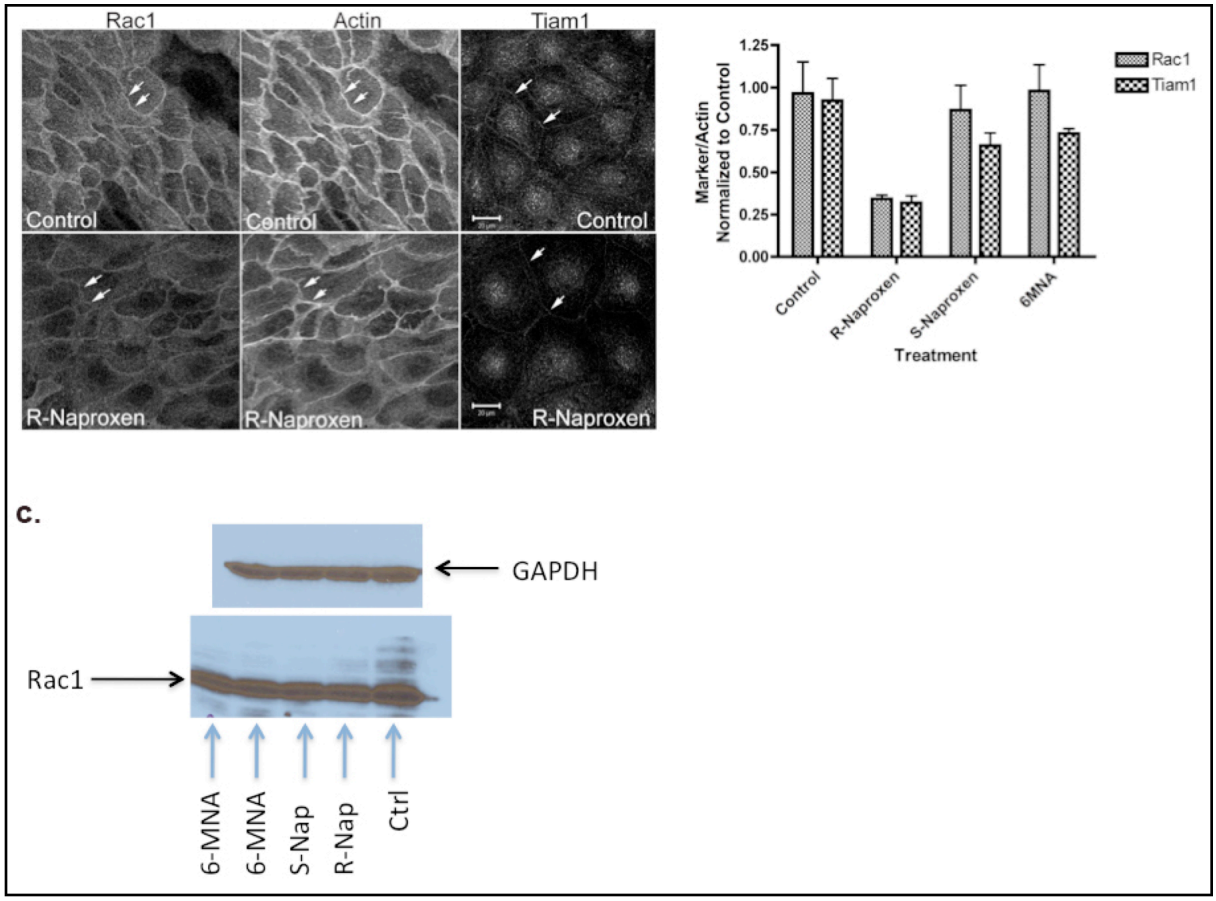

Figure 16: R-Naproxen blocks membrane localization of Rac1 and Tiam1 in OVCA433 cells. (**a**) Rac1 redistributes from the plasma membrane in the presence of 300 μM of R-Naproxen. (**b**). Quantification of fluorescence intensity from immunostaining of Rac1 in OVCA433 cells. (**c**). R-Naproxen does not affect overall protein levels of Rac1 in OVCA433 cells. The cells were treated for 1 hr with R-Naproxen or indicated NSAID.

Based on these results, first, we hypothesized that R-Naproxen could be interfering with interaction of Rac1 with its regulatory proteins such as GEFs and if that held, it would qualify R-Naproxen as an allosteric inhibitor in a cellular context (138, 237-239). Second, we hypothesized that R-Naproxen might be stabilizing Rac1 in a GDP-bound (inactive) state in a non-competitive fashion. Both cases can technically lead to less Rac1-GTP and interfere with downstream effector activation and actin remodeling required for proliferation, migration and invasion. To address these hypotheses, an in vitro qualitative assay was established to directly test the effect of R-Naproxen on Rac1 interaction with Tiam1 GEF.

R-Naproxen small molecule does not interfere with Tiam1 GEF activity on Rac1 under in vitro conditions.

A Tiam1 GEF-Rac activation assay is described in the methods section. Myc-Tiam1 protein was purified by immunoprecipiation for use in the assay. Tiam1 was first shown to be active as a Rac1 GEF in the presence of the phosphatidylinositol 4,5-bisphosphate lipid activator +/- 1% DMSO (Fig. 17a). DMSO did not interfere with Tiam1 driven GEF response (Fig. 17a). His-Rac1 was treated with 100 μM of R-Naproxen or 6-MNA and assayed for mant-GTP binding in the presence of Tiam1 GEF. Contrary to the first

hypothesis, no inhibition of Tiam1 mediated guanine nucleotide exchange by Rac1 was observed in the presence of either R-Naproxen or 6-MNA (Fig. 17b-c) suggesting that R-Naproxen may not be binding the switch regions of Rac1. R-Naproxen could be inhibiting Rac1 in the cell lines assayed via a different mechanism yet to be elucidated. This then prompted us to assess if molecular docking prediction could yield a clue on the most probable binding site of R-Naproxen on Rac1 and if so, that may be used as a guide for designing future alternative experimental approaches to assay the mechanism of R-Naproxen inhibition of Rac1 function.

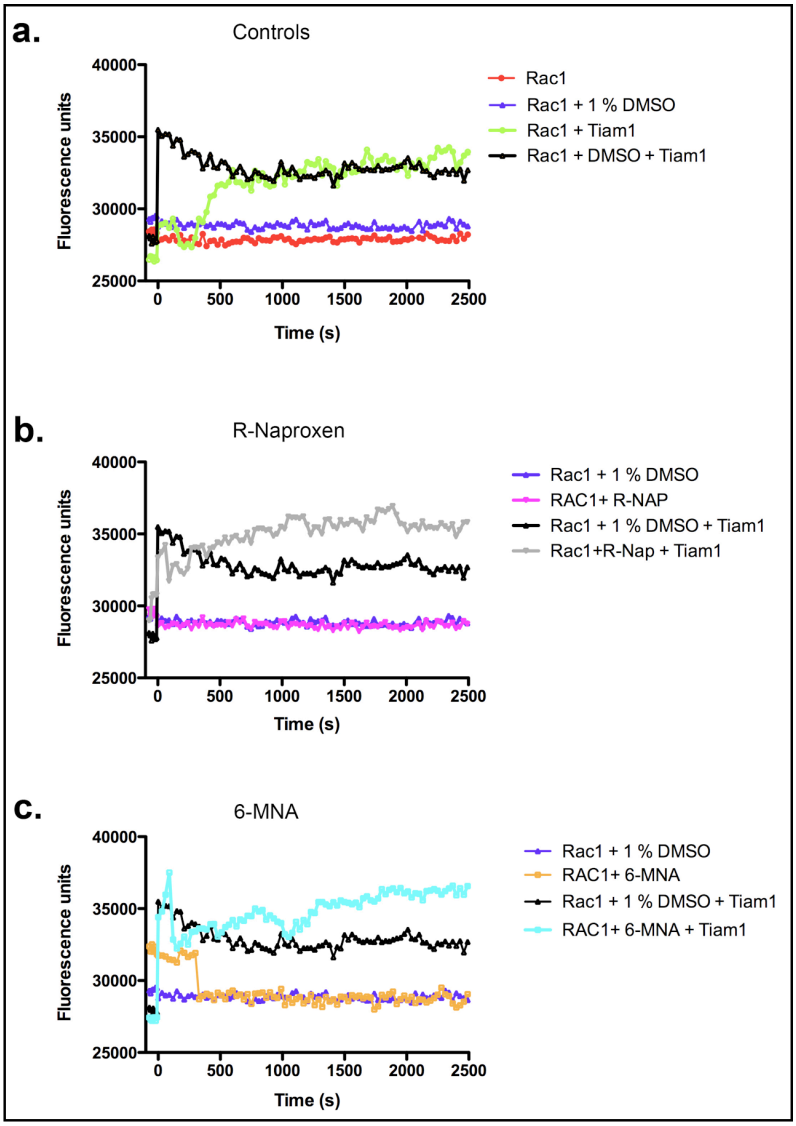

Figure 17: R-Naproxen does not block Rac1 interaction with Tiam1 GEF. (**a**) Controls showing Tiam1 GEF activity effect on Rac1 treated with water and 1 % DMSO. (**b**). Rac1 undergoes normal Tiam1 mediated transition to GDP bound state when treated with 100 µM R-Naproxen, 1 µM Tiam1 and 10 µM of phosphatidylinositol 4,5-bisphosphate lipid. (**c**) Rac1 undergoes normal Tiam1 mediated transition to GDP bound state when treated with 100 µM µM 6-MNA, 1 µM Tiam1 and 10 µM of phosphatidylinositol 4,5-bisphosphate lipid. Phosphatidylinositol 4,5-bisphosphate binds and activates the lipid homology domain of Tiam1.

Molecular docking of R-Naproxen on GDP bound Rac1 predicts possible binding of R-Naproxen to the nucleotide binding pocket

Molecular docking of R-Naproxen in the nucleotide binding pocket of GDP bound Rac1 was prompted by experimental data obtained from cell based assays as well as the in vitro Tiam1 GEF assay. The docking was performed using molecular docking OpenEye Fred docking software. The docking results (Fig. 18) predict that GDP bound Rac1 state relative to the GTP bound Rac1 is the most favorable orientation which may allow R-Naproxen to form H-bonds with Thr17 and Asp57 residues in the nucleotide binding pocket. Further examination showed that R-Naproxen may also form hydrogen bonds with Mg^{+2} cofactor in the nucleotide pocket via Naproxen carboxylic group. The GTP bound state of Rac1 is missing the nucleotide binding pocket orientation present in the GDP bound state which can accommodate R-Naproxen molecule. This suggests that R-Naproxen may prefer the GDP bound Rac1 and thus may explain results obtained in OVCA433 and Swiss 3T3 cells.

Compared to R-Naproxen, the docking of S-Naproxen yielded an unfavorable orientation of carboxyl oxygen with respect to favorable interaction with Mg^{2+} and formation of H-bonds with Thr17 and Asp57 amino acid residues. Thr17 residue is required for Rac1 activation (240). Taken together, both in vitro and cell based

experimental results present R-Naproxen as a small molecule that can functionally inhibit Rac1 in ovarian cancer cell lines. Future studies will test the mechanism of action predicted by Cheminformatic analysis (Fig. 18).

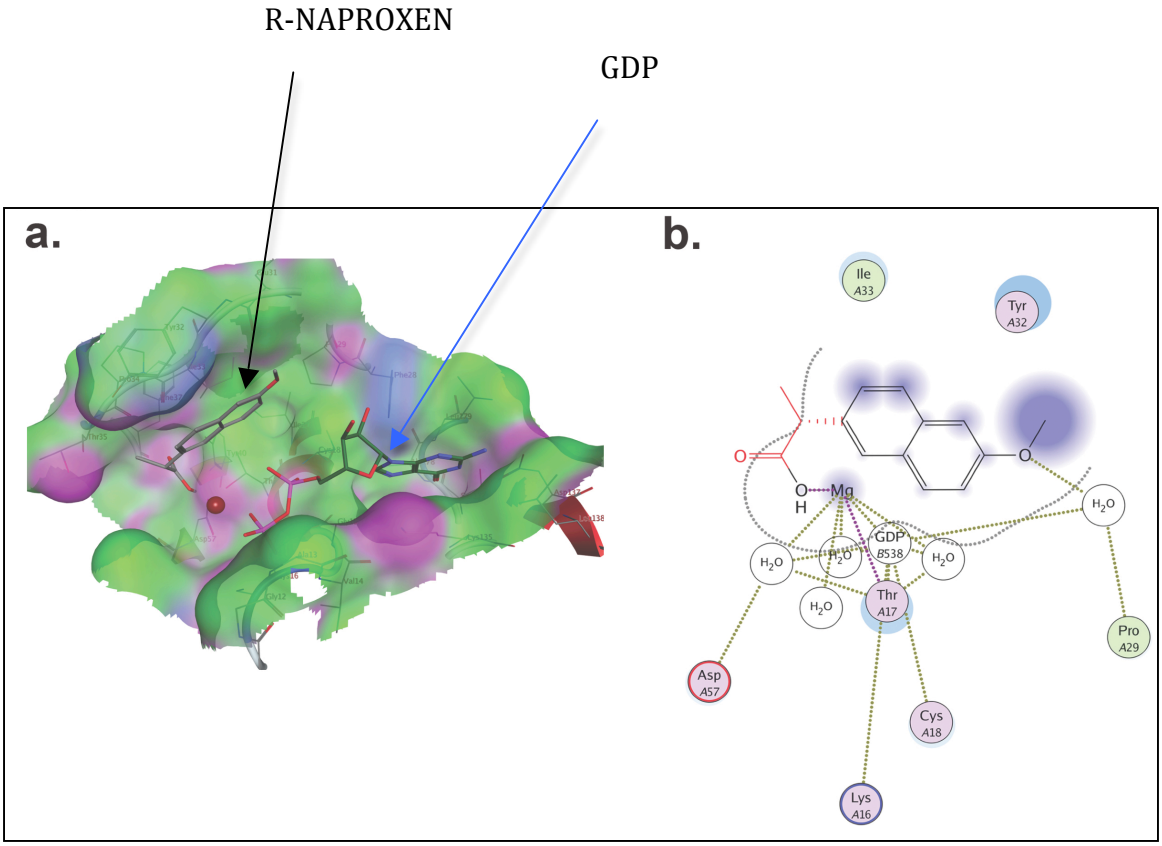

Figure 18: R-Naproxen docks optimally in the nucleotide binding pocket of GDP bound Rac1 (**a-b**) R-Naproxen docked in the nucleotide binding site of Rac1 in the (GDP)- bound (PDB code: 1I4D) conformation. Molecular docking carried out using Fred docking software. Both GDP and R-Naproxen are shown simultaneously docked in the pocket. (**c**) Interaction map for Rac1-GDP and R-Naproxen showing potential hydrogen bonding involving R-Naproxen.

Discussion and conclusion

Use of cyclooxygenase (Cox) inhibitors to modulate cancer is a field gaining currency. Rho GTPases are increasingly being targeted in cancer research due to overwhelming evidence suggesting either overexpression or deregulation of some Rho GTPases downstream signaling components in a number of human cancers (241, 242). While many studies have delineated the downstream effectors of RhoA, Rac1 and Cdc42 as responsible for tumor growth and metastasis, direct targeting of these small GTPases with small molecules is an area which has not received significant attention. In this study, data is presented on the functional characterization of Rac1 using off patent molecules of Naproxen and 6-MNA non-steroidal anti-inflammatory drugs (NSAIDs). Rac1 is shown to be functionally inhibited by the R-Naproxen isoform in ovarian cancer (OVCA433) cells and Swiss 3T3 fibroblast cells at physiologically tolerable concentrations. This is characterized by lower levels of activated Rac1 (GTP bound) and redistribution of Rac1 from the plasma membrane in the presence of R-Naproxen. Functional inhibition of Rac1 by R-Naproxen is correlated with inhibition of cell-cell adhesion and cell migration in ovarian cancer cell lines (Hudson unpublished observations). The functional role of Rac1 in ovarian cancer cells is similar to reported role of Rac1 in NSCLA SP cells where Rac1 was found to regulate cell migration, invasion and lung metastasis (212).

Earlier studies have reported that Rho GTPases are involved in the alteration of cell–cell adhesion status of tumor cells (243). Rho GTPases alter adhesion by coordinating the disassembly as well as destabilization of E-cadherin based adhesions (244, 244). Rac1 in particular has been shown to promote disassembly of cadherin-dependent adhesion via its interaction with PAK1 effector (245). Together, these studies reinforce our findings that the inhibition of cell-cell adhesion by R-Naproxen correlates with functional inhibition of Rac1. R-Naproxen was shown to alter Tiam1 distribution in the plasma membrane in OVCA433 cells even though it did not prevent in vitro Rac1-Tiam1 interaction. The observed Tiam1 membrane re-distribution is consistent with loss of OVCA433 cell-cell junction and migratory ability. Previous in vitro studies have revealed that Tiam1-mediated Rac activation is required for proper cell junction formation (246). This is further backed by a study which showed that loss of Tiam1 promotes EMT in vitro and the progression of mouse skin tumours in vivo (247, 247). There is also evidence suggesting that Tiam1 promotes apical-basal cell polarization in epithelial cells as well as promoting directional migration in freely migrating epithelial cells (246, 248, 248). Thus R-Naproxen dependent loss of Tiam1 from the membrane of OVCA433 cells may contribute to the inhibition of migration and invasion. Like other small GTPases, interaction between Rac1 and its regulatory proteins such as Tiam1 occurs via the switch

1 and switch 2 regions.

In the present study, a possible explanation for the inability of R-Naproxen to inhibit Rac1-Tiam1 interaction is that the mode of interaction involving Rac1 and R-Naproxen may not involve the Rac1 switch regions. One possible R-Naproxen binding site may be the Rac1 nucleotide binding pocket. As a prelude to address the most likely mode of action of R-Naproxen, we have employed a cheminformatics approach to show that R-Naproxen can be docked on the nucleotide binding pocket of GDP bound Rac1 relative to that of the GTP bound Rac1. This molecular docking prediction is based on the hypothesis that R-Naproxen by binding the nucleotide binding site of Rac1, may stabilize Rac1 in the GDP state.

R-Naproxen like other NSAIDs is a cyclooxygenase (COX) enzyme inhibitor. NSAIDs are known to inhibit the activity of both COX-1 and COX-2, a characteristic that accounts for their shared therapeutic and side effects (249). Their ability to inhibit both enzymes has to a large extent been attributed to physico–chemical parameter of lipophilicity (250). While the inhibition of COX-2 accounts for their common use as anti-flammatory drugs, inhibition of COX-1 may explain their often unwanted side effects such as gastric damage (249, 251). Different processes ranging from inflammation to

diseases such as cancer have been linked to COX-2 upregulation (252, 253). In terms of drug response, different NSAIDs including R-Naproxen manifest different inhibitory potency levels against COX-1 and COX-2 isoenzymes (**Appendix F**; Glaser et al. Eur J Pharmacol, 1995, 281, 107-11; Dannhardt and Kiefer, 2001, Eur J Med Chem, 36, 109-26). In the data obtained by contracted commercial entity (CEREP, Seattle, USA), R-Naproxen relative to S-Naproxen, shows lower potency against both COX-1 and COX-2 enzymes (**Appendix F**). This further emphasizes the impact of stereoselectivity between the two isoforms of Naproxen. In addition to their known function as COX inhibitors, NSAIDs have been shown to have off target effects that may contribute to their in vivo effect. Examples include modulation of γ-secretase enzyme, inhibition of the Rho small GTPase and its associated kinase Rock, inhibition of translocation of the transcription factor NF-κB which activates many genes that promote inflammation, induction of mda-7/IL-24 expression and inhibition of vascular endothelial growth factor production among others (254, 255). All these off target effects are contextually relevant in different disease states.

In this study, R-Naproxen is shown to be a novel inhibitor of Rac1 activity in OVCA333 and Swiss 3T3 cells via COX enzyme independent pathway. This is premised on the fact that structurally similar 6-MNA which like Naproxen is a classical COX

inhibitor, did not yield statistically significant inhibitory effect on Rac1 activation and associated cellular processes in the cell lines considered. More so, there are documented studies in different cancer cell lines showing that COX-2 activation occurs downstream of Rac1 activation (256, 257). The data shown hear together with other data that are part of a comprehensive collaborative study show that R-Naproxen inhibits Rac1 driven processes of ovarian cancer cell migration, invasion and proliferation. These are key processes that define tumor cell metastasis and therefore the study presents Rac1 as a novel therapeutic target in ovarian cancer.

Implications and significance of R-Naproxen functional inhibition of Rac1

There are significant and potential spinoffs of the current study. More importantly, it has presented a relatively easy route for Rho GTPase targeting in cancer using small molecule. Naproxen is an off patent and cost effective molecule which has survived all the rigors of drug development and therefore can be safely used in patients. Secondly, since the role of Rac1 in actin remodeling is coordinatively linked to other molecules, questions can be posed as to how R-Naproxen (by inhibiting Rac1 activation) may affect associated partners such as assembly of the downstream Arp2/3 complex (258, 259), nucleating promoting factors (260, 261) and insulin receptor tyrosine kinase substrate p53

(IRSp53) (262). These proteins are intimately associated with Rac1 function in actin remodeling and associated processes of migration and invasion. Functional inhibition of Rac1 also presents an opportunity to target other members of Rho GTPases that together with Rac1 define cancer metastasis. There is a need to assess how R-Naproxen isoform may functionally modulate Rho (A, B or C) and Cdc42 GTPases in the context of ovarian cancer.

There is already published evidence on the inhibition of RhoA GTPase associated signaling pathway by NSAID, Ibuprofen. The latter was shown to surmount axon growth restrictions from myelin and proteoglycans by potently inhibiting downstream pathway linked to RhoA (263). The same study also reported that, like Rho and Rock inhibitors, Ibuprofen stimulated significant neurite growth in cultured dorsal root ganglion neurons. This was confirmed by an independent group which also showed that Ibuprofen reduces ligand-induced Rho signaling and myelin-induced inhibition of neurite outgrowth in vitro (264). There are also suggestions that ibuprofen and its derivatives may prevent Alzheimer's disease by modulating astrocyte reactivity through Rho-GTPase/PAK/ERK-dependent signaling (265). All these precedents affirm the need to investigate how R-Naproxen may modulate Rho small GTPase function in cancer models. Preliminary findings by Elsa Romero in the Wandinger-Ness laboratory suggest that R-Naproxen also

inhibits Cdc42 activation in Swiss 3T3 cells (unpublished) that correlates with disruption of Cdc42 membrane localization in OVCA429 cells (Vestling, unpublished). Both findings suggest that Rho GTPase may also be a potential R-Naproxen target since Rac1, Cdc42 and Rho GTPases are functionally interdependent.

It is important to point out that RhoA and Rac1 are involved in the control of the levels of matrix metallopro-teinases (MMPs) that degrade the extracellular matrix (ECM) in addition to influencing the remodeling of the ECM by regulating tissue inhibitors of metalloproteinases (TIMPs) (245). Degradation of the ECM is a key ingredient in cancer cell migration which therefore makes RhoA targeting by R-Naproxen plausible approach. It has also been reported that Tiam1 functionally upregulates the transcription of TIMP-1 and posttranslational levels of TIMP-2 in renal-cell carcinomas (266). This also presents an option to investigate if R-Naproxen by causing Tiam1 redistribution from the plasma membrane, also affects the levels of TIMP-1 and TIMP-2.

Another point for potential extrapolation of the study is in ovarian cancer animal models. Establishing Rac1 functional inhibition by R-Naproxen in animal models will not only strengthen the current in vitro findings but may also act as a platform for translational clinical research applying Naproxen molecule in a cancer context. Taken together, this study has shown that Rac1 GTPase and associated cellular processes can be

potential targets in ovarian cancer. It has also established that a commonly used NSAID Naproxen can be used to target molecular pathways in cancer, a finding which may offer potential therapeutic opportunities. In a wider context, this study joins the rank of other investigations centered on understanding molecular processes dictating ovarian cancer metastasis and how small molecules can be used to modulate them.

CHAPTER FOUR

FUTURE PERSPECTIVES

Abstract

Different strategies can be employed to characterize a small GTPase protein using a small molecule. In this dissertation, it has been shown that CID1067700 small molecule competitively inhibits nucleotide binding by Rab7 while R-Naproxen allosterically inhibits Rac1 function. Both small molecules can potentially be optimized as probes for selective targeting of small GTPases. These findings present an important route as far as understanding how these important proteins are regulated in diverse cellular processes. To date, only few cases about use of small molecules to selectively target small GTPase proteins exist much as they dictate the progress of a number of diseases. The best examples include small molecule specific inhibition of Golgi trafficking by the fungal metabolite brefeldin A and prenylation inhibitors. The latter are however complicated by lack specificity since the approach may target a plethora of GTPases. The situation thus necessitates the need to explore other small molecules whether allosteric or competitive modulators that may be adapted for selective small GTPase targeting. The entire small GTPase activation cycle presents diverse points for potential small molecule intervention

that may ultimately provide new ideas on mechanism of action. From prenylation inhibitors to protein-protein interactions modulators, research on small molecules targeting small GTPases may open a new window of opportunity with respect to identifying new therapeutic targets in disease states as well as enabling an easier way of characterizing protein function.

Characterized molecular targets and precedents emerging from the current study

There have been some limited attempts to find small molecule modulators of small GTPase proteins of Rab and Rho sub-families. The small molecules that have been characterized to date have centered on modulation of membrane association, nucleotide binding or exchange, and inhibition of protein-protein interactions (Fig. 19). The strategy of blocking membrane recruitment through inhibition of protein prenylation (267), has proven to be effective even though it is limited due to the broad cellular importance of lipid modifications for the proper functioning of many GTPase families among other proteins. Currently, prenylation inhibitors are primarily geared towards targeting Ras GTPases. A major disadvantage of such compounds, however, is the lack of specificity/selectivity required for many applications due to overlapping inhibitor activity against farnesyl transferases and geranylgeranyl transferases. That notwithstanding, the

quest for more specific prenylation inhibitors against the GTPases is aggressively being pursued (10, 11, 268, 269, 269, 270). Even if not specific, the prenylation inhibitor results suggest that the strategy of delocalizing GTPases from membranes can be effective in some cases.

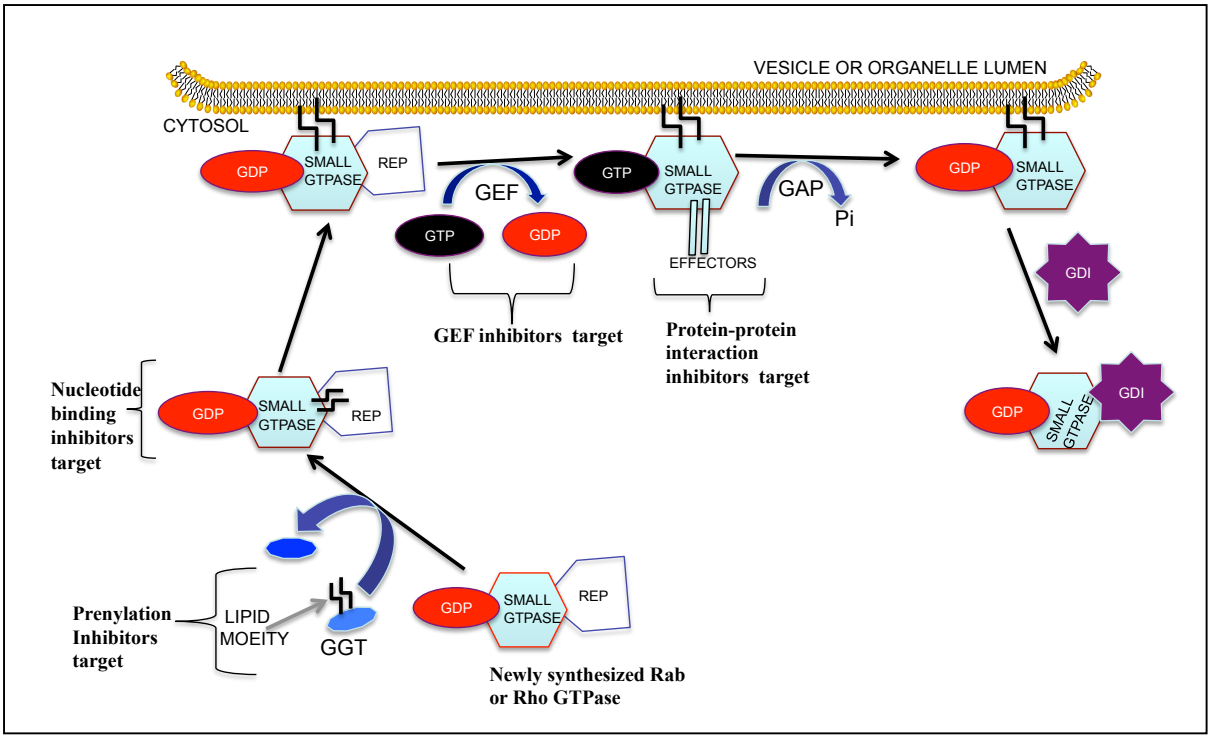

Figure 19. Regulation of small GTPases and potential small molecule modulation sites. Newly synthesized small GTPases are modified on C-terminal cysteine residues by lipid moieties (prenyl or farnesyl chains) to ensure membrane recruitment via REP. GEFs and GAPs analogously act as small GTPase signal activators and attenuators, respectively. GDI serves to regulate membrane-cytosol cycling. Potential points for targeted intervention through small molecules are denoted by brackets.

Another approach for modulating small GTPase function by small molecule is through the inhibition of regulatory protein interactions (Fig. 19). Some of the characterized examples include the fungal metabolite brefeldin A which has been successfully studied as an inhibitor of ADP-ribosylation factor 1 (Arf1) GTPase (271, 272). Brefeldin A functions by targeting specific guanine nucleotide exchange factors (GEFs), including Golgi complex-specific Brefeldin A resistance factor 1 (GBF1). A stable complex of Brefeldin A-GDP-Arf1-GEF on membranes prevents GDP/GTP exchange of Arf1 on membrane surfaces and disrupts Golgi morphology (273). Among the Rho-family of GTPases, GEF inhibitors such as NSC23766 and its analogs have been identified and characterized as allosteric regulators of protein-protein interactions that block Rac1 interaction with its GEF protein partners (14, 274). In our context, R-Naproxen may also modulate Rac1 function in cells via an allosteric mechanism by binding a site distinct from the nucleotide binding site. This may be marked by a direct or indirect inhibition of Rac1 interaction with its regulatory proteins. Inhibition of Rac1 in this way can be significant in situations such as cancer metastasis where blocking of Rac1 dependent cell migration is important. While some GEF small molecule inhibitors for the Rho family of GTPases have been characterized, none have yet been translated to clinical trials possibly due to the immense cost of preclinical studies and drug development of new chemical

entities. Hence the application of an FDA approved molecule could have significant advantages.

The therapeutic success and selectivity of competitive adenine nucleotide binding inhibitors for targeting tyrosine kinases provided the impetus for screens to identify guanine nucleotide binding small molecule inhibitors of GTPases (Fig. 19) (135). Inhibitors may come in different types. They can either be competitive or non-competitive inhibitors or just activators of nucleotide binding by the GTPase. As discussed above, there are currently few compounds that have been characterized with activity against GTPases. EHT1864 is one further example of a small molecule, which is demonstrated to inhibit Rac family GTPases albeit in a non-allosteric fashion by placing Rac1 in an inert and inactive state (guanine nucleotide displacement mechanism) and in the process interfering with Rac1-mediated functions in vivo (223). The screen performed as a collaboration between the Wandinger-Ness lab and the UNM Center for Molecular Discovery was the first to comprehensively identify both inhibitors and activators for Rho and Rab GTPase family members (135). Based on molecular docking prediction, one of our running hypotheses in this study is that R-Naproxen may modulate Rac1 function in cells in similar way as EHT1864 does by stabilizing Rac1 in the GDP bound state. If this holds, it suggests a non-competitive mechanism of inhibition of Rac1 function by R-

Naproxen and significantly, will lead to inhibition of Rac1 associated downstream signaling events that can also be useful against cancer. The caveat will be if the specificity of R-Naproxen is sufficient to avoid affecting other GTPases.

Prior to the present study, there were no known competitive inhibitors of nucleotide binding by small GTPases let alone by the Rab family. Thus, identifying CID1067700 as a competitive inhibitor of Rab7 nucleotide binding, not only presents a good platform for characterizing GTPase enzymology, but also opens new possibilities for probe development that can be extended to other GTPases. One caveat in the use of CID1067700 for cell based studies may be its potential to act as a pan inhibitor against other GTPases. However, given the SAR data presented in this study and multiplex assays performed by Center for Molecular Discovery, chemical modifications show promise of selectivity for Rab7 as compared to Rho family GTPases. This is consistent with previous studies from the Wandinger-Ness laboratory that Rab7 showed exquisite selectivity by binding BODIPY FL GTP analogues labeled on the 2' or 3' oxygen of the ribose ring, but not BODIPY FL GTP-γ-NH labeled on the γ-phosphate (133). RhoA on the other hand bound both analogues equally well, indicating nucleotide binding pocket differences that affect small molecule binding.

In a physiologic context, small molecule activators or inhibitors of small GTPase are expected to be useful in therapeutic applications for various disease states. For instance, activators may be useful for diseases where wild-type GTPase expression is reduced or there is altered activity. Typical examples include, Niemann-Pick type C disease, Huntington's disease, Charcot-Marie-Tooth disease, and some cancers and ciliopathies. On the other hand, inhibitors of guanine nucleotide binding like CID1067700 or allosteric inhibitors such as R-Naproxen can be useful for blocking activation in cells, and with refinement of specificity may offer great opportunities for modulating individual pathways in diseases where overexpression and hyperactivation of GTPases are a problem, e.g. cancers, neurodegenerative and infectious diseases. Through the mechanistic assessment of small molecules such as CID1067700 and R-Naproxen, both an enhanced understanding of the Rab and Rho GTPases with respect to their coordination with regulatory proteins, downstream effector proteins and their potential for targeted therapies may be gained.

APPENDICES

Appendix A. **Rab GTPase functions, networks and disease associations.** Rab GTPases are clustered according to their functions in: 1) Endocytosis and recycling; 2) Degradation, autophagy, phagocytosis and pinocytosis

Rab	GTPase partners	Localization	Rab Function	Pathological condition	Reference
Endocytosis and recycling					
Rab4a	Rab5a, Rab11, Rab14	Early endosomes and recycling endosomes	Regulates sorting and endocytic recycling to the plasma membrane; trafficking of human P-glycoprotein responsible for multidrug resistance of tumors; functions with Rab14 through shared effector RUFY1/Rabip4	Upregulated in rodent model of diabetic cardiomyopathy, human systemic lupus erythematosus, Alzheimer's disease and Down's syndrome; inhibited in Niemann-Pick disease; downregulated in tumor cells	(275-282)
Rab5a	Rab4a, Rab11, Rab15, Rab21	Plasma membrane, clatherin coated vesicles and early endosomes	Regulates endocytosis, early endosome fusion, nuclear signaling through APPL	Hyperactivated in lung adenocarcinoma due to upregulated Rin GEF; upregulated in Alzheimer's Disease	(276, 277, 283-287)
Rab9a	Rab7a	Late endosomes	Implicated in transport from Endosome to trans-Golgi network; lipid transport; lysosome and Lysosome related organelle	Inhibited in Niemann-Pick C disease; increased function beneficial in lipid clearance in Niemann-Pick disease and Cystic fibrosis;	(288-305)

			biogenesis	antagonized by pathogens	
Rab11a, Rab11b (neuron specific)	Arf4, Rab8a, Rab10, Cdc42	Golgi and recycling endosomes, early endosomes, phagosomes	Regulates trafficking from the trans-Golgi network to apical recycling endosomes and plasma membrane; dopamine transporter and beta2-adrenergic receptor trafficking; polarized trafficking in epithelia; phagocytosis in macrophages	Upregulated in Barrett's epithelia; neurodegeneratio n in Huntington's disease due to inactivation; Schwann cell demyelination in Charcot-Marie-Tooth type 4C disease caused by disruption of SH3TC2-Rab11 intreaction; Batten disease disrupts Hook mediated interaction of CLN3 and Rab11	(306-319)
Rab14	Rab4, Rab39	Early endosome, Golgi	Endocytic recycling of transferrin; MHC class I cross-presentation in dendritic cells; TGN to apical trafficking in epithelia; surfactant secretion in alveolar cells; insulin-dependent GLUT4 translocation; functions cooperatively with Rab4 through shared effector RUFY1/Rabip4; regulation of embryonic development through interaction with Kif16B and transport of FGF		(281, 282, 320-327)
Rab15	Rab5a	Early/sorting endosome, recycling endosome	Trafficking through sorting/recycling endosomes to the plasma membrae; attenuates Rab5 function		(328, 329)

Rab17		Recycling endosome	Epithelial transcytosis; polarized trafficking in kidney		(330-332)
Rab20		Phagosomes, mitochondria, endosomes	Vacuolar ATPase trafficking in kidney; target of HIF in hypoxia induced apoptosis; phagosome acidification and maturation; Gap junction biogenesis	Modulated by pathogens; overexpressed in pancreatic and breast cancers	(48, 333-338)
Rab21	Rab5a	Early endosomes; macropinosomes	Endocytosis of integrins, cell-extracellular matrix adhesion and motility; cytokinesis; macropinocytosis shares effectors and GEFs with Rab 5 (APPL, Rabex-5 VARP)	Involved in cancer cell motility	(339-348)
Rab22a	Rab5a, Rab7a	Early endosome, plasma membrane	Transport of transferrin from sorting endosomes to recycling endosomes; pathogen phagocytosis; enriched in glia; shares effectors and GEFs with Rab5 (Rabex-5, EEA1)	Upregulated in hepatocellular carcinoma; mycobacterium tuberculosis inhibits phagosome maturation by blocking Rab22a to Rab7 transition required for late endosome fusion and phagolysosome formation	(340, 349-356)
Rab25	Rab11a	Recycling endosome	Apical recycling in epithelia, microtubule dependent transformation	Tumor progression and cancer invasiveness (down regulated in breast and intestinal cancers; upregulated in ovarian cancer and hepatocellular carcinoma)	(306, 347, 351, 357-370)
Rab31/ Rab22b		Trans Golgi network (TGN) and	Mannose 6-phosphate transport from		(371)

		endosomes	TGN to endosomes; enriched in glia; transport of proteins involved in myelination from TGN to plasma membrane via endosomes		
Rab34	Rab7a, Rab36	Golgi and endosomes	Endosomes, macropinosome formation, phagosome maturation, lysosome morphogenesis, functions with Rab36 and Rab7 through shared effector (RILP)	Diabetic nephropathy	(48, 372-379)
Rab35	Cdc42	Endosomes and plasma membrane	Fast endocytic recycling; MHC class I and II endocytosis and recycling; Tcell recpetor recycling; phosphoinositide regulation; neurite outgrowth through interfaces with Cdc42; actin remodeling through fascin effector leading to filopodia formation	Pathogen phagocytosis and trafficking	(380-388)
Rab36	Rab7a, Rab34	Golgi	Late endosome and lysosome clustering; functions with Rab7 and Rab34 through shared effector RILP	Potential function as tumor suppressor	(372, 389, 390)
Rab39	Rab14	Golgi and early endosomes, AP1 membrane domains	Caspase-dependent-IL-1beta secretion; homology to Rab14; phagosomal acidification		(48, 325, 391, 392)
Autophagy, Phagocytosis and Degradation					

Rab7a	Rab5a, Rab9a, Rab34, Arf6, Rac1	Late endosomes and lysosomes; stage I and II melanosomes; surfactant endocytosis and signaling	Transport from early to late endosomes and late endosome to lysosome fusion; bidirectional transport of signaling endosomes, autophagosomes, multivesicular bodies, and melanosomes on microtubules in association with dynein and kinesin motor proteins; axon viability; phosphoinositide homeostasis; lipid transport; activation of mTOR signaling; lung innate and adaptive immunity based on upregulation in alveolar macrophages by surfactant SP-A	Mutant in Charcot-Marie-Tooth Disease Type 2B (CMT2B); modified to promote intracellular pathogen survival; increased function beneficial in lipid clearance in Niemann Pick disease; upregulated in Alzheimer's Disease, thyroid cancer, diffuse peritoneal malignant mesothelioma, adult-onset obesity; mutation of downstream effector Vps33b causal in arthrogryposis-renal-cholestasis	(21, 27, 30, 32-34, 37, 38, 49, 51, 61, 63, 69, 71, 117, 122, 125, 287, 365, 393-398)
Rab24		Autophagosomes, nuclear inclusions	Myelination; autophagosome formation	Activated in cell culture models of neuronal and cardiomyocyte injury leading to the increased autophagy; upregulated in hepatocellular carcinoma	(351, 355, 399-403)
Rab32		Perinuclear vesicles, mitochondria, autophagic vesicles	Post-Golgi trafficking of melanogenic enzymes; ER stress mediated apoptosis; mitochondrial dynamics	Rab32 gene methylated in inflammatory bowel disease at transition to invasive growth	(346, 404-408)
Rab33		Golgi, autophagosomes	Autophagosome formation; interacts with Atg16L		(409, 410)
Rab43		Phagosome	Cathepsin D transport to phagosomes		(48)

APPENDIX B. Rab GTPase effector regulators and associated cellular functions

Rab	Rab Effector	Effector function	References
Rab4a-GTP	Rabaptin-4	Assists in the docking of transport vesicles en route from early endosomes to recycling endosomes	(411)
	Rabaptin-5	Activates Rab5 through complex with Rabex-5 and links Rab5 with Rab4	(412, 413)
	Rabip4	Regulates transport through early endosomes	(414)
Rab5a-GTP	EEA1	Coordinates tethering and fusion	(415-417)
	p110beta/p85 PI 3-kinase	Ensures coupling of the lipid kinase product to its downstream target, protein kinase B.	(418)
	Phosphoinositide 3-kinase (hVps34/hVps15)	Regulates SNARE complex formation or disassembly	(419)
	Rabaptin-5	Activates Rab5 through a complex with Rabex-5, Links Rab5 with Rab4, and facilitates membrane docking and fusion.	(412, 420, 421)
	Rabaptin-5beta	Stabilizes Rabex-5 recruitment and facilitates membrane fusion in concert with Rabaptin-5	(421, 422)
	Rabenosyn-5	Required for CCV-EE and EE-EE fusion, regulates the functional link between Rab5 and Rab4 domains	(423, 424)
	Rabip4	Regulates transport through early endosomes	(414)
Rab5a-GDP	Rabex-5	GEF for Rab5	(421, 425, 426)
	RIN1	GEF for Rab5 and activated by growth factor signaling	(427)
	RIN2	May function as upstream activator and downstream effector	(428)

Rab7a-GTP	ANKFY1	Possible role in vesicular trafficking. Novel interactor of Rab7. Specific role yet to be established	(125, 429)
	Armus/Rac1	Regulates cytoskeleton organization, ruffled border formation in osteoclasts, inactivates Rab7 and regulates E-cadherin degradation.	(21, 303)
	ATP6V0A1	Component of vacuolar ATPase that regulates organelle acidification required for protein sorting, receptor mediated endocytosis, zymogen activation and synaptic vesicle proton gradient. Novel interactor of Rab7. Specific role yet to be established	(125, 430)
	FYCO1 (FYVE and coiled-coil domain containing 1)	Implicated in microtubule plus end transport of autophagosomes presumably through interaction with kinesin.	(41)
	GNB2L1	Role in intracellular signaling and activation of protein kinase C and possible interaction with Rab7 via WD40 domain. Novel interactor of Rab7. Specific role yet to be established	(125)
	HOPS complex (Vps11,-16,-18,-33,-39 and-41)	Involved in endo-lysosomal transport. Vps39 binds Mon1-Ccz1 complex that serves as a Rab7 GEF in yeast.	(115, 431, 432)
	hVps39	In yeast, cooperates with Mon1-Ccz1 complex to promote Rab7 nucleotide exchange.	(141, 431)
	IMMT (Mitofilin)	Maintains mitochondrial morphology and suggested role in protein import. Novel interactor of Rab7. Specific role yet to be established.	(125)
	KIF3A (kinesin + adapter?)	Associates with late endosomes along with dynein, Rab7 and dynactin. Possible mediator of Rab7 regulated anterograde transport.	(70)
	Mon1a-Mon1b	Mammalian homologs of C. elegans SAND1. Mon1a-Mon1b causes Rab5 GEF displacement and Mon1b interacts with the HOPS complex. HPS1	(116, 433-435)

	ORP1L	Required for activation of dynein/ dynactin motor, regulates late endosome/lysosome morphogenesis and transport.	(78)
	Phosphoinositide 3-kinase (hVps34/hVps15)	Regulates activity of Vps34 and generates PI3P to control endosomal trafficking and signaling.	(18)
	Plekhm1 [pleckstrin homology domain containing, family M (with RUN domain) member]	Regulates vesicular transport in osteoclasts.	(304)
	Prohibitin	Negative regulator of cell proliferation and a possible tumor suppressor. Novel interactor of Rab7, specific role yet to be established.	(125)
	Rabring7	Rab7 interacting RING finger protein, functions as E3 ligase that ubiquitinates itself and controls EGFR degradation.	(85)
	Retromer (Vps26, Vps29, Vps35)	Regulates retrograde transport from late endosome to trans-Golgi network (TGN) through direct interaction with Vps26.	(436)
	RILP (Rab7 interacting lysosomal protein)	Involved in late endosomal/lysosomal maturation. Recruits dynein-dynactin motor protein complex.	(69)
	Rubicon	Regulates endosome maturation through differential interaction with UVRAG and Rab7.	(437)
	Spg21	Involved in vesicular transport. Novel interactor of Rab7. Specific role yet to be established.	(125, 438)
	Stomatin like 2 (STOML2)	Negatively modulates mitochondrial sodium calcium exchange. Novel interactor of Rab7. Specific role yet to be established.	(125)
	TrkA	Interacts with Rab7 and regulates endocytic trafficking and signaling as well as influencing neurite outgrowth.	(33, 439)

	UVRAG/Beclin1	UVRAG/C-Vps complex regulates Rab7 activity during autophagic and endocytic maturation.	(38)
	VapB	Involved in vesicular trafficking and novel interactor of Rab7. Specific role yet to be established.	(125)
	Vps13c	Vacuolar protein sorting and novel interactor of Rab7. Specific role yet to be established.	(125)
Rab7a-GTP, GDP	Ccz1	Recruited to endosomes by Mon1a/Mon1b and acts as Rab7 GEF in yeast. Possible human homolog C7orf28B also some similarity to HPS4 involved in biogenesis of lysosome related organelles.	(116, 433-435)
	TBC1D5	Negatively regulates retromer recruitment and causes Rab7 to dissociate from membrane.	(110)
	TBC1D15	Functions as Rab7 GAP. Reduces its interaction with RILP, fragments lysosomes and confers resistance to growth factor withdrawal induced cell death.	(109, 142)
	XAPC7/PSMA7 alpha proteasome subunit	Negative regulator of late endocytic transport. Overexpression inhibits EGFR degradation.	(71)
Rab7b	SP-A (Surfactant Protein A)	Transiently enhances the expression of Rab7 and Rab7b and makes them functionally active to increase the endolysosomal trafficking in alveolar macrophages.	(398)
Rab8a-GTP	Cpn 0585	Facilitates Rab8 recruitment to Cpn inclusion membrane	(440)
	FIP-2	May be implicated in morphogenesis	(441)
	TRIP8b	Regulates secretory pathway	(442)
	MAP4K2 (Rab8IP)	Rab-regulated protein phosphorylation, secretion pathway	(286, 443)
	Ahi	Ciliogenesis	(444)

	BBSome	Ciliogenesis; cilial transport	(445)
	Cenexin3 (OFD2 splice variant)	Binds microtubules and basal bodies, ciliary biogenesis	(446)
	Ellipsa (via Rabaptin5)	Intraflagellar transport	(447)
	FIP-2	Recruitment of Huntingtin to Rab8-positive vesicular structures; Polarization	(441)
	GDI-2	GDI	(448)
	GLUT4	Glucose transport	(449)
	JRAB/MICAL-L2	Adherens junction and tight junction assembly	(450)
	MICAL-L1	EHD1-Rab8a interaction, membrane tuble localization	(451)
	MSS4	Weak GEF or chaparone	(452, 453)
	Myosin Vb	Motor - Insulin-induced GLUT4 translocation	(321)
	Noc2	Effector	(454)
	OCRL1	Phosphatase	(455, 456)
	Optineurin/FIP2	Post-Golgi trafficking/exocytosis	(457)
	Otoferlin	Trans-Golgi trafficking	(458)
	Rabaptin-5	Molecular bridge for intraflagella transport	(447)
	RIM2	Scaffold	(454)
	Sro7(Sec4p-Yeast homologue)	Potential SNARE regulation	(459)
	XM_037557	GAP	(446)
Rab8a-GDP	Rabin8	GEF	(460)
	Rabin3(rat)	GEF	(460)
Rab8b	TRIP8b	Secretory pathway regulation	(442)
Rab9a-GTP	P40	Mediates late-endosome-to-TGN vesicular transport	(461)
	TIP47	Facilitates MPRs transport	(291)
	GCC185	Involved in MPRs recycling	(462)
	INPP5B	Could be facilitating secretory	(463)

		pathway	
Rab10	Cpn 0585	Facilitates Rab10 recruitment to Cpn inclusion membrane	(440)
	EVI5	Potential GAP	(456, 464)
	Exocyst	Cilial trafficking	(465)
	GDI-1	GDI	(466)
	MSS4	Chaparone	(452)
	Myosin Va,Vb,Vc	Motor	(467)
	Rim1	Scaffold	(454)
	TBC1D4	GAP	(22)
Rab11a-GTP	RIP11	Regulates multiple distinct membrane trafficking events	(468)
	RCP	Regulates protein sorting in tubular endosomes	(469)
	FIP5/RIP11	Endocytic recycling; exocytosis	(470)
	Evi5	GAP	(471)
	FIP3/Arfophilin/ Eferin	Mediate transport to the endosomal-recycling compartment, endocytic regulation, abscission	(472)
	Rab11BP/Rabphilin 11	Vesicle recycling	(286, 473)
	Sec15	Exocyst component, endocytic recycling	(474)
	FIP1	Recycling	(475)
	FIP4	Recycling, Regulation of retinal development, abscission	(476)
	FIP2	Recycling	(477)
	Presenilin 1	Trafficking chaparone	(478)
	Presenilin 2	Trafficking chaparone	(478)
	PI4-kinase β	Localization of rab11 to the Golgi complex, post-Golgi trafficking	(479)
	Myosin Va	Motor	(476, 480)
	Myosin Vb,	Motor	(481)

	D-AKAP2	Endosome morphology and protein accumulation	(482)
	D. melanogaster nuclear fallout (Nuf)	Recycling endosomes, Cleavage furrow membrane integrity, actin remodeling	(64)
	Rab6 interacting protein 1	Rab6-Rab11 interaction	(483)
	SH3TC2	Recycling endosome	(317)
	Syntaxin 4A	t-SNARE, regulatator of secretion	(484)
	Sec15	Exocyst component, endocytic recycling	(474)
Rab11a-GDP	GDP dissociation inhibitor 2	GDI	(448)
Rab11b-GTP (neuron specific)	myosin vb	Cargo recycling	(485)
	Rabphilin-11	Vesicle recycling	(473)
	Rab6 interacting protein	Links Rab6 and Rab11	(483)
	Cpn 0585	Facilitates Rab11b recruitment to Cpn inclusion membrane	(440)
	Evi5	Coordination of vesicular trafficking, cytokinesis, and cell cycle regulation	(319, 471)
Rab15	Rab15 effector protein	Regulates receptor recycling from the recycling compartment	(328)
	Cpn 0585	Facilitates Rab15 recruitment to Cpn inclusion membrane	(440)
	FIP1	Recycling	(475)
	FIP2	Recycling	(475)
	FIP3	Recycling	(475)
	Myosin Vb	Motor	(486)
	RIP11	Insulin granule exocytosis	(487)
Rab17	TBC1D7	GAP	(22, 446)
Rab21	alpha-integrin subunit	Regulates vesicular motility of integrins	(344)
	Varp	GEF for Rab21	(488)

Rab22a	EEA1	May be linking Rab22a with early endocytic pathways	(352)
	Rabex-5	Links Rab22-Rab5 signaling cascade	(356)
	Rabenosyn-5	May be involved in endosomal tethering	(489)
Rab23	EVI5-like	GAP	(22, 446)
Rab25	Integrin beta-1 subunit	Promotes cell migration	(359)
Rab27a	Exophilin4	Mediates the peripheral localization of melanosome and glucagon granules	(490-492)
Rab27a/b	Melanophilin	Mediates the peripheral localization of melanosome and glucagon granules	(493-496)
Rab27a-GDP	Granuphilin	Regulates dense-core vesicle exocytosis	(497)
Rab27a/b	Rabphilin	Modulates secretory vesicle exocytosis	(498)
Rab27a/b	Noc2	Modulates dense-core vesicle exocytosis	(498, 499)
Rab27a/b	Munc13-4	Modulates dense-granule secretion from platelets	(500)
Rab27a/b	Slp2a	Regulates melanosome transport	(490)
Rab32	Varp	Regulates Tyrp1 trafficking in Melanocytes	(339, 346)
	PKA	Regulates melanosome transport	(501)
Rab33a	ATG16L	Regulates autophagosome formation involving Rab33a	(409)
	GM130	May be involved in the docking and fusion of vesicles in the Golgi apparatus	(502)
	Rabaptin-5	May be involved in the docking and fusion of vesicles in the Golgi apparatus	(502)
Rab33b	ATG16L	Regulates autophagosome formation involving Rab33b	(410)
	Rabex-5	May be involved in the docking and fusion of vesicles in the Golgi apparatus	(502)
Rab34	RILP	Regulate lysosome	(379)

		morphogenesis	
	Hmunc13	Mediates lysosome-Golgi trafficking	(375)
Rab35	Fascin	May stimulate actin bundling	(388)
Rab36	RILP	Regulates spatial distribution of late endosomes and lysosomes	(372)
	GAPCenA	Acts as a GAP	(503)
Rab38	Varp	Regulates Tyrp1 Trafficking in Melanocytes	(346, 504)

APPENDIX C: Conformational state of Rab7 when bound to Rab7: Interaction between CID1067700 and Rab7 does not cause transition of Rab7 to GTP conformation. GST-RILP is mobilized on glutathione beads and then interaction between RILP and His-SUMO-GFP-Rab7 with Rab7 in the GTP bound state is measured using flow cytometry. Incubation with either CID1067700 or GDP precludes interaction. Fluorescence output from GFP is a measure of Rab7 binding.

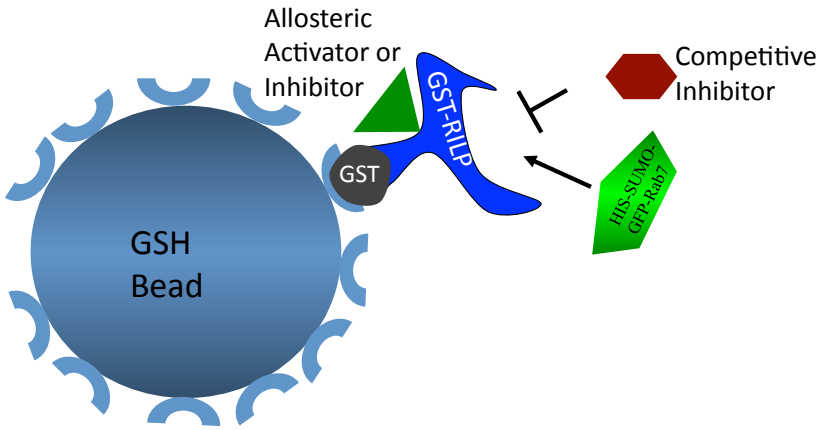

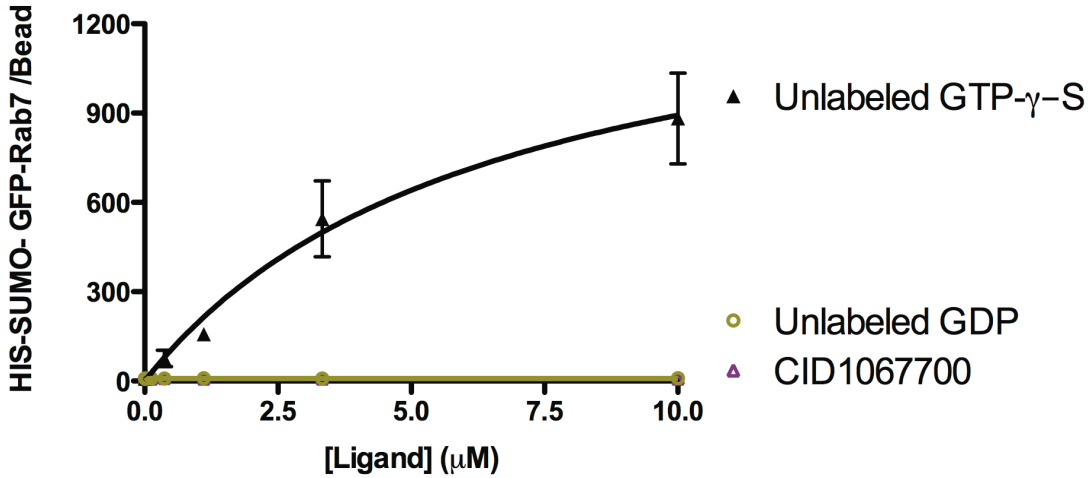

APPENDIX D. Rho GTPase (1). Key functions, (2). Some of the characterized GEFs and GAPs, and (3). Association with cancer

Rho GTPase protein	**Key function**	**Characterized GEF**	**Characterized GAP**	**Cancer link**	**Reference**
Cdc42	Regulates formation of and filopodia, maintenance of cadherin-mediated cell-cell adhesion	Dbs; Intersectin,Tuba, CopE, Fgd1, Vav1/2/3, Ephexin, Asef, DOCK2/9	p50rhoGAP (GMPPNP), n-Chimaerin	Breast, melanoma, squamous-cell carcinoma (SCC), colorectal, testicular	(180, 505-514)
Rac1a	Regulates cell membrane ruffling, formation of lamellipodia, maintenance of cadherin-mediated cell-cell adhesion	Tiam1, Vav1/2/3, Ephexin, Trio, Sos1/2, Asef, Dock4	β2-chimaerin, n-Chimaerin, ArhGAP15	Breast, melanoma, SCC, colorectal, lung, testicular, gastric, renal	(180, 193, 507, 511, 511-518).
Rac1b	Suspected to promote cellular transformation			Colon, breast	(207, 512, 519)
Rac2	Regulation of NADPH oxidase activity,	DOCK2/9, P-Rex1		Head and neck squamous-cell carcinoma, chronic myelogenous leukemia	(520-524)
Rac3	Regulates cell invasion			Non-IBC	(512, 525)

RhoA	Regulates formation of actin stress fibers and focal adhesions, Implicated in thrombin-, serum-, and LPA-induced neurite retraction and cell rounding, maintenance of cadherin-mediated cell-cell adhesion, regulates cytokinesis	XPLN, Vav1/2/3, Ephexin, Syx, p63RhoGEF, Tech, Arhgef5,	ARAP3, MgcRacGAP	Colon, breast, lung, testicular germ cell, head and neck squamous-cell carcinoma; melanoma, colorectal, pancreas, lung, testicular, ovarian, gastric, liver, pelvic ureteric, prostrate, neuroblastona, bladder, leukemias AML, sarcoma, hepatocellular carcinoma	(180, 511, 512, 520, 526-540)
RhoB	Mediates apoptosis	XPLN		Breast, lung and HNSCCa	(537, 541-546)
RhoC	Modulates induction of angiogenic factors	SmgGDS		Inflammatory breast cancer, pancreatic ductal adenocarcinoma; breast IBC; non-IBC; melanoma; SCC; pancreas; lung; non-small cell lung cancer; ovarian, gastric; bladder; Hodgkin's, hepatocellular carcinoma, prostrate	(512, 539, 547-550, 550-554)
RhoD	Regulates cell migration and cytokinesis,				(555, 556)
RhoE/Rnd3	Cytoskeletal organization and cell cycle progression, regulates activity of RhoA			Non-small cell lung carcinoma	(557, 558)
RhoG	Regulates endothelial apical cup assembly, regulates the neutrophil NADPH oxidase, regulates gene expression and the	Trio		Non-IBC	(512, 559, 560)

	actin cytoskeleton in lymphocytes				
RhoH	Acts as an adaptor molecule in TCR signaling pathway			Non-Hodgkin's lymphoma, multiple myeloma Diffuse large B-cell lymphomas	(512, 561, 562)
Rnd1/2/3	Regulates axon guidance and neurite extension, regulates formation of stress fibers			Non-IBC	(512, 557, 563)

Appendix E. **Comparative functional effect of other NSAIDs on Rac1:** i) Aspirin; ii) Ibuprofen; iii) Fenoprofen; iv) Ketoprofen, do not show significant effect on membrane localization of Rac1 GTPase in OVCA433 cells at similar concentration of treatment and duration as R-Naproxen.

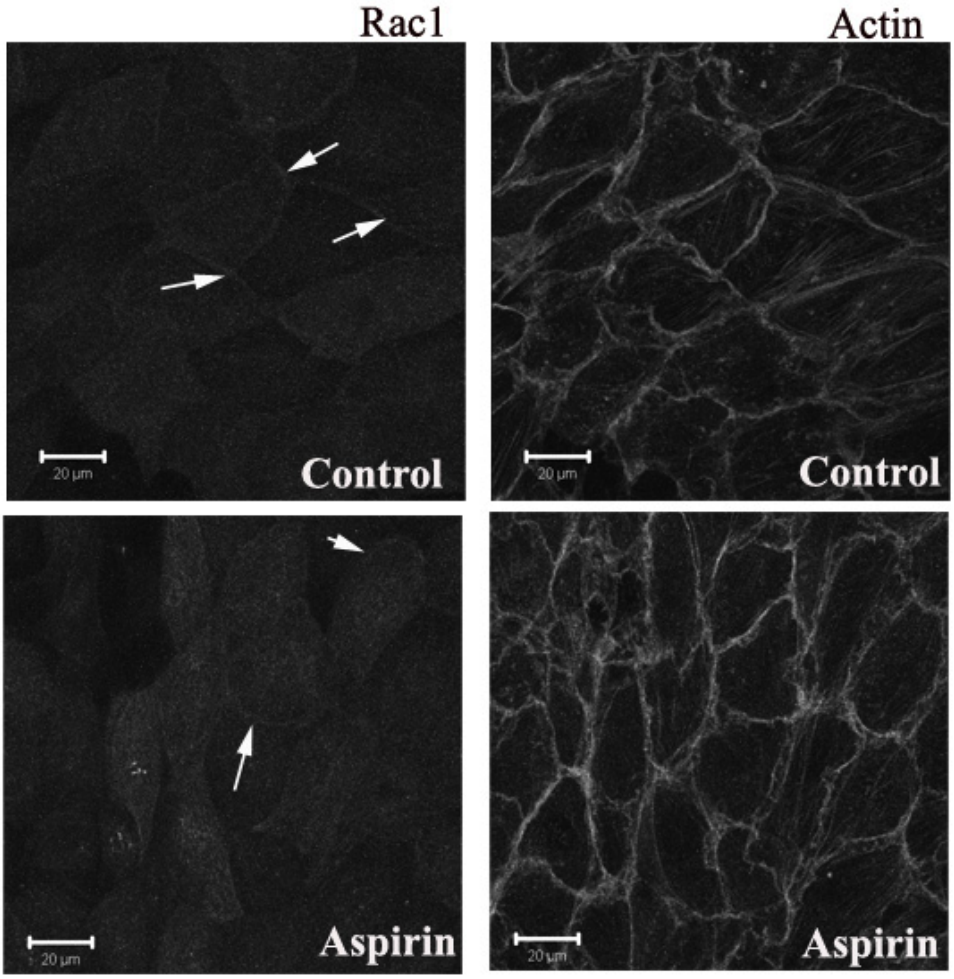

Appedix E (**i**): Relative to control (0.2 % DMSO), 300 μM of Aspirin does not cause significant membrane redistribution of Rac1 in OVCA433 cells after 1hr of treatment. This is unlike the case of R-Naproxen at the same concentration and duration of treatment.

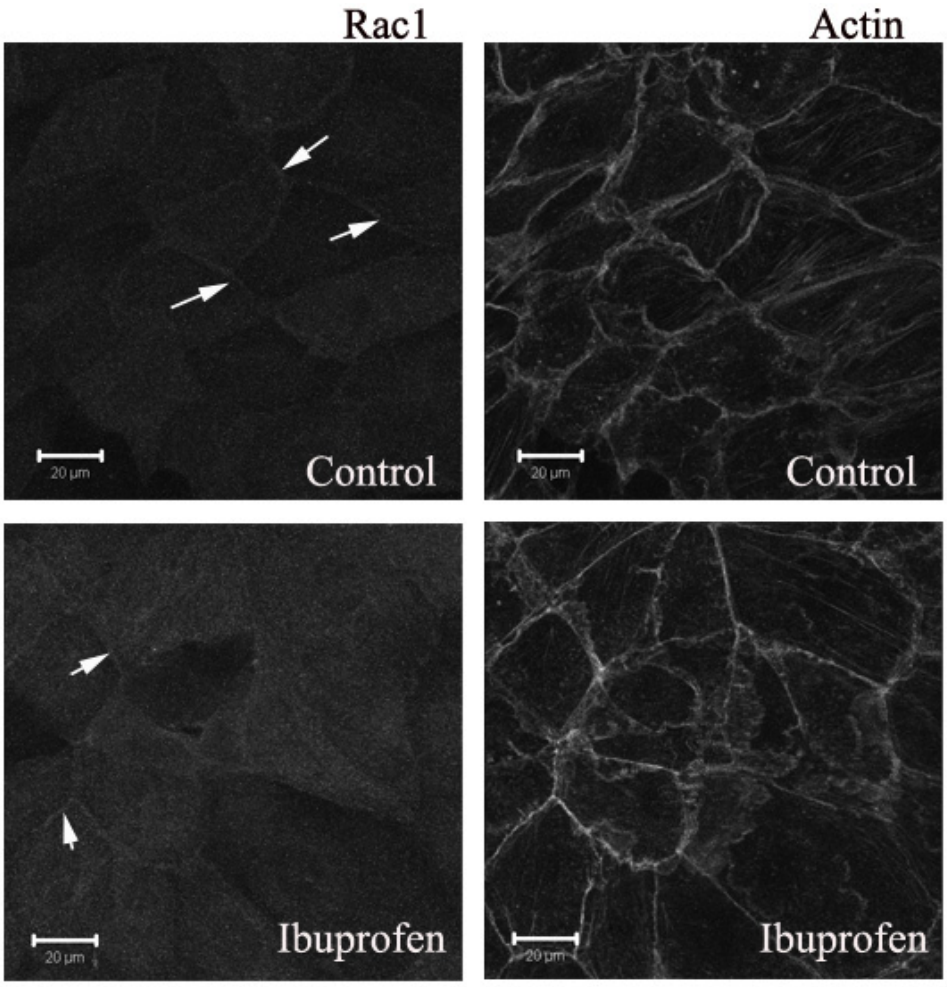

Appedix E (ii): Relative to control (0.2 % DMSO) and also compared to R-Naproxen, 300 µM of Ibuprofen does not cause significant membrane redistribution of Rac1 in OVCA433 cells after 1 h of treatment.

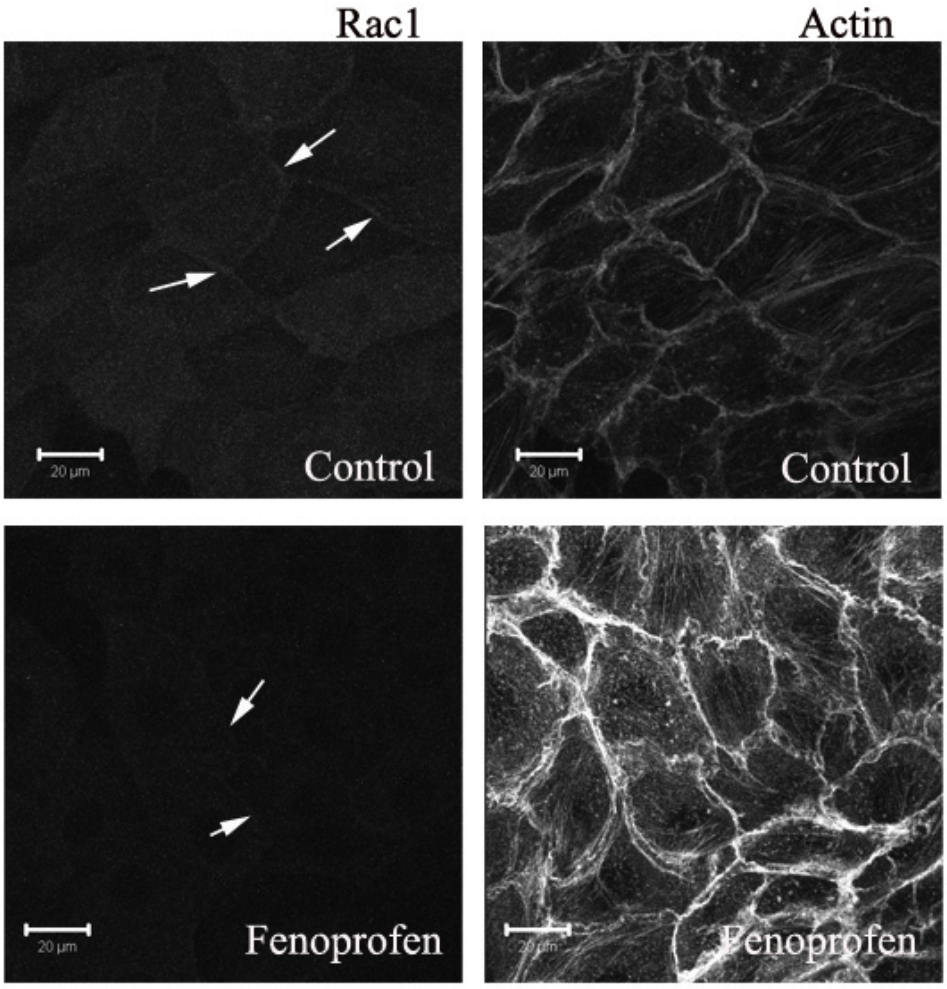

Appedix E (**iii**): Relative to control (0.2 % DMSO), 300 μM of Fenoprofen does not cause significant membrane redistribution of Rac1 to the cytosol in OVCA433 cells after 1 h of treatment unlike R-Naproxen at the same concentration and duration of treatment.

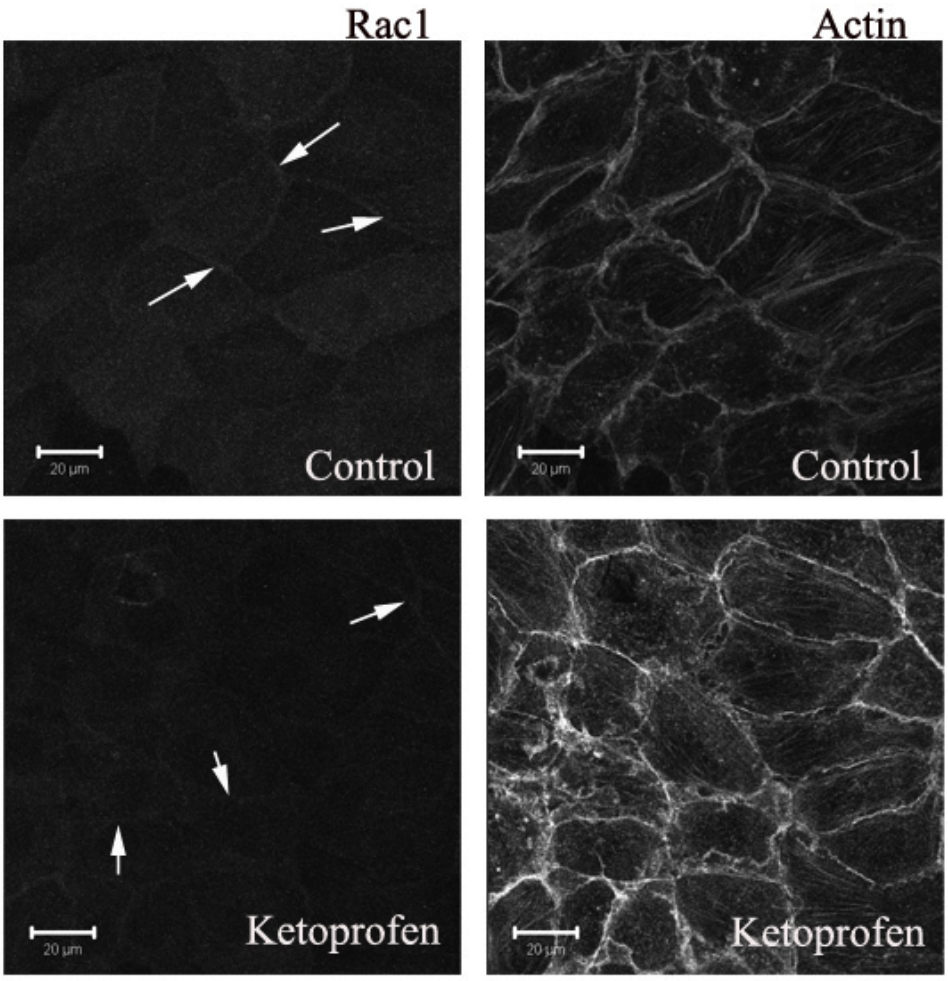

Appedix E (**iv**): Relative to control (0.2 % DMSO), 300 μM of Ketoprofen does not cause significant membrane redistribution of Rac1 in OVCA433 cells after 1 h of treatment. Rac1 is still significantly present at the plasma membrane unlike the case of R-Naproxen at the same concentration and duration of treatment.

Appendix F: COX enzyme inhibitory activity of a panel of NSAIDs

COX-1	**IC50 (M)**	
Compound		**nH**
1-6MNA	2.80E-05	1
2-R-Nap	7.20E-06	0.6
3-S-Nap	5.90E-08	0.9
Pub Chem: CID2950007	1.80E-06	0.9
5-R-Keto	9.90E-07	0.9
6-S-Keto	<1.0E-0.8	NA
COX-2		
Compound		
1-6MNA	>1.0E-04	NA
2-R-Nap	4.20E-06	0.9
3-S-Nap	7.00E-08	1.3
Pub Chem: CID2950007	5.80E-07	0.8
5-R-Keto	>1.0E-04	NA
6-S-Keto	8.5E-0.8	1.4

6-MNA: 6-Methoxy-2-naphthalene acetic acid

Assay performed through a contract agreement with CEREP, Seattle, U.S.A.

References

1. Wittinghofer A, Pai EF. The structure of Ras protein: a model for a universal molecular switch. Trends Biochem Sci. 1991;16:382-387.

2. Eathiraj S, Pan X, Ritacco C, Lambright DG. Structural basis of family-wide Rab GTPase recognition by rabenosyn-5. Nature. 2005;436:415-419.

3. Fenwick RB, Prasannan S, Campbell LJ et al. Solution structure and dynamics of the small GTPase RalB in its active conformation: significance for effector protein binding. Biochemistry. 2009;48:2192-2206.

4. Grant BJ, Gorfe AA, McCammon JA. Ras conformational switching: simulating nucleotide-dependent conformational transitions with accelerated molecular dynamics. PLoS Comput Biol. 2009;5:e1000325.

5. Eberth A, Ahmadian MR. In vitro GEF and GAP assays. Curr Protoc Cell Biol. 2009;Chapter 14:Unit 14.9.

6. Bos JL, Rehmann H, Wittinghofer A. GEFs and GAPs: critical elements in the control of small G proteins. Cell. 2007;129:865-877.

7. Sebti SM, Hamilton AD. Inhibition of Rho GTPases using protein geranylgeranyltransferase I inhibitors. Methods Enzymol. 2000;325:381-388.

8. Sousa SF, Fernandes PA, Ramos MJ. Farnesyltransferase inhibitors: a detailed chemical view on an elusive biological problem. Curr Med Chem. 2008;15:1478-1492.

9. Sane KM, Mynderse M, Lalonde DT et al. A novel geranylgeranyl transferase inhibitor in combination with lovastatin inhibits proliferation and induces autophagy in STS-26T MPNST cells. J Pharmacol Exp Ther. 2010;333:23-33.

10. Machida S, Kato N, Harada K, Ohkanda J. Bivalent inhibitors for disrupting protein surface-substrate interactions and for dual inhibition of protein prenyltransferases. J Am Chem Soc. 2011;133:958-963.

11. Fletcher S, Keaney EP, Cummings CG et al. Structure-based design and synthesis of potent, ethylenediamine-based, mammalian farnesyltransferase inhibitors as anticancer agents. J Med Chem. 2010;53:6867-6888.

12. McKenna CE, Kashemirov BA, Blazewska KM et al. Synthesis, chiral high performance liquid chromatographic resolution and enantiospecific activity of a potent new geranylgeranyl transferase inhibitor, 2-hydroxy-3-imidazo[1,2-a]pyridin-3-yl-2-phosphonopropionic acid. J Med Chem. 2010;53:3454-3464.

13. Vigil D, Cherfils J, Rossman KL, Der CJ. Ras superfamily GEFs and GAPs: validated and tractable targets for cancer therapy? Nat Rev Cancer. 2010;10:842-857.

14. Nassar N, Cancelas J, Zheng J, Williams DA, Zheng Y. Structure-function based design of small molecule inhibitors targeting Rho family GTPases. Curr Top Med Chem. 2006;6:1109-1116.

15. Pelish HE, Ciesla W, Tanaka N et al. The Cdc42 inhibitor secramine B prevents cAMP-induced K+ conductance in intestinal epithelial cells. Biochem Pharmacol. 2006;71:1720-1726.

16. Shutes A, Onesto C, Picard V, Leblond B, Schweighoffer F, Der CJ. Specificity and mechanism of action of EHT 1864, a novel small molecule inhibitor of Rac family small GTPases. J Biol Chem. 2007;282:35666-35678.

17. Hartmann JT, Haap M, Kopp HG, Lipp HP. Tyrosine kinase inhibitors - a review on pharmacology, metabolism and side effects. Curr Drug Metab. 2009;10:470-481.

18. Stein MP, Cao C, Tessema M et al. Interaction and functional analyses of human VPS34/p150 phosphatidylinositol 3-kinase complex with Rab7. Methods Enzymol. 2005;403:628-649.

19. Palamidessi A, Frittoli E, Garre M et al. Endocytic trafficking of Rac is required for the spatial restriction of signaling in cell migration. Cell. 2008;134:135-147.

20. Zech T, Machesky L. Rab5 and rac team up in cell motility. Cell. 2008;134:18-20.

21. Frasa MA, Maximiano FC, Smolarczyk K et al. Armus is a Rac1 effector that inactivates Rab7 and regulates E-cadherin degradation. Curr Biol. 2010;20:198-208.

22. Barr F, Lambright DG. Rab GEFs and GAPs. Curr Opin Cell Biol. 2010;22:461-470.

23. Salminen A, Novick PJ. A ras-like protein is required for a post-Golgi event in yeast secretion. Cell. 1987;49:527-538.

24. Goud B, Salminen A, Walworth NC, Novick PJ. A GTP-binding protein required for secretion rapidly associates with secretory vesicles and the plasma membrane in yeast. Cell. 1988;53:753-768.

25. Touchot N, Chardin P, Tavitian A. Four additional members of the ras gene superfamily isolated by an oligonucleotide strategy: molecular cloning of YPT-related cDNAs from a rat brain library. Proc Natl Acad Sci U S A. 1987;84:8210-8214.

26. Colicelli J. Human RAS superfamily proteins and related GTPases. Sci STKE. 2004;2004:RE13.

27. Schwartz SL, Cao C, Pylypenko O, Rak A, Wandinger-Ness A. Rab GTPases at a glance. Journal of Cell Science. 2007;120:3905.

28. Hutagalung AH, Novick PJ. Role of Rab GTPases in membrane traffic and cell physiology. Physiol Rev. 2011;91:119-149.

29. Agola JO, Jim PA, Ward HH, Basuray S, Wandinger-Ness A. Rab GTPases as regulators of endocytosis, targets of disease and therapeutic opportunities. Clin Genet. 2011

30. Feng Y, Press B, Wandinger-Ness A. Rab 7: an important regulator of late endocytic membrane traffic. J Cell Biol. 1995;131:1435-1452.

31. Progida C, Malerod L, Stuffers S, Brech A, Bucci C, Stenmark H. RILP is required for the proper morphology and function of late endosomes. J Cell Sci. 2007;120:3729-3737.

32. Vanlandingham PA, Ceresa BP. Rab7 regulates late endocytic trafficking downstream of multivesicular body biogenesis and cargo sequestration. J Biol Chem. 2009;284:12110-12124.

33. BasuRay S, Mukherjee S, Romero E, Wilson MC, Wandinger-Ness A. Rab7 mutants associated with Charcot-Marie-Tooth disease exhibit enhanced NGF-stimulated signaling. PLoS One. 2010;5:e15351.

34. Croizet-Berger K, Daumerie C, Couvreur M, Courtoy PJ, van den Hove MF. The endocytic catalysts, Rab5a and Rab7, are tandem regulators of thyroid hormone production. Proc Natl Acad Sci U S A. 2002;99:8277-8282.

35. Roepstorff K, Grovdal L, Grandal M, Lerdrup M, van Deurs B. Endocytic downregulation of ErbB receptors: mechanisms and relevance in cancer. Histochem Cell Biol. 2008;129:563-578.

36. Bains M, Zaegel V, Mize-Berge J, Heidenreich KA. IGF-I stimulates Rab7-RILP interaction during neuronal autophagy. Neurosci Lett. 2011;488:112-117.

37. Gutierrez MG, Munafo DB, Beron W, Colombo MI. Rab7 is required for the normal progression of the autophagic pathway in mammalian cells. J Cell Sci. 2004;117:2687-2697.

38. Liang C, Lee JS, Inn KS et al. Beclin1-binding UVRAG targets the class C Vps complex to coordinate autophagosome maturation and endocytic trafficking. Nat Cell Biol. 2008;10:776-787.

39. Eskelinen EL. Maturation of autophagic vacuoles in Mammalian cells. Autophagy. 2005;1:1-10.

40. Tabata K, Matsunaga K, Sakane A, Sasaki T, Noda T, Yoshimori T. Rubicon and PLEKHM1 negatively regulate the endocytic/autophagic pathway via a novel Rab7-binding domain. Mol Biol Cell. 2010;21:4162-4172.

41. Pankiv S, Alemu EA, Brech A et al. FYCO1 is a Rab7 effector that binds to LC3 and PI3P to mediate microtubule plus end-directed vesicle transport. J Cell Biol. 2010;188:253-269.

42. Jager S, Bucci C, Tanida I et al. Role for Rab7 in maturation of late autophagic vacuoles. J Cell Sci. 2004;117:4837-4848.

43. Deretic V. Autophagy in infection. Curr Opin Cell Biol. 2010;22:252-262.

44. Wong E, Cuervo AM. Autophagy gone awry in neurodegenerative diseases. Nat Neurosci. 2010;13:805-811.

45. Mehrpour M, Esclatine A, Beau I, Codogno P. Overview of macroautophagy regulation in mammalian cells. Cell Res. 2010;20:748-762.

46. Ohashi Y, Munro S. Membrane delivery to the yeast autophagosome from the Golgi-endosomal system. Mol Biol Cell. 2010;21:3998-4008.

47. Saito F, Kuwata H, Oiki E et al. Inefficient phagosome maturation in infant macrophages. Biochem Biophys Res Commun. 2008;375:113-118.

48. Seto S, Tsujimura K, Koide Y. Rab GTPases regulating phagosome maturation are differentially recruited to mycobacterial phagosomes. Traffic. 2011;12:407-420.

49. Jordens I, Westbroek W, Marsman M et al. Rab7 and Rab27a control two motor protein activities involved in melanosomal transport. Pigment Cell Res. 2006;19:412-423.

50. Hida T, Sohma H, Kokai Y et al. Rab7 is a critical mediator in vesicular transport of tyrosinase-related protein 1 in melanocytes. J Dermatol. 2011;38:432-441.

51. Kawakami A, Sakane F, Imai S et al. Rab7 regulates maturation of melanosomal matrix protein gp100/Pmel17/Silv. J Invest Dermatol. 2008;128:143-150.

52. Hirosaki K, Yamashita T, Wada I, Jin HY, Jimbow K. Tyrosinase and tyrosinase-related protein 1 require Rab7 for their intracellular transport. J Invest Dermatol. 2002;119:475-480.

53. Palokangas H, Mulari M, Vaananen HK. Endocytic pathway from the basal plasma membrane to the ruffled border membrane in bone-resorbing osteoclasts. J Cell Sci. 1997;110:1767-1780.

54. Mulari M, Vaaraniemi J, Vaananen HK. Intracellular membrane trafficking in bone resorbing osteoclasts. Microsc Res Tech. 2003;61:496-503.

55. de Saint Basile G, Menasche G, Fischer A. Molecular mechanisms of biogenesis and exocytosis of cytotoxic granules. Nat Rev Immunol. 2010;10:568-579.

56. Green DR. Apoptosis and sphingomyelin hydrolysis. The flip side. J Cell Biol. 2000;150:F5-7.

57. van Meer G, Holthuis JC. Sphingolipid transport in eukaryotic cells. Biochim Biophys Acta. 2000;1486:145-170.

58. Pagano RE. Endocytic trafficking of glycosphingolipids in sphingolipid storage diseases. Philos Trans R Soc Lond B Biol Sci. 2003;358:885-891.

59. Ory DS. The niemann-pick disease genes; regulators of cellular cholesterol homeostasis. Trends Cardiovasc Med. 2004;14:66-72.

60. Liscum L, Arnio E, Anthony M, Howley A, Sturley SL, Agler M. Identification of a pharmaceutical compound that partially corrects the Niemann-Pick C phenotype in cultured cells. J Lipid Res. 2002;43:1708-1717.

61. Choudhury A, Dominguez M, Puri V et al. Rab proteins mediate Golgi transport of caveola-internalized glycosphingolipids and correct lipid trafficking in Niemann-Pick C cells. J Clin Invest. 2002;109:1541-1550.

62. Stein MP, Feng Y, Cooper KL, Welford AM, Wandinger-Ness A. Human VPS34 and p150 are Rab7 interacting partners. Traffic. 2003;4:754-771.

63. Cao C, Laporte J, Backer JM, Wandinger-Ness A, Stein MP. Myotubularin lipid phosphatase binds the hVPS15/hVPS34 lipid kinase complex on endosomes. Traffic. 2007;8:1052-1067.

64. Cao C, Backer JM, Laporte J, Bedrick EJ, Wandinger-Ness A. Sequential actions of myotubularin lipid phosphatases regulate endosomal PI(3)P and growth factor receptor trafficking. Mol Biol Cell. 2008;19:3334-3346.

65. Rocha N, Kuijl C, van der Kant R et al. Cholesterol sensor ORP1L contacts the ER protein VAP to control Rab7-RILP-p150 Glued and late endosome positioning. J Cell Biol. 2009;185:1209-1225.

66. Emery G, Knoblich JA. Endosome dynamics during development. Curr Opin Cell Biol. 2006;18:407-415.

67. Palacios F, Tushir JS, Fujita Y, D'Souza-Schorey C. Lysosomal targeting of E-cadherin: a unique mechanism for the down-regulation of cell-cell adhesion during epithelial to mesenchymal transitions. Mol Cell Biol. 2005;25:389-402.

68. Cantalupo G, Alifano P, Roberti V, Bruni CB, Bucci C. Rab-interacting lysosomal protein (RILP): the Rab7 effector required for transport to lysosomes. EMBO J. 2001;20:683-693.

69. Jordens I, Fernandez-Borja M, Marsman M et al. The Rab7 effector protein RILP controls lysosomal transport by inducing the recruitment of dynein-dynactin motors. Curr Biol. 2001;11:1680-1685.

70. Bananis E, Nath S, Gordon K et al. Microtubule-dependent movement of late endocytic vesicles in vitro: requirements for Dynein and Kinesin. Mol Biol Cell. 2004;15:3688-3697.

71. Dong J, Chen W, Welford A, Wandinger-Ness A. The proteasome alpha-subunit XAPC7 interacts specifically with Rab7 and late endosomes. J Biol Chem. 2004;279:21334-21342.

72. Bucci C, De Gregorio L, Bruni CB. Expression analysis and chromosomal assignment of PRA1 and RILP genes. Biochem Biophys Res Commun. 2001;286:815-819.

73. Wu M, Wang T, Loh E, Hong W, Song H. Structural basis for recruitment of RILP by small GTPase Rab7. EMBO J. 2005;24:1491-1501.

74. Wang T, Wong KK, Hong W. A unique region of RILP distinguishes it from its related proteins in its regulation of lysosomal morphology and interaction with Rab7 and Rab34. Mol Biol Cell. 2004;15:815-826.

75. Marsman M, Jordens I, Rocha N, Kuijl C, Janssen L, Neefjes J. A splice variant of RILP induces lysosomal clustering independent of dynein recruitment. Biochem Biophys Res Commun. 2006;344:747-756.

76. Starr T, Ng TW, Wehrly TD, Knodler LA, Celli J. Brucella intracellular replication requires trafficking through the late endosomal/lysosomal compartment. Traffic. 2008;9:678-694.

77. Colucci AM, Campana MC, Bellopede M, Bucci C. The Rab-interacting lysosomal protein, a Rab7 and Rab34 effector, is capable of self-interaction. Biochem Biophys Res Commun. 2005;334:128-133.

78. Johansson M, Rocha N, Zwart W et al. Activation of endosomal dynein motors by stepwise assembly of Rab7-RILP-p150Glued, ORP1L, and the receptor betalll spectrin. J Cell Biol. 2007;176:459-471.

79. Wang T, Hong W. RILP interacts with VPS22 and VPS36 of ESCRT-II and regulates their membrane recruitment. Biochem Biophys Res Commun. 2006;350:413-423.

80. Johansson M, Lehto M, Tanhuanpaa K, Cover TL, Olkkonen VM. The oxysterol-binding protein homologue ORP1L interacts with Rab7 and alters functional properties of late endocytic compartments. Mol Biol Cell. 2005;16:5480-5492.

81. Boudjelal M, Wang Z, Voorhees JJ, Fisher GJ. Ubiquitin/proteasome pathway regulates levels of retinoic acid receptor gamma and retinoid X receptor alpha in human keratinocytes. Cancer Res. 2000;60:2247-2252.

82. Mukherjee S, Dong J, Heincelman C, Lenhart M, Welford A, Wandinger-Ness A. Functional analyses and interaction of the XAPC7 proteasome subunit with Rab7. Methods Enzymol. 2005;403:650-663.

83. Mizuno K, Kitamura A, Sasaki T. Rabring7, a novel Rab7 target protein with a RING finger motif. Mol Biol Cell. 2003;14:3741-3752.

84. Mizuno K, Sakane A, Sasaki T. Rabring7: a target protein for rab7 small g protein. Methods Enzymol. 2005;403:687-696.

85. Sakane A, Hatakeyama S, Sasaki T. Involvement of Rabring7 in EGF receptor degradation as an E3 ligase. Biochem Biophys Res Commun. 2007;357:1058-1064.

86. Murray JT, Backer JM. Analysis of hVps34/hVps15 interactions with Rab5 in vivo and in vitro. Methods Enzymol. 2005;403:789-799.

87. Pertz O. Spatio-temporal Rho GTPase signaling - where are we now? J Cell Sci. 2010;123:1841-1850.

88. Gomez PF, Luo D, Hirosaki K et al. Identification of rab7 as a melanosome-associated protein involved in the intracellular transport of tyrosinase-related protein 1. J Invest Dermatol. 2001;117:81-90.

89. Dupre DJ, Chen Z, Le Gouill C et al. Trafficking, ubiquitination, and down-regulation of the human platelet-activating factor receptor. J Biol Chem. 2003;278:48228-48235.

90. Casey PJ, Seabra MC. Protein prenyltransferases. J Biol Chem. 1996;271:5289-5292.

91. Pereira-Leal JB, Seabra MC. The mammalian Rab family of small GTPases: definition of family and subfamily sequence motifs suggests a mechanism for functional specificity in the Ras superfamily. J Mol Biol. 2000;301:1077-1087.

92. Watanabe M, Fiji HD, Guo L et al. Inhibitors of protein geranylgeranyltransferase I and Rab geranylgeranyltransferase identified from a library of allenoate-derived compounds. J Biol Chem. 2008;283:9571-9579.

93. Kinsella BT, Maltese WA. rab GTP-binding proteins with three different carboxyl-terminal cysteine motifs are modified in vivo by 20-carbon isoprenoids. J Biol Chem. 1992;267:3940-3945.

94. Pfeffer S, Aivazian D. Targeting Rab GTPases to distinct membrane compartments. Nat Rev Mol Cell Biol. 2004;5:886-896.

95. Alexandrov K, Simon I, Yurchenko V et al. Characterization of the ternary complex between Rab7, REP-1 and Rab geranylgeranyl transferase. Eur J Biochem. 1999;265:160-170.

96. Wu YW, Oesterlin LK, Tan KT, Waldmann H, Alexandrov K, Goody RS. Membrane targeting mechanism of Rab GTPases elucidated by semisynthetic protein probes. Nat Chem Biol. 2010;6:534-540.

97. Wu YW, Tan KT, Waldmann H, Goody RS, Alexandrov K. Interaction analysis of prenylated Rab GTPase with Rab escort protein and GDP dissociation inhibitor explains the need for both regulators. Proc Natl Acad Sci U S A. 2007;104:12294-12299.

98. Leung KF, Baron R, Ali BR, Magee AI, Seabra MC. Rab GTPases containing a CAAX motif are processed post-geranylgeranylation by proteolysis and methylation. J Biol Chem. 2007;282:1487-1497.

99. Rak A, Pylypenko O, Niculae A, Pyatkov K, Goody RS, Alexandrov K. Structure of the Rab7:REP-1 complex: insights into the mechanism of Rab prenylation and choroideremia disease. Cell. 2004;117:749-760.

100. Rak A, Pylypenko O, Niculae A, Goody RS, Alexandrov K. Crystallization and preliminary X-ray diffraction analysis of monoprenylated Rab7 GTPase in complex with Rab escort protein 1. J Struct Biol. 2003;141:93-95.

101. Seabra MC. New insights into the pathogenesis of choroideremia: a tale of two REPs. Ophthalmic Genet. 1996;17:43-46.

102. van den Hurk JA, Hendriks W, van de Pol DJ et al. Mouse choroideremia gene mutation causes photoreceptor cell degeneration and is not transmitted through the female germline. Hum Mol Genet. 1997;6:851-858.

103. Thoma NH, Iakovenko A, Goody RS, Alexandrov K. Phosphoisoprenoids modulate association of Rab geranylgeranyltransferase with REP-1. J Biol Chem. 2001;276:48637-48643.

104. Alexandrov K, Horiuchi H, Steele-Mortimer O, Seabra MC, Zerial M. Rab escort protein-1 is a multifunctional protein that accompanies newly prenylated rab proteins to their target membranes. EMBO J. 1994;13:5262-5273.

105. Chavrier P, Gorvel JP, Stelzer E, Simons K, Gruenberg J, Zerial M. Hypervariable C-terminal domain of rab proteins acts as a targeting signal. Nature. 1991;353:769-772.

106. Svejstrup JQ, Li Y, Fellows J, Gnatt A, Bjorklund S, Kornberg RD. Evidence for a mediator cycle at the initiation of transcription. Proc Natl Acad Sci U S A. 1997;94:6075-6078.

107. Pfeffer S. Filling the Rab GAP. Nat Cell Biol. 2005;7:856-857.

108. Plemel RL, Lobingier BT, Brett CL et al. Subunit organization and Rab interactions of Vps-C protein complexes that control endolysosomal membrane traffic. Mol Biol Cell. 2011;22:1353-1363.

109. Zhang XM, Walsh B, Mitchell CA, Rowe T. TBC domain family, member 15 is a novel mammalian Rab GTPase-activating protein with substrate preference for Rab7. Biochem Biophys Res Commun. 2005;335:154-161.

110. Seaman MN, Harbour ME, Tattersall D, Read E, Bright N. Membrane recruitment of the cargo-selective retromer subcomplex is catalysed by the small GTPase Rab7 and inhibited by the Rab-GAP TBC1D5. J Cell Sci. 2009;122:2371-2382.

111. Deretic V. Ay, there's the Rab: organelle maturation by Rab conversion. Dev Cell. 2005;9:446-448.

112. Beraud-Dufour S, Balch W. A journey through the exocytic pathway. J Cell Sci. 2002;115:1779-1780.

113. Markgraf DF, Peplowska K, Ungermann C. Rab cascades and tethering factors in the endomembrane system. FEBS Lett. 2007;581:2125-2130.

114. Grosshans BL, Ortiz D, Novick P. Rabs and their effectors: achieving specificity in membrane traffic. Proc Natl Acad Sci U S A. 2006;103:11821-11827.

115. Rink J, Ghigo E, Kalaidzidis Y, Zerial M. Rab conversion as a mechanism of progression from early to late endosomes. Cell. 2005;122:735-749.

116. Poteryaev D, Datta S, Ackema K, Zerial M, Spang A. Identification of the switch in early-to-late endosome transition. Cell. 2010;141:497-508.

117. Zhang M, Chen L, Wang S, Wang T. Rab7: roles in membrane trafficking and disease. Biosci Rep. 2009;29:193-209.

118. Niemann A, Berger P, Suter U. Pathomechanisms of mutant proteins in Charcot-Marie-Tooth disease. Neuromolecular Med. 2006;8:217-242.

119. Shy ME, Garbern JY, Kamholz J. Hereditary motor and sensory neuropathies: a biological perspective. Lancet Neurol. 2002;1:110-118.

120. Bienfait HM, Baas F, Koelman JH et al. Phenotype of Charcot-Marie-Tooth disease Type 2. Neurology. 2007;68:1658-1667.

121. Verhoeven K, De Jonghe P, Coen K et al. Mutations in the small GTP-ase late endosomal protein RAB7 cause Charcot-Marie-Tooth type 2B neuropathy. Am J Hum Genet. 2003;72:722-727.

122. Spinosa MR, Progida C, De Luca A, Colucci AM, Alifano P, Bucci C. Functional characterization of Rab7 mutant proteins associated with Charcot-Marie-Tooth type 2B disease. J Neurosci. 2008;28:1640-1648.

123. Houlden H, King RH, Muddle JR et al. A novel RAB7 mutation associated with ulcero-mutilating neuropathy. Ann Neurol. 2004;56:586-590.

124. De Luca A, Progida C, Spinosa MR, Alifano P, Bucci C. Characterization of the Rab7K157N mutant protein associated with Charcot-Marie-Tooth type 2B. Biochem Biophys Res Commun. 2008;372:283-287.

125. McCray BA, Skordalakes E, Taylor JP. Disease mutations in Rab7 result in unregulated nucleotide exchange and inappropriate activation. Hum Mol Genet. 2010;19:1033-1047.

126. Cogli L, Progida C, Lecci R, Bramato R, Kruttgen A, Bucci C. CMT2B-associated Rab7 mutants inhibit neurite outgrowth. Acta Neuropathol. 2010;120:491-501.

127. Kwon JM, Elliott JL, Yee WC et al. Assignment of a second Charcot-Marie-Tooth type II locus to chromosome 3q. Am J Hum Genet. 1995;57:853-858.

128. Cogli L, Piro F, Bucci C. Rab7 and the CMT2B disease. Biochem Soc Trans. 2009;37:1027-1031.

129. Wang T, Ming Z, Xiaochun W, Hong W. Rab7: role of its protein interaction cascades in endo-lysosomal traffic. Cell Signal. 2011;23:516-521.

130. Mitra S, Cheng KW, Mills GB. Rab GTPases implicated in inherited and acquired disorders. Semin Cell Dev Biol. 2011;22:57-68.

131. Segev N. GTPases in intracellular trafficking: an overview. Semin Cell Dev Biol. 2011;22:1-2.

132. Segev N. Coordination of intracellular transport steps by GTPases. Semin Cell Dev Biol. 2011;22:33-38.

133. Schwartz SL, Tessema M, Buranda T et al. Flow cytometry for real-time measurement of guanine nucleotide binding and exchange by Ras-like GTPases. Anal Biochem. 2008;381:258-266.

134. Tessema M, Simons PC, Cimino DF et al. Glutathione-S-transferase-green fluorescent protein fusion protein reveals slow dissociation from high site density beads and measures free GSH. Cytometry A. 2006;69:326-334.

135. Surviladze Z, Waller A, Wu Y et al. Identification of a small GTPase inhibitor using a high-throughput flow cytometry bead-based multiplex assay. J Biomol Screen. 2010;15:10-20.

136. Ramirez S, Aiken CT, Andrzejewski B, Sklar LA, Edwards BS. High-throughput flow cytometry: validation in microvolume bioassays. Cytometry A. 2003;53:55-65.

137. Simon I, Zerial M, Goody RS. Kinetics of interaction of Rab5 and Rab7 with nucleotides and magnesium ions. J Biol Chem. 1996;271:20470-20478.

138. Gao Y, Dickerson JB, Guo F, Zheng J, Zheng Y. Rational design and characterization of a Rac GTPase-specific small molecule inhibitor. Proc Natl Acad Sci U S A. 2004;101:7618-7623.

139. Manara MC, Nicoletti G, Zambelli D et al. NVP-BEZ235 as a new therapeutic option for sarcomas. Clin Cancer Res. 2010;16:530-540.

140. Takei H, Fujita S, Shirakawa T, Koshikawa N, Kobayashi M. Insulin facilitates repetitive spike firing in rat insular cortex via phosphoinositide 3-kinase but not mitogen activated protein kinase cascade. Neuroscience. 2010;170:1199-1208.

141. Flinn RJ, Yan Y, Goswami S, Parker PJ, Backer JM. The late endosome is essential for mTORC1 signaling. Mol Biol Cell. 2010;21:833-841.

142. Peralta ER, Martin BC, Edinger AL. Differential effects of TBC1D15 and mammalian Vps39 on Rab7 activation state, lysosomal morphology, and growth factor dependence. J Biol Chem. 2010;285:16814-16821.

143. Seto S, Matsumoto S, Tsujimura K, Koide Y. Differential recruitment of CD63 and Rab7-interacting-lysosomal-protein to phagosomes containing Mycobacterium tuberculosis in macrophages. Microbiol Immunol. 2010;54:170-174.

144. Bishop AL, Hall A. Rho GTPases and their effector proteins. Biochem J. 2000;348 Pt 2:241-255.

145. Hall A. Rho GTPases and the actin cytoskeleton. Science. 1998;279:509-514.

146. Etienne-Manneville S, Hall A. Rho GTPases in cell biology. Nature. 2002;420:629-635.

147. Ridley AJ, Hall A. The small GTP-binding protein rho regulates the assembly of focal adhesions and actin stress fibers in response to growth factors. Cell. 1992;70:389-399.

148. Ridley AJ, Paterson HF, Johnston CL, Diekmann D, Hall A. The small GTP-binding protein rac regulates growth factor-induced membrane ruffling. Cell. 1992;70:401-410.

149. Nobes CD, Hall A. Rho, rac, and cdc42 GTPases regulate the assembly of multimolecular focal complexes associated with actin stress fibers, lamellipodia, and filopodia. Cell. 1995;81:53-62.

150. Kozma R, Ahmed S, Best A, Lim L. The Ras-related protein Cdc42Hs and bradykinin promote formation of peripheral actin microspikes and filopodia in Swiss 3T3 fibroblasts. Mol Cell Biol. 1995;15:1942-1952.

151. Mabuchi I, Hamaguchi Y, Fujimoto H, Morii N, Mishima M, Narumiya S. A rho-like protein is involved in the organisation of the contractile ring in dividing sand dollar eggs. Zygote. 1993;1:325-331.

152. Drechsel DN, Hyman AA, Hall A, Glotzer M. A requirement for Rho and Cdc42 during cytokinesis in Xenopus embryos. Curr Biol. 1997;7:12-23.

153. Prokopenko SN, Saint R, Bellen HJ. Untying the Gordian knot of cytokinesis. Role of small G proteins and their regulators. J Cell Biol. 2000;148:843-848.

154. Cox D, Chang P, Zhang Q, Reddy PG, Bokoch GM, Greenberg S. Requirements for both Rac1 and Cdc42 in membrane ruffling and phagocytosis in leukocytes. J Exp Med. 1997;186:1487-1494.

155. Caron E, Hall A. Identification of two distinct mechanisms of phagocytosis controlled by different Rho GTPases. Science. 1998;282:1717-1721.

156. Nobes CD, Hall A. Rho GTPases control polarity, protrusion, and adhesion during cell movement. J Cell Biol. 1999;144:1235-1244.

157. Allen WE, Zicha D, Ridley AJ, Jones GE. A role for Cdc42 in macrophage chemotaxis. J Cell Biol. 1998;141:1147-1157.

158. Settleman J. Rho GTPases in development. Prog Mol Subcell Biol. 1999;22:201-229.

159. Luo L, Jan LY, Jan YN. Rho family GTP-binding proteins in growth cone signalling. Curr Opin Neurobiol. 1997;7:81-86.

160. Matos P, Skaug J, Marques B et al. Small GTPase Rac1: structure, localization, and expression of the human gene. Biochem Biophys Res Commun. 2000;277:741-751.

161. Moll J, Sansig G, Fattori E, van der Putten H. The murine rac1 gene: cDNA cloning, tissue distribution and regulated expression of rac1 mRNA by disassembly of actin microfilaments. Oncogene. 1991;6:863-866.

162. Shirsat NV, Pignolo RJ, Kreider BL, Rovera G. A member of the ras gene superfamily is expressed specifically in T, B and myeloid hemopoietic cells. Oncogene. 1990;5:769-772.

163. Haataja L, Groffen J, Heisterkamp N. Characterization of RAC3, a novel member of the Rho family. J Biol Chem. 1997;272:20384-20388.

164. Xudong L, Guangyi W. Effect of blocking Rac1 expression in cholangiocarcinoma QBC939 cells. Braz J Med Biol Res. 2011;44:483-488.

165. Gonzalez E, Kou R, Michel T. Rac1 modulates sphingosine 1-phosphate-mediated activation of phosphoinositide 3-kinase/Akt signaling pathways in vascular endothelial cells. J Biol Chem. 2006;281:3210-3216.

166. Nakagawa M, Fukata M, Yamaga M, Itoh N, Kaibuchi K. Recruitment and activation of Rac1 by the formation of E-cadherin-mediated cell-cell adhesion sites. J Cell Sci. 2001;114:1829-1838.

167. Braga VM, Machesky LM, Hall A, Hotchin NA. The small GTPases Rho and Rac are required for the establishment of cadherin-dependent cell-cell contacts. J Cell Biol. 1997;137:1421-1431.

168. Vicente-Manzanares M, Zareno J, Whitmore L, Choi CK, Horwitz AF. Regulation of protrusion, adhesion dynamics, and polarity by myosins IIA and IIB in migrating cells. J Cell Biol. 2007;176:573-580.

169. Quast T, Eppler F, Semmling V et al. CD81 is essential for the formation of membrane protrusions and regulates Rac1-activation in adhesion-dependent immune cell migration. Blood. 2011

170. Kimura F, Iwaya K, Kawaguchi T et al. Epidermal growth factor-dependent enhancement of invasiveness of squamous cell carcinoma of the breast. Cancer Sci. 2010;101:1133-1140.

171. Miki H, Suetsugu S, Takenawa T. WAVE, a novel WASP-family protein involved in actin reorganization induced by Rac. EMBO J. 1998;17:6932-6941.

172. Yamazaki D, Suetsugu S, Miki H et al. WAVE2 is required for directed cell migration and cardiovascular development. Nature. 2003;424:452-456.

173. Itoh RE, Kurokawa K, Ohba Y, Yoshizaki H, Mochizuki N, Matsuda M. Activation of rac and cdc42 video imaged by fluorescent resonance energy transfer-based single-molecule probes in the membrane of living cells. Mol Cell Biol. 2002;22:6582-6591.

174. Kraynov VS, Chamberlain C, Bokoch GM, Schwartz MA, Slabaugh S, Hahn KM. Localized Rac activation dynamics visualized in living cells. Science. 2000;290:333-337.

175. Gardiner EM, Pestonjamasp KN, Bohl BP, Chamberlain C, Hahn KM, Bokoch GM. Spatial and temporal analysis of Rac activation during live neutrophil chemotaxis. Curr Biol. 2002;12:2029-2034.

176. Li JY, Cao RF, Wang H et al. [Correlation between the PTEN/MMAC1/TEP1 expression and cell proliferation and apoptosis in human renal cell carcinoma (RCC)]. Ai Zheng. 2003;22:607-611.

177. Merlot S, Firtel RA. Leading the way: Directional sensing through phosphatidylinositol 3-kinase and other signaling pathways. J Cell Sci. 2003;116:3471-3478.

178. Brugnera E, Haney L, Grimsley C et al. Unconventional Rac-GEF activity is mediated through the Dock180-ELMO complex. Nat Cell Biol. 2002;4:574-582.

179. Cote JF, Vuori K. Identification of an evolutionarily conserved superfamily of DOCK180-related proteins with guanine nucleotide exchange activity. J Cell Sci. 2002;115:4901-4913.

180. Schmidt A, Hall A. Guanine nucleotide exchange factors for Rho GTPases: turning on the switch. Genes Dev. 2002;16:1587-1609.

181. Bernards A. GAPs galore! A survey of putative Ras superfamily GTPase activating proteins in man and Drosophila. Biochim Biophys Acta. 2003;1603:47-82.

182. Olofsson B. Rho guanine dissociation inhibitors: pivotal molecules in cellular signalling. Cell Signal. 1999;11:545-554.

183. Hart MJ, Sharma S, elMasry N et al. Identification of a novel guanine nucleotide exchange factor for the Rho GTPase. J Biol Chem. 1996;271:25452-25458.

184. Habets GG, Scholtes EH, Zuydgeest D et al. Identification of an invasion-inducing gene, Tiam-1, that encodes a protein with homology to GDP-GTP exchangers for Rho-like proteins. Cell. 1994;77:537-549.

185. Habets GG, van der Kammen RA, Stam JC, Michiels F, Collard JG. Sequence of the human invasion-inducing TIAM1 gene, its conservation in evolution and its expression in tumor cell lines of different tissue origin. Oncogene. 1995;10:1371-1376.

186. Stam JC, Sander EE, Michiels F et al. Targeting of Tiam1 to the plasma membrane requires the cooperative function of the N-terminal pleckstrin homology domain and an adjacent protein interaction domain. J Biol Chem. 1997;272:28447-28454.

187. Michiels F, Stam JC, Hordijk PL et al. Regulated membrane localization of Tiam1, mediated by the NH2-terminal pleckstrin homology domain, is required for Rac-dependent membrane ruffling and C-Jun NH2-terminal kinase activation. J Cell Biol. 1997;137:387-398.

188. Lambert JM, Lambert QT, Reuther GW et al. Tiam1 mediates Ras activation of Rac by a PI(3)K-independent mechanism. Nat Cell Biol. 2002;4:621-625.

189. Fleming IN, Elliott CM, Collard JG, Exton JH. Lysophosphatidic acid induces threonine phosphorylation of Tiam1 in Swiss 3T3 fibroblasts via activation of protein kinase C. J Biol Chem. 1997;272:33105-33110.

190. Fleming IN, Elliott CM, Buchanan FG, Downes CP, Exton JH. Ca2+/calmodulin-dependent protein kinase II regulates Tiam1 by reversible protein phosphorylation. J Biol Chem. 1999;274:12753-12758.

191. Fleming IN, Elliott CM, Exton JH. Phospholipase C-gamma, protein kinase C and Ca2+/calmodulin-dependent protein kinase II are involved in platelet-derived growth factor-induced phosphorylation of Tiam1. FEBS Lett. 1998;429:229-233.

192. Aili M, Telepnev M, Hallberg B, Wolf-Watz H, Rosqvist R. In vitro GAP activity towards RhoA, Rac1 and Cdc42 is not a prerequisite for YopE induced HeLa cell cytotoxicity. Microb Pathog. 2003;34:297-308.

193. Seoh ML, Ng CH, Yong J, Lim L, Leung T. ArhGAP15, a novel human RacGAP protein with GTPase binding property. FEBS Lett. 2003;539:131-137.

194. Caloca MJ, Wang H, Kazanietz MG. Characterization of the Rac-GAP (Rac-GTPase-activating protein) activity of beta2-chimaerin, a 'non-protein kinase C' phorbol ester receptor. Biochem J. 2003;375:313-321.

195. Klawitter J, Shokati T, Moll V, Christians U, Klawitter J. Effects of lovastatin on breast cancer cells: a proteo-metabonomic study. Breast Cancer Res. 2010;12:R16.

196. Yoneda M, Hirokawa YS, Ohashi A et al. RhoB enhances migration and MMP1 expression of prostate cancer DU145. Exp Mol Pathol. 2010;88:90-95.

197. Sanchez-Aguilera A, Rattmann I, Drew DZ et al. Involvement of RhoH GTPase in the development of B-cell chronic lymphocytic leukemia. Leukemia. 2010;24:97-104.

198. Islam M, Lin G, Brenner JC et al. RhoC expression and head and neck cancer metastasis. Mol Cancer Res. 2009;7:1771-1780.

199. Lahoz A, Hall A. DLC1: a significant GAP in the cancer genome. Genes Dev. 2008;22:1724-1730.

200. Bousquet E, Mazieres J, Privat M et al. Loss of RhoB expression promotes migration and invasion of human bronchial cells via activation of AKT1. Cancer Res. 2009;69:6092-6099.

201. Asnaghi L, Vass WC, Quadri R et al. E-cadherin negatively regulates neoplastic growth in non-small cell lung cancer: role of Rho GTPases. Oncogene. 2010;29:2760-2771.

202. Meng XN, Jin Y, Yu Y et al. Characterisation of fibronectin-mediated FAK signalling pathways in lung cancer cell migration and invasion. Br J Cancer. 2009;101:327-334.

203. Feng YX, Zhao JS, Li JJ et al. Liver cancer: EphrinA2 promotes tumorigenicity through Rac1/Akt/NF-kappaB signaling pathway 120:. Hepatology. 2010;51:535-544.

204. Cho HJ, Baek KE, Yoo J. RhoGDI2 as a therapeutic target in cancer. Expert Opin Ther Targets. 2010;14:67-75.

205. Zavarella S, Nakada M, Belverud S et al. Role of Rac1-regulated signaling in medulloblastoma invasion. Laboratory investigation. J Neurosurg Pediatr. 2009;4:97-104.

206. Cannistra SA. Cancer of the ovary. N Engl J Med. 2004;351:2519-2529.

207. Schnelzer A, Prechtel D, Knaus U et al. Rac1 in human breast cancer: overexpression, mutation analysis, and characterization of a new isoform, Rac1b. Oncogene. 2000;19:3013-3020.

208. Rosenblatt AE, Garcia MI, Lyons L et al. Inhibition of the Rho GTPase, Rac1, decreases estrogen receptor levels and is a novel therapeutic strategy in breast cancer. Endocr Relat Cancer. 2011;18:207-219.

209. Miyoshi Y, Murase K, Saito M, Imamura M, Oh K. Mechanisms of estrogen receptor-alpha upregulation in breast cancers. Med Mol Morphol. 2010;43:193-196.

210. Jing MX, Mao XY, Li C, Wei J, Liu C, Jin F. Estrogen receptor-alpha promoter methylation in sporadic basal-like breast cancer of Chinese women. Tumour Biol. 2011

211. Barone I, Brusco L, Gu G et al. Loss of Rho GDIalpha and resistance to tamoxifen via effects on estrogen receptor alpha. J Natl Cancer Inst. 2011;103:538-552.

212. Akunuru S, Palumbo J, Zhai QJ, Zheng Y. Rac1 targeting suppresses human non-small cell lung adenocarcinoma cancer stem cell activity. PLoS One. 2011;6:e16951.

213. Kissil JL, Walmsley MJ, Hanlon L et al. Requirement for Rac1 in a K-ras induced lung cancer in the mouse. Cancer Res. 2007;67:8089-8094.

214. Malliri A, Rygiel TP, van der Kammen RA et al. The rac activator Tiam1 is a Wnt-responsive gene that modifies intestinal tumor development. J Biol Chem. 2006;281:543-548.

215. Liu L, Wu DH, Ding YQ. Tiam1 gene expression and its significance in colorectal carcinoma. World J Gastroenterol. 2005;11:705-707.

216. Espina C, Cespedes MV, Garcia-Cabezas MA et al. A critical role for Rac1 in tumor progression of human colorectal adenocarcinoma cells. Am J Pathol. 2008;172:156-166.

217. Sansom OJ, Reed KR, Hayes AJ et al. Loss of Apc in vivo immediately perturbs Wnt signaling, differentiation, and migration. Genes Dev. 2004;18:1385-1390.

218. Buongiorno P, Pethe VV, Charames GS, Esufali S, Bapat B. Rac1 GTPase and the Rac1 exchange factor Tiam1 associate with Wnt-responsive promoters to enhance beta-catenin/TCF-dependent transcription in colorectal cancer cells. Mol Cancer. 2008;7:73.

219. Korinek V, Barker N, Morin PJ et al. Constitutive transcriptional activation by a beta-catenin-Tcf complex in APC-/- colon carcinoma. Science. 1997;275:1784-1787.

220. Wang H, Linghu H, Wang J et al. The role of Crk/Dock180/Rac1 pathway in the malignant behavior of human ovarian cancer cell SKOV3. Tumour Biol. 2010;31:59-67.

221. Wooster R, Weber BL. Breast and ovarian cancer. N Engl J Med. 2003;348:2339-2347.

222. Cho KR, Shih I. Ovarian cancer. Annu Rev Pathol. 2009;4:287-313.

223. Onesto C, Shutes A, Picard V, Schweighoffer F, Der CJ. Characterization of EHT 1864, a novel small molecule inhibitor of Rac family small GTPases. Methods Enzymol. 2008;439:111-129.

224. Akbar H, Cancelas J, Williams DA, Zheng J, Zheng Y. Rational design and applications of a Rac GTPase-specific small molecule inhibitor. Methods Enzymol. 2006;406:554-565.

225. Hernandez E, De La Mota-Peynado A, Dharmawardhane S, Vlaar CP. Novel inhibitors of Rac1 in metastatic breast cancer. P R Health Sci J. 2010;29:348-356.

226. Chan A, Akhtar M, Brenner M, Zheng Y, Gulko PS, Symons M. The GTPase Rac regulates the proliferation and invasion of fibroblast-like synoviocytes from rheumatoid arthritis patients. Mol Med. 2007;13:297-304.

227. Mahmud SM, Franco EL, Aprikian AG. Use of nonsteroidal anti-inflammatory drugs and prostate cancer risk: a meta-analysis. Int J Cancer. 2010;127:1680-1691.

228. Kawahara T, Ishiguro H, Hoshino K et al. Analysis of NSAID-activated gene 1 expression in prostate cancer. Urol Int. 2010;84:198-202.

229. Park IS, Jo JR, Hong H et al. Aspirin induces apoptosis in YD-8 human oral squamous carcinoma cells through activation of caspases, down-regulation of Mcl-1, and inactivation of ERK-1/2 and AKT. Toxicol In Vitro. 2010;24:713-720.

230. Sidelmann UG, Bjornsdottir I, Shockcor JP, Hansen SH, Lindon JC, Nicholson JK. Directly coupled HPLC-NMR and HPLC-MS approaches for the rapid characterisation of drug metabolites in urine: application to the human metabolism of naproxen. J Pharm Biomed Anal. 2001;24:569-579.

231. Kotilinek LA, Westerman MA, Wang Q et al. Cyclooxygenase-2 inhibition improves amyloid-beta-mediated suppression of memory and synaptic plasticity. Brain. 2008;131:651-664.

232. Carabaza A, Cabre F, Rotllan E et al. Stereoselective inhibition of inducible cyclooxygenase by chiral nonsteroidal antiinflammatory drugs. J Clin Pharmacol. 1996;36:505-512.

233. Kolluri SK, Corr M, James SY et al. The R-enantiomer of the nonsteroidal antiinflammatory drug etodolac binds retinoid X receptor and induces tumor-selective apoptosis. Proc Natl Acad Sci U S A. 2005;102:2525-2530.

234. Crompton AM, Foley LH, Wood A et al. Regulation of Tiam1 nucleotide exchange activity by pleckstrin domain binding ligands. J Biol Chem. 2000;275:25751-25759.

235. Hofmann C, Shepelev M, Chernoff J. The genetics of Pak. J Cell Sci. 2004;117:4343-4354.

236. Bokoch GM. Biology of the p21-activated kinases. Annu Rev Biochem. 2003;72:743-781.

237. Stanford SM, Krishnamurthy D, Falk MD et al. Discovery of a novel series of inhibitors of lymphoid tyrosine phosphatase with activity in human T cells. J Med Chem. 2011;54:1640-1654.

238. Blazer LL, Zhang H, Casey EM, Husbands SM, Neubig RR. A nanomolar-potency small molecule inhibitor of regulator of G-protein signaling proteins. Biochemistry. 2011;50:3181-3192.

239. Sprang SR, Chen Z, Du X. Structural basis of effector regulation and signal termination in heterotrimeric Galpha proteins. Adv Protein Chem. 2007;74:1-65.

240. Zhang H, Sun C, Glogauer M, Bokoch GM. Human neutrophils coordinate chemotaxis by differential activation of Rac1 and Rac2. J Immunol. 2009;183:2718-2728.

241. Aznar S, Lacal JC. Rho signals to cell growth and apoptosis. Cancer Lett. 2001;165:1-10.

242. Sahai E, Marshall CJ. RHO-GTPases and cancer. Nat Rev Cancer. 2002;2:133-142.

243. Thiery JP, Sleeman JP. Complex networks orchestrate epithelial-mesenchymal transitions. Nat Rev Mol Cell Biol. 2006;7:131-142.

244. Lozano E, Betson M, Braga VM. Tumor progression: Small GTPases and loss of cell-cell adhesion. Bioessays. 2003;25:452-463.

245. Lozano E, Frasa MA, Smolarczyk K, Knaus UG, Braga VM. PAK is required for the disruption of E-cadherin adhesion by the small GTPase Rac. J Cell Sci. 2008;121:933-938.

246. Mertens AE, Rygiel TP, Olivo C, van der Kammen R, Collard JG. The Rac activator Tiam1 controls tight junction biogenesis in keratinocytes through binding to and activation of the Par polarity complex. J Cell Biol. 2005;170:1029-1037.

247. Malliri A, van der Kammen RA, Clark K, van der Valk M, Michiels F, Collard JG. Mice deficient in the Rac activator Tiam1 are resistant to Ras-induced skin tumours. Nature. 2002;417:867-871.

248. Pegtel DM, Ellenbroek SI, Mertens AE, van der Kammen RA, de Rooij J, Collard JG. The Par-Tiam1 complex controls persistent migration by stabilizing microtubule-dependent front-rear polarity. Curr Biol. 2007;17:1623-1634.

249. Vane JR. Inhibition of prostaglandin synthesis as a mechanism of action for aspirin-like drugs. Nature. 1971;231:232-235.

250. Dannhardt G, Kiefer W. Cyclooxygenase inhibitors--current status and future prospects. Eur J Med Chem. 2001;36:109-126.

251. Mizushima T. Development of new type of NSAIDs with lower gastric side effects. Inflammation and Regeneration. 2008

252. Taketo MM. Cyclooxygenase-2 inhibitors in tumorigenesis (part I). J Natl Cancer Inst. 1998;90:1529-1536.

253. Turini ME, DuBois RN. Cyclooxygenase-2: a therapeutic target. Annu Rev Med. 2002;53:35-57.

254. Gupta RA, Tejada LV, Tong BJ et al. Cyclooxygenase-1 is overexpressed and promotes angiogenic growth factor production in ovarian cancer. Cancer Res. 2003;63:906-911.

255. Wyss-Coray T. Inflammation in Alzheimer disease: driving force, bystander or beneficial response? Nat Med. 2006;12:1005-1015.

256. Wu R, Abramson AL, Symons MH, Steinberg BM. Pak1 and Pak2 are activated in recurrent respiratory papillomas, contributing to one pathway of Rac1-mediated COX-2 expression. Int J Cancer. 2010;127:2230-2237.

257. Wu R, Coniglio SJ, Chan A, Symons MH, Steinberg BM. Up-regulation of Rac1 by epidermal growth factor mediates COX-2 expression in recurrent respiratory papillomas. Mol Med. 2007;13:143-150.

258. Urban E, Jacob S, Nemethova M, Resch GP, Small JV. Electron tomography reveals unbranched networks of actin filaments in lamellipodia. Nat Cell Biol. 2010;12:429-435.

259. Pollard TD, Blanchoin L, Mullins RD. Molecular mechanisms controlling actin filament dynamics in nonmuscle cells. Annu Rev Biophys Biomol Struct. 2000;29:545-576.

260. Campellone KG, Welch MD. A nucleator arms race: cellular control of actin assembly. Nat Rev Mol Cell Biol. 2010;11:237-251.

261. Chesarone MA, Goode BL. Actin nucleation and elongation factors: mechanisms and interplay. Curr Opin Cell Biol. 2009;21:28-37.

262. Miki H, Yamaguchi H, Suetsugu S, Takenawa T. IRSp53 is an essential intermediate between Rac and WAVE in the regulation of membrane ruffling. Nature. 2000;408:732-735.

263. Fu Q, Hue J, Li S. Nonsteroidal anti-inflammatory drugs promote axon regeneration via RhoA inhibition. J Neurosci. 2007;27:4154-4164.

264. Wang X, Budel S, Baughman K, Gould G, Song KH, Strittmatter SM. Ibuprofen enhances recovery from spinal cord injury by limiting tissue loss and stimulating axonal growth. J Neurotrauma. 2009;26:81-95.

265. Lichtenstein MP, Carriba P, Baltrons MA et al. Secretase-independent and RhoGTPase/PAK/ERK-dependent regulation of cytoskeleton dynamics in astrocytes by NSAIDs and derivatives. J Alzheimers Dis. 2010;22:1135-1155.

266. Engers R, Springer E, Michiels F, Collard JG, Gabbert HE. Rac affects invasion of human renal cell carcinomas by up-regulating tissue inhibitor of metalloproteinases (TIMP)-1 and TIMP-2 expression. J Biol Chem. 2001;276:41889-41897.

267. Sebti SM, Hamilton AD. Farnesyltransferase and geranylgeranyltransferase I inhibitors and cancer therapy: lessons from mechanism and bench-to-bedside translational studies. Oncogene. 2000;19:6584-6593.

268. Coxon FP, Helfrich MH, Larijani B et al. Identification of a novel phosphonocarboxylate inhibitor of Rab geranylgeranyl transferase that specifically prevents Rab prenylation in osteoclasts and macrophages. J Biol Chem. 2001;276:48213-48222.

269. Yuasa T, Kimura S, Ashihara E, Habuchi T, Maekawa T. Zoledronic acid - a multiplicity of anti-cancer action. Curr Med Chem. 2007;14:2126-2135.

270. Ali BR, Nouvel I, Leung KF, Hume AN, Seabra MC. A novel statin-mediated "prenylation block-and-release" assay provides insight into the membrane targeting mechanisms of small GTPases. Biochem Biophys Res Commun. 2010;397:34-41.

271. Ivessa NE, Gravotta D, De Lemos-Chiarandini C, Kreibich G. Functional protein prenylation is required for the brefeldin A-dependent retrograde transport from the Golgi apparatus to the endoplasmic reticulum. J Biol Chem. 1997;272:20828-20834.

272. Dong C, Zhang X, Zhou F et al. ADP-ribosylation factors modulate the cell surface transport of G protein-coupled receptors. J Pharmacol Exp Ther. 2010;333:174-183.

273. Anders N, Jurgens G. Large ARF guanine nucleotide exchange factors in membrane trafficking. Cell Mol Life Sci. 2008;65:3433-3445.

274. Ferri N, Corsini A, Bottino P, Clerici F, Contini A. Virtual screening approach for the identification of new Rac1 inhibitors. J Med Chem. 2009;52:4087-4090.

275. Mohrmann K, Leijendekker R, Gerez L, van Der Sluijs P. rab4 regulates transport to the apical plasma membrane in Madin-Darby canine kidney cells. J Biol Chem. 2002;277:10474-10481.

276. Cataldo AM, Petanceska S, Peterhoff CM et al. App gene dosage modulates endosomal abnormalities of Alzheimer's disease in a segmental trisomy 16 mouse model of down syndrome. J Neurosci. 2003;23:6788-6792.

277. Cataldo AM, Peterhoff CM, Troncoso JC, Gomez-Isla T, Hyman BT, Nixon RA. Endocytic pathway abnormalities precede amyloid beta deposition in sporadic Alzheimer's disease and Down syndrome: differential effects of APOE genotype and presenilin mutations. Am J Pathol. 2000;157:277-286.

278. Choudhury A, Sharma DK, Marks DL, Pagano RE. Elevated endosomal cholesterol levels in Niemann-Pick cells inhibit rab4 and perturb membrane recycling. Mol Biol Cell. 2004;15:4500-4511.

279. Etzion S, Etzion Y, DeBosch B, Crawford PA, Muslin AJ. Akt2 deficiency promotes cardiac induction of Rab4a and myocardial beta-adrenergic hypersensitivity. J Mol Cell Cardiol. 2010;49:931-940.

280. Fernandez DR, Telarico T, Bonilla E et al. Activation of mammalian target of rapamycin controls the loss of TCRzeta in lupus T cells through HRES-1/Rab4-regulated lysosomal degradation. J Immunol. 2009;182:2063-2073.

281. Ferrandiz-Huertas C, Fernandez-Carvajal A, Ferrer-Montiel A. Rab4 interacts with the human P-glycoprotein and modulates its surface expression in multidrug resistant K562 cells. Int J Cancer. 2011;128:192-205.

282. Yamamoto H, Koga H, Katoh Y, Takahashi S, Nakayama K, Shin HW. Functional cross-talk between Rab14 and Rab4 through a dual effector, RUFY1/Rabip4. Mol Biol Cell. 2010;21:2746-2755.

283. McLauchlan H, Newell J, Morrice N, Osborne A, West M, Smythe E. A novel role for Rab5-GDI in ligand sequestration into clathrin-coated pits. Curr Biol. 1998;8:34-45.

284. Woodman PG. Biogenesis of the sorting endosome: the role of Rab5. Traffic. 2000;1:695-701.

285. Tomshine JC, Severson SR, Wigle DA et al. Cell proliferation and epidermal growth factor signaling in non-small cell lung adenocarcinoma cell lines are dependent on Rin1. J Biol Chem. 2009;284:26331-26339.

286. Zerial M, McBride H. Rab proteins as membrane organizers. Nat Rev Mol Cell Biol. 2001;2:107-117.

287. Ginsberg SD, Mufson EJ, Counts SE et al. Regional selectivity of rab5 and rab7 protein upregulation in mild cognitive impairment and Alzheimer's disease. J Alzheimers Dis. 2010;22:631-639.

288. Carroll KS, Hanna J, Simon I, Krise J, Barbero P, Pfeffer SR. Role of Rab9 GTPase in facilitating receptor recruitment by TIP47. Science. 2001;292:1373-1376.

289. Diaz E, Schimmoller F, Pfeffer SR. A novel Rab9 effector required for endosome-to-TGN transport. J Cell Biol. 1997;138:283-290.

290. Ganley IG, Pfeffer SR. Cholesterol accumulation sequesters Rab9 and disrupts late endosome function in NPC1-deficient cells. J Biol Chem. 2006;281:17890-17899.

291. Hanna J, Carroll K, Pfeffer SR. Identification of residues in TIP47 essential for Rab9 binding. Proc Natl Acad Sci U S A. 2002;99:7450-7454.

292. Jackson LK, Nawabi P, Hentea C, Roark EA, Haldar K. The Salmonella virulence protein SifA is a G protein antagonist. Proc Natl Acad Sci U S A. 2008;105:14141-14146.

293. Kaptzan T, West SA, Holicky EL et al. Development of a Rab9 transgenic mouse and its ability to increase the lifespan of a murine model of Niemann-Pick type C disease. Am J Pathol. 2009;174:14-20.

294. Kloer DP, Rojas R, Ivan V et al. Assembly of the biogenesis of lysosome-related organelles complex-3 (BLOC-3) and its interaction with Rab9. J Biol Chem. 2010;285:7794-7804.

295. Lombardi D, Soldati T, Riederer MA, Goda Y, Zerial M, Pfeffer SR. Rab9 functions in transport between late endosomes and the trans Golgi network. EMBO J. 1993;12:677-682.

296. Murray JL, Mavrakis M, McDonald NJ et al. Rab9 GTPase is required for replication of human immunodeficiency virus type 1, filoviruses, and measles virus. J Virol. 2005;79:11742-11751.

297. Narita K, Choudhury A, Dobrenis K et al. Protein transduction of Rab9 in Niemann-Pick C cells reduces cholesterol storage. FASEB J. 2005;19:1558-1560.

298. Riederer MA, Soldati T, Shapiro AD, Lin J, Pfeffer SR. Lysosome biogenesis requires Rab9 function and receptor recycling from endosomes to the trans-Golgi network. J Cell Biol. 1994;125:573-582.

299. Shimizu S, Arakawa S, Nishida Y. Autophagy takes an alternative pathway. Autophagy. 2010;6:290-291.

300. Soldati T, Rancano C, Geissler H, Pfeffer SR. Rab7 and Rab9 are recruited onto late endosomes by biochemically distinguishable processes. J Biol Chem. 1995;270:25541-25548.

301. Walter M, Davies JP, Ioannou YA. Telomerase immortalization upregulates Rab9 expression and restores LDL cholesterol egress from Niemann-Pick C1 late endosomes. J Lipid Res. 2003;44:243-253.

302. Worgall TS. Lipid metabolism in cystic fibrosis. Curr Opin Clin Nutr Metab Care. 2009;12:105-109.

303. Sun Y, Buki KG, Ettala O, Vaaraniemi JP, Vaananen HK. Possible role of direct Rac1-Rab7 interaction in ruffled border formation of osteoclasts. J Biol Chem. 2005;280:32356-32361.

304. Van Wesenbeeck L, Odgren PR, Coxon FP et al. Involvement of PLEKHM1 in osteoclastic vesicular transport and osteopetrosis in incisors absent rats and humans. J Clin Invest. 2007;117:919-930.

305. Zhao H, Laitala-Leinonen T, Parikka V, Vaananen HK. Downregulation of small GTPase Rab7 impairs osteoclast polarization and bone resorption. J Biol Chem. 2001;276:39295-39302.

306. Calhoun BC, Goldenring JR. Two Rab proteins, vesicle-associated membrane protein 2 (VAMP-2) and secretory carrier membrane proteins (SCAMPs), are present on immunoisolated parietal cell tubulovesicles. Biochem J. 1997;325:559-564.

307. Chen W, Feng Y, Chen D, Wandinger-Ness A. Rab11 is required for trans-golgi network-to-plasma membrane transport and a preferential target for GDP dissociation inhibitor. Mol Biol Cell. 1998;9:3241-3257.

308. Jing J, Prekeris R. Polarized endocytic transport: the roles of Rab11 and Rab11-FIPs in regulating cell polarity. Histol Histopathol. 2009;24:1171-1180.

309. Knodler A, Feng S, Zhang J et al. Coordination of Rab8 and Rab11 in primary ciliogenesis. Proc Natl Acad Sci U S A. 2010;107:6346-6351.

310. Li X, Sapp E, Chase K et al. Disruption of Rab11 activity in a knock-in mouse model of Huntington's disease. Neurobiol Dis. 2009;36:374-383.

311. Li X, Standley C, Sapp E et al. Mutant huntingtin impairs vesicle formation from recycling endosomes by interfering with Rab11 activity. Mol Cell Biol. 2009;29:6106-6116.

312. Luiro K, Yliannala K, Ahtiainen L et al. Interconnections of CLN3, Hook1 and Rab proteins link Batten disease to defects in the endocytic pathway. Hum Mol Genet. 2004;13:3017-3027.

313. Parent A, Hamelin E, Germain P, Parent JL. Rab11 regulates the recycling of the beta2-adrenergic receptor through a direct interaction. Biochem J. 2009;418:163-172.

314. Ray GS, Lee JR, Nwokeji K, Mills LR, Goldenring JR. Increased immunoreactivity for Rab11, a small GTP-binding protein, in low-grade dysplastic Barrett's epithelia. Lab Invest. 1997;77:503-511.

315. Richards P, Didszun C, Campesan S et al. Dendritic spine loss and neurodegeneration is rescued by Rab11 in models of Huntington's disease. Cell Death Differ. 2011;18:191-200.

316. Roberts RC, Peden AA, Buss F et al. Mistargeting of SH3TC2 away from the recycling endosome causes Charcot-Marie-Tooth disease type 4C. Hum Mol Genet. 2010;19:1009-1018.

317. Stendel C, Roos A, Kleine H et al. SH3TC2, a protein mutant in Charcot-Marie-Tooth neuropathy, links peripheral nerve myelination to endosomal recycling. Brain. 2010;133:2462-2474.

318. Ullrich O, Reinsch S, Urbe S, Zerial M, Parton RG. Rab11 regulates recycling through the pericentriolar recycling endosome. J Cell Biol. 1996;135:913-924.

319. Westlake CJ, Baye LM, Nachury MV et al. Primary cilia membrane assembly is initiated by Rab11 and transport protein particle II (TRAPPII) complex-dependent trafficking of Rabin8 to the centrosome. Proc Natl Acad Sci U S A. 2011;108:2759-2764.

320. Gou D, Mishra A, Weng T et al. Annexin A2 interactions with Rab14 in alveolar type II cells. J Biol Chem. 2008;283:13156-13164.

321. Ishikura S, Klip A. Muscle cells engage Rab8A and myosin Vb in insulin-dependent GLUT4 translocation. Am J Physiol Cell Physiol. 2008;295:C1016-25.

322. Junutula JR, De Maziere AM, Peden AA et al. Rab14 is involved in membrane trafficking between the Golgi complex and endosomes. Mol Biol Cell. 2004;15:2218-2229.

323. Kitt KN, Hernandez-Deviez D, Ballantyne SD, Spiliotis ET, Casanova JE, Wilson JM. Rab14 regulates apical targeting in polarized epithelial cells. Traffic. 2008;9:1218-1231.

324. Kyei GB, Vergne I, Chua J et al. Rab14 is critical for maintenance of Mycobacterium tuberculosis phagosome maturation arrest. EMBO J. 2006;25:5250-5259.

325. Proikas-Cezanne T, Gaugel A, Frickey T, Nordheim A. Rab14 is part of the early endosomal clathrin-coated TGN microdomain. FEBS Lett. 2006;580:5241-5246.

326. Saveanu L, Carroll O, Weimershaus M et al. IRAP identifies an endosomal compartment required for MHC class I cross-presentation. Science. 2009;325:213-217.

327. Ueno H, Huang X, Tanaka Y, Hirokawa N. KIF16B/Rab14 molecular motor complex is critical for early embryonic development by transporting FGF receptor. Dev Cell. 2011;20:60-71.

328. Strick DJ, Elferink LA. Rab15 effector protein: a novel protein for receptor recycling from the endocytic recycling compartment. Mol Biol Cell. 2005;16:5699-5709.

329. Zuk PA, Elferink LA. Rab15 differentially regulates early endocytic trafficking. J Biol Chem. 2000;275:26754-26764.

330. Beaumont KA, Hamilton NA, Moores MT et al. The recycling endosome protein Rab17 regulates melanocytic filopodia formation and melanosome trafficking. Traffic. 2011;12:627-643.

331. Lehtonen S, Lehtonen E, Olkkonen VM. Vesicular transport and kidney development. Int J Dev Biol. 1999;43:425-433.

332. Zacchi P, Stenmark H, Parton RG et al. Rab17 regulates membrane trafficking through apical recycling endosomes in polarized epithelial cells. J Cell Biol. 1998;140:1039-1053.

333. Amillet JM, Ferbus D, Real FX et al. Characterization of human Rab20 overexpressed in exocrine pancreatic carcinoma. Hum Pathol. 2006;37:256-263.

334. Curtis LM, Gluck S. Distribution of Rab GTPases in mouse kidney and comparison with vacuolar H+-ATPase. Nephron Physiol. 2005;100:p31-42.

335. Das Sarma J, Kaplan BE, Willemsen D, Koval M. Identification of rab20 as a potential regulator of connexin 43 trafficking. Cell Commun Adhes. 2008;15:65-74.

336. Hackenbeck T, Huber R, Schietke R et al. The GTPase RAB20 is a HIF target with mitochondrial localization mediating apoptosis in hypoxia. Biochim Biophys Acta. 2011;1813:1-13.

337. Lutcke A, Parton RG, Murphy C et al. Cloning and subcellular localization of novel rab proteins reveals polarized and cell type-specific expression. J Cell Sci. 1994;107:3437-3448.

338. Turner N, Lambros MB, Horlings HM et al. Integrative molecular profiling of triple negative breast cancers identifies amplicon drivers and potential therapeutic targets. Oncogene. 2010;29:2013-2023.

339. Burgo A, Sotirakis E, Simmler MC et al. Role of Varp, a Rab21 exchange factor and TI-VAMP/VAMP7 partner, in neurite growth. EMBO Rep. 2009;10:1117-1124.

340. Delprato A, Lambright DG. Structural basis for Rab GTPase activation by VPS9 domain exchange factors. Nat Struct Mol Biol. 2007;14:406-412.

341. Egami Y, Araki N. Characterization of Rab21-positive tubular endosomes induced by PI3K inhibitors. Exp Cell Res. 2008;314:729-737.

342. Egami Y, Araki N. Dynamic changes in the spatiotemporal localization of Rab21 in live RAW264 cells during macropinocytosis. PLoS One. 2009;4:e6689.

343. Pal'gova IV, Korobko EV, Korobko IV. [Multiadaptor 4.1 and RanBP9 protein family members as putative interaction partners for VARP, a Rab21 GTPase guanine nucleotide exchange factor]. Mol Biol (Mosk). 2007;41:1009-1013.

344. Pellinen T, Arjonen A, Vuoriluoto K, Kallio K, Fransen JA, Ivaska J. Small GTPase Rab21 regulates cell adhesion and controls endosomal traffic of beta1-integrins. J Cell Biol. 2006;173:767-780.

345. Pellinen T, Tuomi S, Arjonen A et al. Integrin trafficking regulated by Rab21 is necessary for cytokinesis. Dev Cell. 2008;15:371-385.

346. Tamura K, Ohbayashi N, Maruta Y, Kanno E, Itoh T, Fukuda M. Varp is a novel Rab32/38-binding protein that regulates Tyrp1 trafficking in melanocytes. Mol Biol Cell. 2009;20:2900-2908.

347. Tang BL, Ng EL. Rabs and cancer cell motility. Cell Motil Cytoskeleton. 2009;66:365-370.

348. Zhu G, Chen J, Liu J et al. Structure of the APPL1 BAR-PH domain and characterization of its interaction with Rab5. EMBO J. 2007;26:3484-3493.

349. Magadan JG, Barbieri MA, Mesa R, Stahl PD, Mayorga LS. Rab22a regulates the sorting of transferrin to recycling endosomes. Mol Cell Biol. 2006;26:2595-2614.

350. Roberts EA, Chua J, Kyei GB, Deretic V. Higher order Rab programming in phagolysosome biogenesis. J Cell Biol. 2006;174:923-929.

351. He H, Dai F, Yu L et al. Identification and characterization of nine novel human small GTPases showing variable expressions in liver cancer tissues. Gene Expr. 2002;10:231-242.

352. Kauppi M, Simonsen A, Bremnes B et al. The small GTPase Rab22 interacts with EEA1 and controls endosomal membrane trafficking. J Cell Sci. 2002;115:899-911.

353. Mesa R, Salomon C, Roggero M, Stahl PD, Mayorga LS. Rab22a affects the morphology and function of the endocytic pathway. J Cell Sci. 2001;114:4041-4049.

354. Ng EL, Tang BL. Rab GTPases and their roles in brain neurons and glia. Brain Res Rev. 2008;58:236-246.

355. Olkkonen VM, Dupree P, Killisch I, Lutcke A, Zerial M, Simons K. Molecular cloning and subcellular localization of three GTP-binding proteins of the rab subfamily. J Cell Sci. 1993;106:1249-1261.

356. Zhu H, Liang Z, Li G. Rabex-5 is a Rab22 effector and mediates a Rab22-Rab5 signaling cascade in endocytosis. Mol Biol Cell. 2009;20:4720-4729.

357. Agarwal R, Jurisica I, Mills GB, Cheng KW. The emerging role of the RAB25 small GTPase in cancer. Traffic. 2009;10:1561-1568.

358. Bigelow RL, Williams BJ, Carroll JL, Daves LK, Cardelli JA. TIMP-1 overexpression promotes tumorigenesis of MDA-MB-231 breast cancer cells and alters expression of a subset of cancer promoting genes in vivo distinct from those observed in vitro. Breast Cancer Res Treat. 2009;117:31-44.

359. Caswell PT, Spence HJ, Parsons M et al. Rab25 associates with alpha5beta1 integrin to promote invasive migration in 3D microenvironments. Dev Cell. 2007;13:496-510.

360. Cheng JM, Ding M, Aribi A, Shah P, Rao K. Loss of RAB25 expression in breast cancer. Int J Cancer. 2006;118:2957-2964.

361. Cheng JM, Volk L, Janaki DK, Vyakaranam S, Ran S, Rao KA. Tumor suppressor function of Rab25 in triple-negative breast cancer. Int J Cancer. 2010;126:2799-2812.

362. Cheng KW, Lahad JP, Kuo WL et al. The RAB25 small GTPase determines aggressiveness of ovarian and breast cancers. Nat Med. 2004;10:1251-1256.

363. Cheng KW, Lu Y, Mills GB. Assay of Rab25 function in ovarian and breast cancers. Methods Enzymol. 2005;403:202-215.

364. Chia WJ, Tang BL. Emerging roles for Rab family GTPases in human cancer. Biochim Biophys Acta. 2009;1795:110-116.

365. Davidson B, Zhang Z, Kleinberg L et al. Gene expression signatures differentiate ovarian/peritoneal serous carcinoma from diffuse malignant peritoneal mesothelioma. Clin Cancer Res. 2006;12:5944-5950.

366. Goldenring JR, Nam KT. Rab25 as a tumour suppressor in colon carcinogenesis. Br J Cancer. 2011;104:33-36.

367. Lapierre LA, Avant KM, Caldwell CM et al. Characterization of immunoisolated human gastric parietal cells tubulovesicles: identification of regulators of apical recycling. Am J Physiol Gastrointest Liver Physiol. 2007;292:G1249-62.

368. Lapierre LA, Caldwell CM, Higginbotham JN et al. Transformation of rat intestinal epithelial cells by overexpression of Rab25 is microtubule dependent. Cytoskeleton (Hoboken). 2011;68:97-111.

369. Nam KT, Lee HJ, Smith JJ et al. Loss of Rab25 promotes the development of intestinal neoplasia in mice and is associated with human colorectal adenocarcinomas. J Clin Invest. 2010;120:840-849.

370. Sheach LA, Adeney EM, Kucukmetin A et al. Androgen-related expression of G-proteins in ovarian cancer. Br J Cancer. 2009;101:498-503.

371. Rodriguez-Gabin AG, Yin X, Si Q, Larocca JN. Transport of mannose-6-phosphate receptors from the trans-Golgi network to endosomes requires Rab31. Exp Cell Res. 2009;315:2215-2230.

372. Chen L, Hu J, Yun Y, Wang T. Rab36 regulates the spatial distribution of late endosomes and lysosomes through a similar mechanism to Rab34. Mol Membr Biol. 2010;27:24-31.

373. Goldenberg NM, Grinstein S, Silverman M. Golgi-bound Rab34 is a novel member of the secretory pathway. Mol Biol Cell. 2007;18:4762-4771.

374. Goldenberg NM, Silverman M. Rab34 and its effector munc13-2 constitute a new pathway modulating protein secretion in the cellular response to hyperglycemia. Am J Physiol Cell Physiol. 2009;297:C1053-8.

375. Speight P, Silverman M. Diacylglycerol-activated Hmunc13 serves as an effector of the GTPase Rab34. Traffic. 2005;6:858-865.

376. Sun P, Endo T. Assays for functional properties of Rab34 in macropinosome formation. Methods Enzymol. 2005;403:229-243.

377. Sun P, Yamamoto H, Suetsugu S, Miki H, Takenawa T, Endo T. Small GTPase Rah/Rab34 is associated with membrane ruffles and macropinosomes and promotes macropinosome formation. J Biol Chem. 2003;278:4063-4071.

378. Wang T, Hong W. Interorganellar regulation of lysosome positioning by the Golgi apparatus through Rab34 interaction with Rab-interacting lysosomal protein. Mol Biol Cell. 2002;13:4317-4332.

379. Wang T, Hong W. Assay and functional properties of Rab34 interaction with RILP in lysosome morphogenesis. Methods Enzymol. 2005;403:675-687.

380. Allaire PD, Marat AL, Dall'Armi C, Di Paolo G, McPherson PS, Ritter B. The Connecdenn DENN domain: a GEF for Rab35 mediating cargo-specific exit from early endosomes. Mol Cell. 2010;37:370-382.

381. Chevallier J, Koop C, Srivastava A, Petrie RJ, Lamarche-Vane N, Presley JF. Rab35 regulates neurite outgrowth and cell shape. FEBS Lett. 2009;583:1096-1101.

382. Chua CE, Lim YS, Tang BL. Rab35--a vesicular traffic-regulating small GTPase with actin modulating roles. FEBS Lett. 2010;584:1-6.

383. Echard A. Membrane traffic and polarization of lipid domains during cytokinesis. Biochem Soc Trans. 2008;36:395-399.

384. Kouranti I, Sachse M, Arouche N, Goud B, Echard A. Rab35 regulates an endocytic recycling pathway essential for the terminal steps of cytokinesis. Curr Biol. 2006;16:1719-1725.

385. Marat AL, McPherson PS. The connecdenn family, Rab35 guanine nucleotide exchange factors interfacing with the clathrin machinery. J Biol Chem. 2010;285:10627-10637.

386. Shim J, Lee SM, Lee MS, Yoon J, Kweon HS, Kim YJ. Rab35 mediates transport of Cdc42 and Rac1 to the plasma membrane during phagocytosis. Mol Cell Biol. 2010;30:1421-1433.

387. Walseng E, Bakke O, Roche PA. Major histocompatibility complex class II-peptide complexes internalize using a clathrin- and dynamin-independent endocytosis pathway. J Biol Chem. 2008;283:14717-14727.

388. Zhang J, Fonovic M, Suyama K, Bogyo M, Scott MP. Rab35 controls actin bundling by recruiting fascin as an effector protein. Science. 2009;325:1250-1254.

389. Wozniak K, Piaskowski S, Gresner SM et al. BCR expression is decreased in meningiomas showing loss of heterozygosity of 22q within a new minimal deletion region. Cancer Genet Cytogenet. 2008;183:14-20.

390. Zhou J, Fogelgren B, Wang Z, Roe BA, Biegel JA. Isolation of genes from the rhabdoid tumor deletion region in chromosome band 22q11.2. Gene. 2000;241:133-141.

391. Becker CE, Creagh EM, O'Neill LA. Rab39a binds caspase-1 and is required for caspase-1-dependent interleukin-1beta secretion. J Biol Chem. 2009;284:34531-34537.

392. Chen T, Han Y, Yang M et al. Rab39, a novel Golgi-associated Rab GTPase from human dendritic cells involved in cellular endocytosis. Biochem Biophys Res Commun. 2003;303:1114-1120.

393. Li Y, Wandinger-Ness A, Goldenring JR, Cover TL. Clustering and redistribution of late endocytic compartments in response to Helicobacter pylori vacuolating toxin. Mol Biol Cell. 2004;15:1946-1959.

394. Press B, Feng Y, Hoflack B, Wandinger-Ness A. Mutant Rab7 causes the accumulation of cathepsin D and cation-independent mannose 6-phosphate receptor in an early endocytic compartment. J Cell Biol. 1998;140:1075-1089.

395. Vitelli R, Santillo M, Lattero D et al. Role of the small GTPase Rab7 in the late endocytic pathway. J Biol Chem. 1997;272:4391-4397.

396. Ceresa BP, Bahr SJ. rab7 activity affects epidermal growth factor:epidermal growth factor receptor degradation by regulating endocytic trafficking from the late endosome. J Biol Chem. 2006;281:1099-1106.

397. Mukhopadhyay A, Pan X, Lambright DG, Tissenbaum HA. An endocytic pathway as a target of tubby for regulation of fat storage. EMBO Rep. 2007;8:931-938.

398. Sender V, Moulakakis C, Stamme C. Pulmonary surfactant protein A enhances endolysosomal trafficking in alveolar macrophages through regulation of Rab7. J Immunol. 2011;186:2397-2411.

399. Marambio P, Toro B, Sanhueza C et al. Glucose deprivation causes oxidative stress and stimulates aggresome formation and autophagy in cultured cardiac myocytes. Biochim Biophys Acta. 2010;1802:509-518.

400. Munafo DB, Colombo MI. Induction of autophagy causes dramatic changes in the subcellular distribution of GFP-Rab24. Traffic. 2002;3:472-482.

401. Overmeyer JH, Maltese WA. Tyrosine phosphorylation of Rab proteins. Methods Enzymol. 2005;403:194-202.

402. Schardt A, Brinkmann BG, Mitkovski M, Sereda MW, Werner HB, Nave KA. The SNARE protein SNAP-29 interacts with the GTPase Rab3A: Implications for membrane trafficking in myelinating glia. J Neurosci Res. 2009;87:3465-3479.

403. Wu M, Yin G, Zhao X et al. Human RAB24, interestingly and predominantly distributed in the nuclei of COS-7 cells, is colocalized with cyclophilin A and GABARAP. Int J Mol Med. 2006;17:749-754.

404. Alto NM, Soderling J, Scott JD. Rab32 is an A-kinase anchoring protein and participates in mitochondrial dynamics. J Cell Biol. 2002;158:659-668.

405. Bui M, Gilady SY, Fitzsimmons RE et al. Rab32 modulates apoptosis onset and mitochondria-associated membrane (MAM) properties. J Biol Chem. 2010;285:31590-31602.

406. Hirota Y, Tanaka Y. A small GTPase, human Rab32, is required for the formation of autophagic vacuoles under basal conditions. Cell Mol Life Sci. 2009;66:2913-2932.

407. Wasmeier C, Romao M, Plowright L, Bennett DC, Raposo G, Seabra MC. Rab38 and Rab32 control post-Golgi trafficking of melanogenic enzymes. J Cell Biol. 2006;175:271-281.

408. Schulmann K, Mori Y, Croog V et al. Molecular phenotype of inflammatory bowel disease-associated neoplasms with microsatellite instability. Gastroenterology. 2005;129:74-85.

409. Fukuda M, Itoh T. Direct link between Atg protein and small GTPase Rab: Atg16L functions as a potential Rab33 effector in mammals. Autophagy. 2008;4:824-826.

410. Itoh T, Fujita N, Kanno E, Yamamoto A, Yoshimori T, Fukuda M. Golgi-resident small GTPase Rab33B interacts with Atg16L and modulates autophagosome formation. Mol Biol Cell. 2008;19:2916-2925.

411. Nagelkerken B, Van Anken E, Van Raak M et al. Rabaptin4, a novel effector of the small GTPase rab4a, is recruited to perinuclear recycling vesicles. Biochem J. 2000;346 Pt 3:593-601.

412. Stenmark H, Vitale G, Ullrich O, Zerial M. Rabaptin-5 is a direct effector of the small GTPase Rab5 in endocytic membrane fusion. Cell. 1995;83:423-432.

413. Vitale G, Rybin V, Christoforidis S et al. Distinct Rab-binding domains mediate the interaction of Rabaptin-5 with GTP-bound Rab4 and Rab5. EMBO J. 1998;17:1941-1951.

414. Fouraux MA, Deneka M, Ivan V et al. Rabip4' is an effector of rab5 and rab4 and regulates transport through early endosomes. Mol Biol Cell. 2004;15:611-624.

415. Gaullier JM, Simonsen A, D'Arrigo A, Bremnes B, Stenmark H, Aasland R. FYVE fingers bind PtdIns(3)P.[letter]. Nature 1998;394(6692):432-433.

416. Simonsen A, Lippe R, Christoforidis S et al. EEA1 links PI(3)K function to Rab5 regulation of endosome fusion. Nature. 1998;394:494-498.

417. Christoforidis S, McBride HM, Burgoyne RD, Zerial M. The Rab5 effector EEA1 is a core component of endosome docking. Nature. 1999;397:621-625.

418. Kurosu H, Katada T. Association of phosphatidylinositol 3-kinase composed of p110beta-catalytic and p85-regulatory subunits with the small GTPase Rab5. J Biochem. 2001;130:73-78.

419. Murray JT, Panaretou C, Stenmark H, Miaczynska M, Backer JM. Role of Rab5 in the recruitment of hVps34/p150 to the early endosome. Traffic. 2002;3:416-427.

420. Korobko E, Kiselev S, Olsnes S, Stenmark H, Korobko I. The Rab5 effector Rabaptin-5 and its isoform Rabaptin-5delta differ in their ability to interact with the small GTPase Rab4. FEBS J. 2005;272:37-46.

421. Lippe R, Miaczynska M, Rybin V, Runge A, Zerial M. Functional synergy between Rab5 effector Rabaptin-5 and exchange factor Rabex-5 when physically associated in a complex. Mol Biol Cell. 2001;12:2219-2228.

422. Gournier H, Stenmark H, Rybin V, Lippe R, Zerial M. Two distinct effectors of the small GTPase Rab5 cooperate in endocytic membrane fusion. EMBO J. 1998;17:1930-1940.

423. Nielsen E, Christoforidis S, Uttenweiler-Joseph S et al. Rabenosyn-5, a novel Rab5 effector, is complexed with hVPS45 and recruited to endosomes through a FYVE finger domain. J Cell Biol. 2000;151:601-612.

424. de Renzis S, Sonnichsen B, Zerial M. Divalent Rab effectors regulate the sub-compartmental organization and sorting of early endosomes. Nat Cell Biol. 2002;4:124-133.

425. Horiuchi H, Lippe R, McBride HM et al. A novel Rab5 GDP/GTP exchange factor complexed to Rabaptin-5 links nucleotide exchange to effector recruitment and function. Cell. 1997;90:1149-1159.

426. Zhu H, Zhu G, Liu J, Liang Z, Zhang XC, Li G. Rabaptin-5-independent membrane targeting and Rab5 activation by Rabex-5 in the cell. Mol Biol Cell. 2007;18:4119-4128.

427. Bliss JM, Venkatesh B, Colicelli J. The RIN family of Ras effectors. Methods Enzymol. 2006;407:335-344.

428. Saito K, Murai J, Kajiho H, Kontani K, Kurosu H, Katada T. A novel binding protein composed of homophilic tetramer exhibits unique properties for the small GTPase Rab5. J Biol Chem. 2002;277:3412-3418.

429. Kuriyama H, Asakawa S, Minoshima S et al. Characterization and chromosomal mapping of a novel human gene, ANKHZN. Gene. 2000;253:151-160.

430. Dautry-Varsat A. Receptor-mediated endocytosis: the intracellular journey of transferrin and its receptor. Biochimie. 1986;68:375-381.

431. Wurmser AE, Sato TK, Emr SD. New component of the vacuolar class C-Vps complex couples nucleotide exchange on the Ypt7 GTPase to SNARE-dependent docking and fusion. J Cell Biol. 2000;151:551-562.

432. Seals DF, Eitzen G, Margolis N, Wickner WT, Price A. A Ypt/Rab effector complex containing the Sec1 homolog Vps33p is required for homotypic vacuole fusion. Proc Natl Acad Sci U S A. 2000;97:9402-9407.

433. Nordmann M, Cabrera M, Perz A et al. The Mon1-Ccz1 complex is the GEF of the late endosomal Rab7 homolog Ypt7. Curr Biol. 2010;20:1654-1659.

434. Cheli VT, Dell'Angelica EC. Early origin of genes encoding subunits of biogenesis of lysosome-related organelles complex-1, -2 and -3. Traffic. 2010;11:579-586.

435. Kinchen JM, Ravichandran KS. Identification of two evolutionarily conserved genes regulating processing of engulfed apoptotic cells. Nature. 2010;464:778-782.

436. Nakada-Tsukui K, Saito-Nakano Y, Ali V, Nozaki T. A retromerlike complex is a novel Rab7 effector that is involved in the transport of the virulence factor cysteine protease in the enteric protozoan parasite Entamoeba histolytica. Mol Biol Cell. 2005;16:5294-5303.

437. Sun Q, Westphal W, Wong KN, Tan I, Zhong Q. Rubicon controls endosome maturation as a Rab7 effector. Proc Natl Acad Sci U S A. 2010;107:19338-19343.

438. Hanna MC, Blackstone C. Interaction of the SPG21 protein ACP33/maspardin with the aldehyde dehydrogenase ALDH16A1. Neurogenetics. 2009;10:217-228.

439. Saxena S, Bucci C, Weis J, Kruttgen A. The small GTPase Rab7 controls the endosomal trafficking and neuritogenic signaling of the nerve growth factor receptor TrkA. J Neurosci. 2005;25:10930-10940.

440. Cortes C, Rzomp KA, Tvinnereim A, Scidmore MA, Wizel B. Chlamydia pneumoniae inclusion membrane protein Cpn0585 interacts with multiple Rab GTPases. Infect Immun. 2007;75:5586-5596.

441. Hattula K, Peranen J. FIP-2, a coiled-coil protein, links Huntingtin to Rab8 and modulates cellular morphogenesis. Curr Biol. 2000;10:1603-1606.

442. Chen S, Liang MC, Chia JN, Ngsee JK, Ting AE. Rab8b and its interacting partner TRIP8b are involved in regulated secretion in AtT20 cells. J Biol Chem. 2001;276:13209-13216.

443. Ren M, Zeng J, De Lemos-Chiarandini C, Rosenfeld M, Adesnik M, Sabatini DD. In its active form, the GTP-binding protein rab8 interacts with a stress-activated protein kinase. Proc Natl Acad Sci U S A. 1996;93:5151-5155.

444. Hsiao YC, Tong ZJ, Westfall JE, Ault JG, Page-McCaw PS, Ferland RJ. Ahi1, whose human ortholog is mutated in Joubert syndrome, is required for Rab8a localization, ciliogenesis and vesicle trafficking. Hum Mol Genet. 2009;18:3926-3941.

445. Nachury MV, Loktev AV, Zhang Q et al. A core complex of BBS proteins cooperates with the GTPase Rab8 to promote ciliary membrane biogenesis. Cell. 2007;129:1201-1213.

446. Yoshimura S, Egerer J, Fuchs E, Haas AK, Barr FA. Functional dissection of Rab GTPases involved in primary cilium formation. J Cell Biol. 2007;178:363-369.

447. Omori Y, Zhao C, Saras A et al. Elipsa is an early determinant of ciliogenesis that links the IFT particle to membrane-associated small GTPase Rab8. Nat Cell Biol. 2008;10:437-444.

448. Shisheva A, Chinni SR, DeMarco C. General role of GDP dissociation inhibitor 2 in membrane release of Rab proteins: modulations of its functional interactions by in vitro and in vivo structural modifications. Biochemistry. 1999;38:11711-11721.

449. Randhawa VK, Ishikura S, Talior-Volodarsky I et al. GLUT4 vesicle recruitment and fusion are differentially regulated by Rac, AS160, and Rab8A in muscle cells. J Biol Chem. 2008;283:27208-27219.

450. Yamamura R, Nishimura N, Nakatsuji H, Arase S, Sasaki T. The interaction of JRAB/MICAL-L2 with Rab8 and Rab13 coordinates the assembly of tight junctions and adherens junctions. Mol Biol Cell. 2008;19:971-983.

451. Sharma M, Giridharan SS, Rahajeng J, Naslavsky N, Caplan S. MICAL-L1 links EHD1 to tubular recycling endosomes and regulates receptor recycling. Mol Biol Cell. 2009;20:5181-5194.

452. Burton JL, Burns ME, Gatti E, Augustine GJ, De Camilli P. Specific interactions of Mss4 with members of the Rab GTPase subfamily. EMBO J. 1994;13:5547-5558.

453. Wixler V, Wixler L, Altenfeld A, Ludwig S, Goody RS, Itzen A. Identification and characterisation of novel Mss4-binding Rab GTPases. Biol Chem. 2011;392:239-248.

454. Fukuda M. Distinct Rab binding specificity of Rim1, Rim2, rabphilin, and Noc2. Identification of a critical determinant of Rab3A/Rab27A recognition by Rim2. J Biol Chem. 2003;278:15373-15380.

455. Hyvola N, Diao A, McKenzie E, Skippen A, Cockcroft S, Lowe M. Membrane targeting and activation of the Lowe syndrome protein OCRL1 by rab GTPases. EMBO J. 2006;25:3750-3761.

456. Fukuda M, Kanno E, Ishibashi K, Itoh T. Large scale screening for novel rab effectors reveals unexpected broad Rab binding specificity. Mol Cell Proteomics. 2008;7:1031-1042.

457. Sahlender DA, Roberts RC, Arden SD et al. Optineurin links myosin VI to the Golgi complex and is involved in Golgi organization and exocytosis. J Cell Biol. 2005;169:285-295.

458. Heidrych P, Zimmermann U, Bress A et al. Rab8b GTPase, a protein transport regulator, is an interacting partner of otoferlin, defective in a human autosomal recessive deafness form. Hum Mol Genet. 2008;17:3814-3821.

459. Grosshans BL, Novick P. Identification and verification of Sro7p as an effector of the Sec4p Rab GTPase. Methods Enzymol. 2008;438:95-108.

460. Hattula K, Furuhjelm J, Arffman A, Peranen J. A Rab8-specific GDP/GTP exchange factor is involved in actin remodeling and polarized membrane transport. Mol Biol Cell. 2002;13:3268-3280.

461. Sbrissa D, Ikonomov OC, Shisheva A. Analysis of potential binding of the recombinant Rab9 effector p40 to phosphoinositide-enriched synthetic liposomes. Methods Enzymol. 2005;403:696-705.

462. Hayes GL, Brown FC, Haas AK, Nottingham RM, Barr FA, Pfeffer SR. Multiple Rab GTPase binding sites in GCC185 suggest a model for vesicle tethering at the trans-Golgi. Mol Biol Cell. 2009;20:209-217.

463. Williams C, Choudhury R, McKenzie E, Lowe M. Targeting of the type II inositol polyphosphate 5-phosphatase INPP5B to the early secretory pathway. J Cell Sci. 2007;120:3941-3951.

464. Itoh T, Satoh M, Kanno E, Fukuda M. Screening for target Rabs of TBC (Tre-2/Bub2/Cdc16) domain-containing proteins based on their Rab-binding activity. Genes Cells. 2006;11:1023-1037.

465. Babbey CM, Bacallao RL, Dunn KW. Rab10 associates with primary cilia and the exocyst complex in renal epithelial cells. Am J Physiol Renal Physiol. 2010;299:F495-506.

466. Chen Y, Deng Y, Zhang J, Yang L, Xie X, Xu T. GDI-1 preferably interacts with Rab10 in insulin-stimulated GLUT4 translocation. Biochem J. 2009;422:229-235.

467. Roland JT, Lapierre LA, Goldenring JR. Alternative splicing in class V myosins determines association with Rab10. J Biol Chem. 2009;284:1213-1223.

468. Horgan CP, McCaffrey MW. The dynamic Rab11-FIPs. Biochem Soc Trans. 2009;37:1032-1036.

469. Peden AA, Schonteich E, Chun J, Junutula JR, Scheller RH, Prekeris R. The RCP-Rab11 complex regulates endocytic protein sorting. Mol Biol Cell. 2004;15:3530-3541.

470. Prekeris R, Klumperman J, Scheller RH. A Rab11/Rip11 protein complex regulates apical membrane trafficking via recycling endosomes. Mol Cell. 2000;6:1437-1448.

471. Dabbeekeh JT, Faitar SL, Dufresne CP, Cowell JK. The EVI5 TBC domain provides the GTPase-activating protein motif for RAB11. Oncogene. 2007;26:2804-2808.

472. Prekeris R, Davies JM, Scheller RH. Identification of a novel Rab11/25 binding domain present in Eferin and Rip proteins. J Biol Chem. 2001;276:38966-38970.

473. Mammoto A, Ohtsuka T, Hotta I, Sasaki T, Takai Y. Rab11BP/Rabphilin-11, a downstream target of rab11 small G protein implicated in vesicle recycling. J Biol Chem. 1999;274:25517-25524.

474. Zhang XM, Ellis S, Sriratana A, Mitchell CA, Rowe T. Sec15 is an effector for the Rab11 GTPase in mammalian cells. J Biol Chem. 2004;279:43027-43034.

475. Hales CM, Griner R, Hobdy-Henderson KC et al. Identification and characterization of a family of Rab11-interacting proteins. J Biol Chem. 2001;276:39067-39075.

476. Muto A, Aoki Y, Watanabe S. Mouse Rab11-FIP4 regulates proliferation and differentiation of retinal progenitors in a Rab11-independent manner. Dev Dyn. 2007;236:214-225.

477. Lindsay AJ, McCaffrey MW. Rab11-FIP2 functions in transferrin recycling and associates with endosomal membranes via its COOH-terminal domain. J Biol Chem. 2002;277:27193-27199.

478. Dumanchin C, Czech C, Campion D et al. Presenilins interact with Rab11, a small GTPase involved in the regulation of vesicular transport. Hum Mol Genet. 1999;8:1263-1269.

479. de Graaf P, Zwart WT, van Dijken RA et al. Phosphatidylinositol 4-kinasebeta is critical for functional association of rab11 with the Golgi complex. Mol Biol Cell. 2004;15:2038-2047.

480. Hickson GR, Matheson J, Riggs B et al. Arfophilins are dual Arf/Rab 11 binding proteins that regulate recycling endosome distribution and are related to Drosophila nuclear fallout. Mol Biol Cell. 2003;14:2908-2920.

481. Hobdy-Henderson KC, Hales CM, Lapierre LA, Cheney RE, Goldenring JR. Dynamics of the apical plasma membrane recycling system during cell division. Traffic. 2003;4:681-693.

482. Eggers CT, Schafer JC, Goldenring JR, Taylor SS. D-AKAP2 interacts with Rab4 and Rab11 through its RGS domains and regulates transferrin receptor recycling. J Biol Chem. 2009;284:32869-32880.

483. Miserey-Lenkei S, Waharte F, Boulet A et al. Rab6-interacting protein 1 links Rab6 and Rab11 function. Traffic. 2007;8:1385-1403.

484. Band AM, Ali H, Vartiainen MK et al. Endogenous plasma membrane t-SNARE syntaxin 4 is present in rab11 positive endosomal membranes and associates with cortical actin cytoskeleton. FEBS Lett. 2002;531:513-519.

485. Lapierre LA, Goldenring JR. Interactions of myosin vb with rab11 family members and cargoes traversing the plasma membrane recycling system. Methods Enzymol. 2005;403:715-723.

486. Lapierre LA, Kumar R, Hales CM et al. Myosin vb is associated with plasma membrane recycling systems. Mol Biol Cell. 2001;12:1843-1857.

487. Sugawara K, Shibasaki T, Mizoguchi A, Saito T, Seino S. Rab11 and its effector Rip11 participate in regulation of insulin granule exocytosis. Genes Cells. 2009;14:445-456.

488. Zhang X, He X, Fu XY, Chang Z. Varp is a Rab21 guanine nucleotide exchange factor and regulates endosome dynamics. J Cell Sci. 2006;119:1053-1062.

489. Mishra A, Eathiraj S, Corvera S, Lambright DG. Structural basis for Rab GTPase recognition and endosome tethering by the C2H2 zinc finger of Early Endosomal Autoantigen 1 (EEA1). Proc Natl Acad Sci U S A. 2010;107:10866-10871.

490. Kuroda TS, Fukuda M. Rab27A-binding protein Slp2-a is required for peripheral melanosome distribution and elongated cell shape in melanocytes. Nat Cell Biol. 2004;6:1195-1203.

491. Yu M, Kasai K, Nagashima K et al. Exophilin4/Slp2-a targets glucagon granules to the plasma membrane through unique Ca2+-inhibitory phospholipid-binding activity of the C2A domain. Mol Biol Cell. 2007;18:688-696.

492. Chavas LM, Ihara K, Kawasaki M et al. Elucidation of Rab27 recruitment by its effectors: structure of Rab27a bound to Exophilin4/Slp2-a. Structure. 2008;16:1468-1477.

493. Wu XS, Rao K, Zhang H et al. Identification of an organelle receptor for myosin-Va. Nat Cell Biol. 2002;4:271-278.

494. Strom M, Hume AN, Tarafder AK, Barkagianni E, Seabra MC. A family of Rab27-binding proteins. Melanophilin links Rab27a and myosin Va function in melanosome transport. J Biol Chem. 2002;277:25423-25430.

495. Nagashima K, Torii S, Yi Z et al. Melanophilin directly links Rab27a and myosin Va through its distinct coiled-coil regions. FEBS Lett. 2002;517:233-238.

496. Fukuda M, Kuroda TS. Missense mutations in the globular tail of myosin-Va in dilute mice partially impair binding of Slac2-a/melanophilin. J Cell Sci. 2004;117:583-591.

497. Torii S, Kusakabe M, Yamamoto T, Maekawa M, Nishida E. Sef is a spatial regulator for Ras/MAP kinase signaling. Dev Cell. 2004;7:33-44.

498. Fukuda M, Yamamoto A. Assay of the Rab-binding specificity of rabphilin and Noc2: target molecules for Rab27. Methods Enzymol. 2005;403:469-481.

499. Cheviet S, Coppola T, Haynes LP, Burgoyne RD, Regazzi R. The Rab-binding protein Noc2 is associated with insulin-containing secretory granules and is essential for pancreatic beta-cell exocytosis. Mol Endocrinol. 2004;18:117-126.

500. Shirakawa R, Higashi T, Tabuchi A et al. Munc13-4 is a GTP-Rab27-binding protein regulating dense core granule secretion in platelets. J Biol Chem. 2004;279:10730-10737.

501. Park M, Serpinskaya AS, Papalopulu N, Gelfand VI. Rab32 regulates melanosome transport in Xenopus melanophores by protein kinase a recruitment. Curr Biol. 2007;17:2030-2034.

502. Valsdottir R, Hashimoto H, Ashman K, Koda T, Storrie B, Nilsson T. Identification of rabaptin-5, rabex-5, and GM130 as putative effectors of rab33b, a regulator of retrograde traffic between the Golgi apparatus and ER. FEBS Lett. 2001;508:201-209.

503. Kanno E, Ishibashi K, Kobayashi H, Matsui T, Ohbayashi N, Fukuda M. Comprehensive screening for novel rab-binding proteins by GST pull-down assay using 60 different mammalian Rabs. Traffic. 2010;11:491-507.

504. Wang F, Zhang H, Zhang X et al. Varp interacts with Rab38 and functions as its potential effector. Biochem Biophys Res Commun. 2008;372:162-167.

505. Kozma R, Ahmed S, Best A, Lim L. The GTPase-activating protein n-chimaerin cooperates with Rac1 and Cdc42Hs to induce the formation of lamellipodia and filopodia. Mol Cell Biol. 1996;16:5069-5080.

506. Zhang B, Zhang Y, Wang Z, Zheng Y. The role of Mg2+ cofactor in the guanine nucleotide exchange and GTP hydrolysis reactions of Rho family GTP-binding proteins. J Biol Chem. 2000;275:25299-25307.

507. Rossman KL, Der CJ, Sondek J. GEF means go: turning on RHO GTPases with guanine nucleotide-exchange factors. Nat Rev Mol Cell Biol. 2005;6:167-180.

508. Rossman KL, Worthylake DK, Snyder JT, Siderovski DP, Campbell SL, Sondek J. A crystallographic view of interactions between Dbs and Cdc42: PH domain-assisted guanine nucleotide exchange. EMBO J. 2002;21:1315-1326.

509. Snyder JT, Worthylake DK, Rossman KL et al. Structural basis for the selective activation of Rho GTPases by Dbl exchange factors. Nat Struct Biol. 2002;9:468-475.

510. Rittinger K, Walker PA, Eccleston JF et al. Crystal structure of a small G protein in complex with the GTPase-activating protein rhoGAP. Nature. 1997;388:693-697.

511. Fritz G, Just I, Kaina B. Rho GTPases are over-expressed in human tumors. Int J Cancer. 1999;81:682-687.

512. Gomez del Pulgar T, Benitah SA, Valeron PF, Espina C, Lacal JC. Rho GTPase expression in tumourigenesis: evidence for a significant link. Bioessays. 2005;27:602-613.

513. Xu B, Bhullar RP. Regulation of Rac1 and Cdc42 activation in thrombin- and collagen-stimulated CHRF-288-11 cells. Mol Cell Biochem. 2011;353:73-79.

514. Zamudio-Meza H, Castillo-Alvarez A, Gonzalez-Bonilla C, Meza I. Cross-talk between Rac1 and Cdc42 GTPases regulates formation of filopodia required for dengue virus type-2 entry into HMEC-1 cells. J Gen Virol. 2009;90:2902-2911.

515. Kai M, Yasuda S, Imai S, Kanoh H, Sakane F. Tyrosine phosphorylation of beta2-chimaerin by Src-family kinase negatively regulates its Rac-specific GAP activity. Biochim Biophys Acta. 2007;1773:1407-1415.

516. Caloca MJ, Delgado P, Alarcon B, Bustelo XR. Role of chimaerins, a group of Rac-specific GTPase activating proteins, in T-cell receptor signaling. Cell Signal. 2008;20:758-770.

517. Pan Y, Bi F, Liu N et al. Expression of seven main Rho family members in gastric carcinoma. Biochem Biophys Res Commun. 2004;315:686-691.

518. Liu SY, Yen CY, Yang SC, Chiang WF, Chang KW. Overexpression of Rac-1 small GTPase binding protein in oral squamous cell carcinoma. J Oral Maxillofac Surg. 2004;62:702-707.

519. Jordan P, Brazao R, Boavida MG, Gespach C, Chastre E. Cloning of a novel human Rac1b splice variant with increased expression in colorectal tumors. Oncogene. 1999;18:6835-6839.

520. Abraham MT, Kuriakose MA, Sacks PG et al. Motility-related proteins as markers for head and neck squamous cell cancer. Laryngoscope. 2001;111:1285-1289.

521. George A, Pushkaran S, Li L et al. Altered phosphorylation of cytoskeleton proteins in sickle red blood cells: the role of protein kinase C, Rac GTPases, and reactive oxygen species. Blood Cells Mol Dis. 2010;45:41-45.

522. Kwofie MA, Skowronski J. Specific recognition of Rac2 and Cdc42 by DOCK2 and DOCK9 guanine nucleotide exchange factors. J Biol Chem. 2008;283:3088-3096.

523. Zhao T, Nalbant P, Hoshino M, Dong X, Wu D, Bokoch GM. Signaling requirements for translocation of P-Rex1, a key Rac2 exchange factor involved in chemoattractant-stimulated human neutrophil function. J Leukoc Biol. 2007;81:1127-1136.

524. Dong X, Mo Z, Bokoch G, Guo C, Li Z, Wu D. P-Rex1 is a primary Rac2 guanine nucleotide exchange factor in mouse neutrophils. Curr Biol. 2005;15:1874-1879.

525. Mira JP, Benard V, Groffen J, Sanders LC, Knaus UG. Endogenous, hyperactive Rac3 controls proliferation of breast cancer cells by a p21-activated kinase-dependent pathway. Proc Natl Acad Sci U S A. 2000;97:185-189.

526. Lee JS, Kamijo K, Ohara N, Kitamura T, Miki T. MgcRacGAP regulates cortical activity through RhoA during cytokinesis. Exp Cell Res. 2004;293:275-282.

527. Krugmann S, Andrews S, Stephens L, Hawkins PT. ARAP3 is essential for formation of lamellipodia after growth factor stimulation. J Cell Sci. 2006;119:425-432.

528. Gambardella L, Hemberger M, Hughes B, Zudaire E, Andrews S, Vermeren S. PI3K signaling through the dual GTPase-activating protein ARAP3 is essential for developmental angiogenesis. Sci Signal. 2010;3:ra76.

529. Estevez MA, Henderson JA, Ahn D et al. The neuronal RhoA GEF, Tech, interacts with the synaptic multi-PDZ-domain-containing protein, MUPP1. J Neurochem. 2008;106:1287-1297.

530. Lutz S, Shankaranarayanan A, Coco C et al. Structure of Galphaq-p63RhoGEF-RhoA complex reveals a pathway for the activation of RhoA by GPCRs. Science. 2007;318:1923-1927.

531. Yeung WW, Wong YH. The RhoA-specific guanine nucleotide exchange factor p63RhoGEF binds to activated Galpha(16) and inhibits the canonical phospholipase Cbeta pathway. Cell Signal. 2009;21:1317-1325.

532. Garnaas MK, Moodie KL, Liu ML et al. Syx, a RhoA guanine exchange factor, is essential for angiogenesis in Vivo. Circ Res. 2008;103:710-716.

533. Goh LL, Manser E. The RhoA GEF Syx is a target of Rnd3 and regulated via a Raf1-like ubiquitin-related domain. PLoS One. 2010;5:e12409.

534. Shamah SM, Lin MZ, Goldberg JL et al. EphA receptors regulate growth cone dynamics through the novel guanine nucleotide exchange factor ephexin. Cell. 2001;105:233-244.

535. Zhang Y, Sawada T, Jing X, Yokote H, Yan X, Sakaguchi K. Regulation of ephexin1, a guanine nucleotide exchange factor of Rho family GTPases, by fibroblast growth factor receptor-mediated tyrosine phosphorylation. J Biol Chem. 2007;282:31103-31112.

536. Abe K, Rossman KL, Liu B et al. Vav2 is an activator of Cdc42, Rac1, and RhoA. J Biol Chem. 2000;275:10141-10149.

537. Arthur WT, Ellerbroek SM, Der CJ, Burridge K, Wennerberg K. XPLN, a guanine nucleotide exchange factor for RhoA and RhoB, but not RhoC. J Biol Chem. 2002;277:42964-42972.

538. Kamai T, Arai K, Tsujii T, Honda M, Yoshida K. Overexpression of RhoA mRNA is associated with advanced stage in testicular germ cell tumour. BJU Int. 2001;87:227-231.

539. Kamai T, Tsujii T, Arai K et al. Significant association of Rho/ROCK pathway with invasion and metastasis of bladder cancer. Clin Cancer Res. 2003;9:2632-2641.

540. Wang Z, Kumamoto Y, Wang P et al. Regulation of immature dendritic cell migration by RhoA guanine nucleotide exchange factor Arhgef5. J Biol Chem. 2009;284:28599-28606.

541. Kim BK, Kim HM, Chung KS et al. Upregulation of RhoB via c-Jun N-terminal kinase signaling induces apoptosis of the human gastric carcinoma NUGC-3 cells treated with NSC12618. Carcinogenesis. 2011;32:254-261.

542. Bravo-Nuevo A, Sugimoto H, Iyer S et al. RhoB loss prevents streptozotocin-induced diabetes and ameliorates diabetic complications in mice. Am J Pathol. 2011;178:245-252.

543. Hu XH, Wu WF, Qing Y et al. [Improved therapeutic effectiveness by combining recombinant human RhoB with low-dose cisplatin in human lung cancer in nude mice]. Sichuan Da Xue Xue Bao Yi Xue Ban. 2011;42:475-479.

544. Fritz G, Brachetti C, Bahlmann F, Schmidt M, Kaina B. Rho GTPases in human breast tumours: expression and mutation analyses and correlation with clinical parameters. Br J Cancer. 2002;87:635-644.

545. Mazieres J, Antonia T, Daste G et al. Loss of RhoB expression in human lung cancer progression. Clin Cancer Res. 2004;10:2742-2750.

546. Adnane J, Muro-Cacho C, Mathews L, Sebti SM, Munoz-Antonia T. Suppression of rho B expression in invasive carcinoma from head and neck cancer patients. Clin Cancer Res. 2002;8:2225-2232.

547. Houchens NW, Merajver SD. Molecular determinants of the inflammatory breast cancer phenotype. Oncology (Williston Park). 2008;22:1556-61; discussion 1561, 1565-8, 1576.

548. Hamel B, Monaghan-Benson E, Rojas RJ et al. SmgGDS is a guanine nucleotide exchange factor that specifically activates RhoA and RhoC. J Biol Chem. 2011;286:12141-12148.

549. MacGrath SM, Koleske AJ. Invadopodia: RhoC runs rings around cofilin. Curr Biol. 2011;21:R280-2.

550. Suwa H, Ohshio G, Imamura T et al. Overexpression of the rhoC gene correlates with progression of ductal adenocarcinoma of the pancreas. Br J Cancer. 1998;77:147-152.

551. van Golen KL, Wu ZF, Qiao XT, Bao LW, Merajver SD. RhoC GTPase, a novel transforming oncogene for human mammary epithelial cells that partially recapitulates the inflammatory breast cancer phenotype. Cancer Res. 2000;60:5832-5838.

552. Kleer CG, Teknos TN, Islam M et al. RhoC GTPase expression as a potential marker of lymph node metastasis in squamous cell carcinomas of the head and neck. Clin Cancer Res. 2006;12:4485-4490.

553. Liu N, Zhang G, Bi F et al. RhoC is essential for the metastasis of gastric cancer. J Mol Med (Berl). 2007;85:1149-1156.

554. Shikada Y, Yoshino I, Okamoto T, Fukuyama S, Kameyama T, Maehara Y. Higher expression of RhoC is related to invasiveness in non-small cell lung carcinoma. Clin Cancer Res. 2003;9:5282-5286.

555. Murphy C, Saffrich R, Olivo-Marin JC et al. Dual function of rhoD in vesicular movement and cell motility. Eur J Cell Biol. 2001;80:391-398.

556. Tsubakimoto K, Matsumoto K, Abe H et al. Small GTPase RhoD suppresses cell migration and cytokinesis. Oncogene. 1999;18:2431-2440.

557. Zhang C, Zhou F, Li N et al. Overexpression of RhoE has a prognostic value in non-small cell lung cancer. Ann Surg Oncol. 2007;14:2628-2635.

558. Cuiyan Z, Jie H, Fang Z et al. Overexpression of RhoE in Non-small Cell Lung Cancer (NSCLC) is associated with smoking and correlates with DNA copy number changes. Cancer Biol Ther. 2007;6:335-342.

559. Jiang WG, Watkins G, Lane J et al. Prognostic value of rho GTPases and rho guanine nucleotide dissociation inhibitors in human breast cancers. Clin Cancer Res. 2003;9:6432-6440.

560. Blangy A, Vignal E, Schmidt S, Debant A, Gauthier-Rouviere C, Fort P. TrioGEF1 controls Rac- and Cdc42-dependent cell structures through the direct activation of rhoG. J Cell Sci. 2000;113:729-739.

561. Preudhomme C, Roumier C, Hildebrand MP et al. Nonrandom 4p13 rearrangements of the RhoH/TTF gene, encoding a GTP-binding protein, in non-Hodgkin's lymphoma and multiple myeloma. Oncogene. 2000;19:2023-2032.

562. Pasqualucci L, Neumeister P, Goossens T et al. Hypermutation of multiple proto-oncogenes in B-cell diffuse large-cell lymphomas. Nature. 2001;412:341-346.

563. Bektic J, Pfeil K, Berger AP et al. Small G-protein RhoE is underexpressed in prostate cancer and induces cell cycle arrest and apoptosis. Prostate. 2005;64:332-340.